UTD Ray and Beam Methods for Analysis of Large EM Wave Problems

Prabhakar H. Pathak (pathak.2@osu.edu)

The Ohio State University, ElectroScience Laboratory
1320 Kinnear Road, Columbus Ohio, 43212, USA

COPYRIGHT

ElectroScience LABORATORY

ABSTRACT

It is well known from the independent works of Keller, Deschamps, and Felsen, respectively, that an electromagnetic (EM) point current source positioned in complex space produces a beam wave field which is highly localized about its forward propagation axis. It is noted that the EM field of a complex source beam (CSB) constitutes an exact solution of Maxwell's equations, and it is simply obtained by an analytic continuation of the exact closed form expression of the EM field for a point current in real space, where the real source coordinates are replaced by complex values. In its paraxial region, a CSB automatically reduces to a Gaussian Beam (GB). By controlling the values of the complex source coordinates, one can produce either a CSB with a very broad (not well focused) beam or a very narrow (highly focused) beam; consequently, such a CSB field can be made to pass smoothly from the field of a real point source to a plane wave field. It is clear that CSBs can serve as highly useful basis functions to represent EM fields, and indeed they have been used in this fashion by some researchers in this area. Here, additional useful methods for developing convergent CSB expansions to represent the fields of EM sources, via appropriate EM equivalence theorems, will be illustrated. Applications of such CSB expansions to analyze a class of electrically large practical antenna and scattering problems will be presented to demonstrate their utility.

Index Terms: Ray Optics, Diffraction, GTD, UTD, PTD, Beams, Hybrid Methods

BIOGRAPHY

Prabhakar Pathak received his Ph.D (NVTP) from the Ohio State Univ (OSU). Currently he is Professor (Emeritus) at OSU. He is also a Courtesy Professor and an Adàunct Professor at Univ. of South Florida. Prof. Pathak is regarded as a co-developer of the uniform geometrical theory of diffraction (UTD). His interests continue to be in the development of new UTD solutions in both frequency and time domains, as well as in the development of fast Beam and Hybrid methods, for solving large antenna/scattering problems of engineering interest. Prof. Pathak has been actively presenting short courses and invited talks at conferences and workshops both in the US and abroad. He has authored/coauthored over a hundred journal and conference papers, as well as contributed chapters to seven books. Prior to NVVP, he served two consecutive terms as an Associate Editor of IEEE Trans. AP-S. He was appointed as an IEEE (AP-S) Distinguished lecturer (DL) from 1991-1993. Prof. Pathak was also appointed as the chair of the IEEE AP-S DL program during 1995 – 2005. He served as a member of the IEEE AP-S AdCom in 2010. He received the 1996 Schelkunoff best paper award from IEEE-AP-S; the ISAP 2009 best paper award; the George Sinclair award (1996) from OSU ElectroScience Laboratory; and, IEEE Third Millennium Medal from AP- S in 2000. Prof. Pathak received the Distinguished Achievement Award from IEEE AP-S in 2013. He is an IEEE Life Fellow, and a member of URSI-commission B.

ElectroScience LABORATORY

• Two Basic Asymptotic High Frequency (HF) Methodologies can be Categorized as follows:

1. **RAY OPTICAL METHODS**
   a) Geometrical Optics (GO)
   b) Geometrical Theory of Diffraction (GTD)
      [GTD = GO + Diffraction]
   c) Uniform Version of the GTD

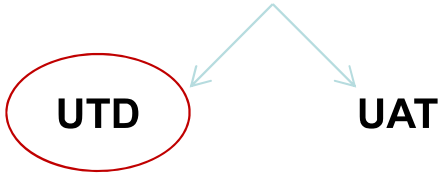

2. **WAVE OPTICAL METHODS**
   a) Physical Optics (PO)
   b) Physical Theory of Diffraction (PTD)
      [PTD = PO + Diffraction Correction]
   c) Incremental Theory of Diffraction (ITD) and Equivalent Current Method (ECM)

ON THE LOCALIZATION OF THE WAVE PROPAGATION AT HF

- The HF localization principle can be demonstrated via asymptotic evaluation of the radiation integral as depicted below:

a) Radiation integral for the scattered field in the spatial domain.

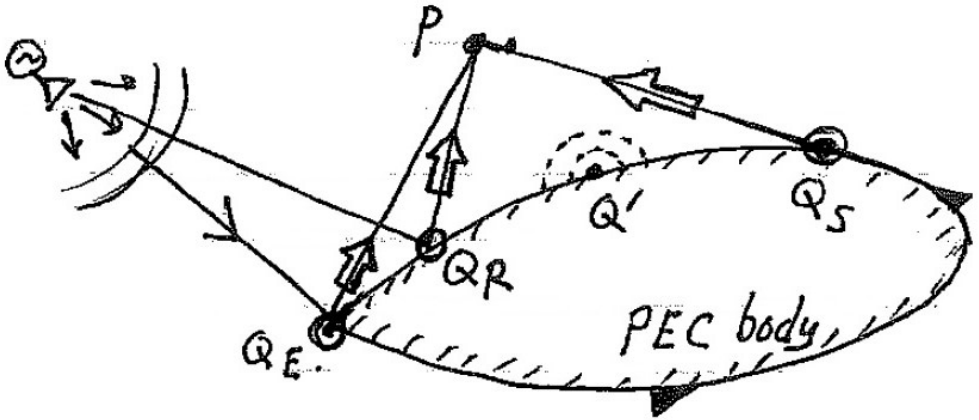

$$\overline{E}(P) = \overline{E}^{i}(P) + \overline{E}^{s}(P)$$

$$\overline{E}^{s}(P) = \int_S \overline{\overline{\Gamma}}_{ee}(P \mid Q') \cdot \overline{J}_S(Q')\, dS'$$

$$\overline{\overline{\Gamma}}_{ee}(\bar{r} \mid \bar{r}') = -j\omega\mu \left(\overline{\overline{I}} + \frac{\nabla\nabla}{k^2} \right) \frac{e^{-jkR}}{R}, \quad \left(R = \left| \bar{r} - \bar{r}' \right| \right)$$

$$\overline{E}^{s}(P) \approx \underbrace{\overline{E}^{r}(P)}_{\text{from } Q'=Q_R} + \underbrace{\overline{E}^{d}(P)}_{\text{from } Q'=Q_E} + \underbrace{\overline{E}^{sd}(P)}_{\text{from } Q'=Q_S}$$

Q_E, Q_R and Q_S are critical points corresp. to end, stationary and confluence of two stationary points, respectively of the integrand. For other values of Q' the integral is negligible due to destructive interference in the asymptotic HF regime.

b) Radiation integral for the scattered field in the spectral domain.

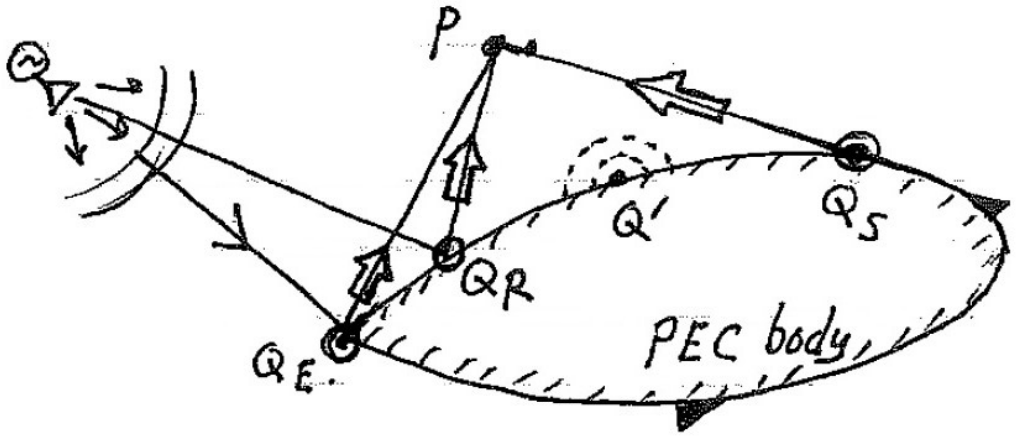

$$\overline{E}^s(P) = \int dk_x \int dk_y \, \overline{f}(k_x, k_y) \cdot e^{-j\bar{k}\cdot\bar{r}}$$

$$\overline{f} = \int_S (-j\omega\mu C)\overline{J}_S(Q')e^{j\bar{k}\cdot\bar{r}'}dS'$$

$$\overline{E}^s(P) \square \overline{E}^r(P) + \overline{E}^d(P) + \overline{E}^{sd}(P)$$

Q_E, Q_R and Q_S transform into critical within the spectrum as poles, saddle points, branch points, etc. Only those plane waves reaching P from the nbhd of Q_E, Q_R and Q_S contribute significantly; all others interfere destructively.

$$\overline{k} = k_x\hat{x} + k_y\hat{y} + k_z\hat{z}$$

$$k_z = \sqrt{k^2 - k_x^2 - k_y^2} = -j\sqrt{k_x^2 + k_y^2 - k^2}\,; \; z > z' \;\text{ assumed}$$

RAY METHODS & SOME APPLICATIONS

• Unlike most other computational electromagnetic (CEM) techniques, asymptotic high frequency (HF) ray methods offer a **simple picture** for describing EM antenna/scattering phenomena.

Examples of EM antenna radiation and coupling problems of interest and some typical UTD rays.

• Rays → wave effects are highly **LOCALIZED** at HF.

• Primary focus here will be on the uniform geometrical theory of diffraction (UTD) type ray solutions.

• The need for UTD arises because classical geometrical optics (GO) ray method **fails** to predict diffraction !

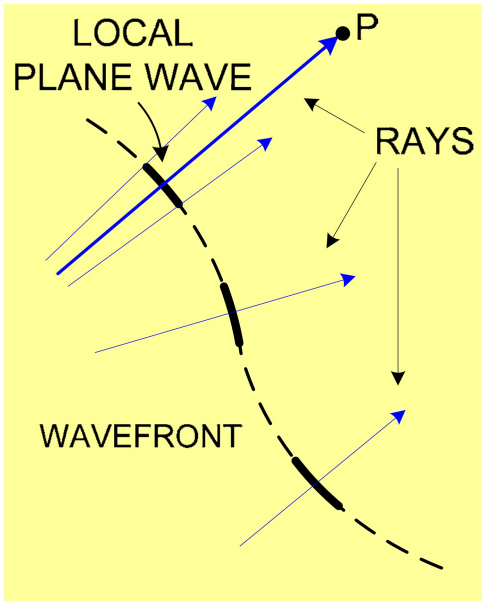

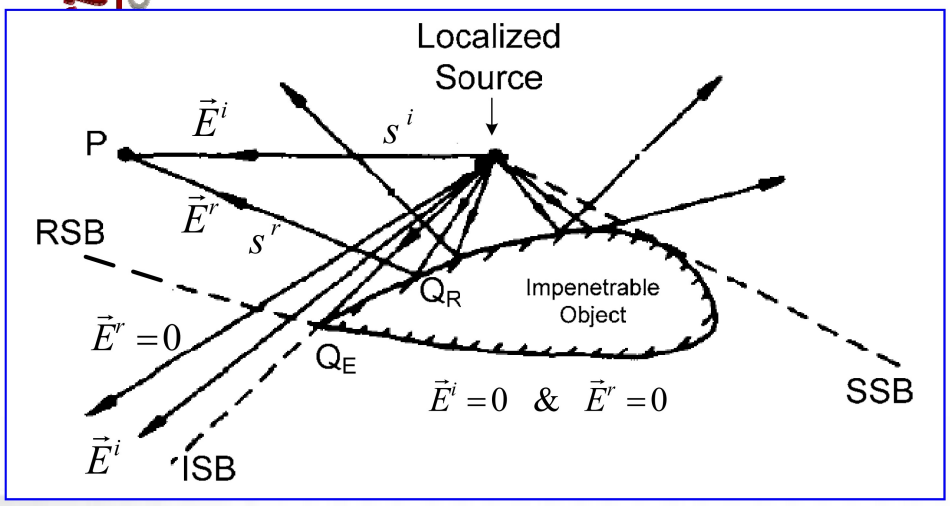

$$\vec{E}^i(P) \sim C_O \vec{P} \frac{e^{-jks^i}}{s^i} U_i$$

$$\vec{E}^r(P) \sim \vec{E}^i(Q_R) \cdot \overline{\overline{R}}(Q_R) f(s^r) e^{-jks^r} U_r$$

$$U_i = \begin{cases} 1, & \text{Lit side of ISB} \\ 0, & \text{Shadow side of ISB} \end{cases}$$

$$U_r = \begin{cases} 1, & \text{Lit side of RSB} \\ 0, & \text{Shadow side of RSB} \end{cases}$$

* $f(s^r)$ depends only on surface and wavefront geometry at & near Q_R

ISB: Incident Shadow Boundary, RSB: Reflection Shadow Boundary, SSB: Surface Shadow Boundary

RAY METHODS & SOME APPLICATIONS (cont.)

- Keller and coworkers (1958; 1962) introduced a **new** class of rays, i.e. diffracted rays, to describe diffraction in his geometrical theory of diffraction (GTD).
- Diffracted rays exist in addition to geometrical optics (GO) rays.
- Diffracted rays are produced at structural and material discontinuities, as well as at grazing incidence on a smooth convex surface.

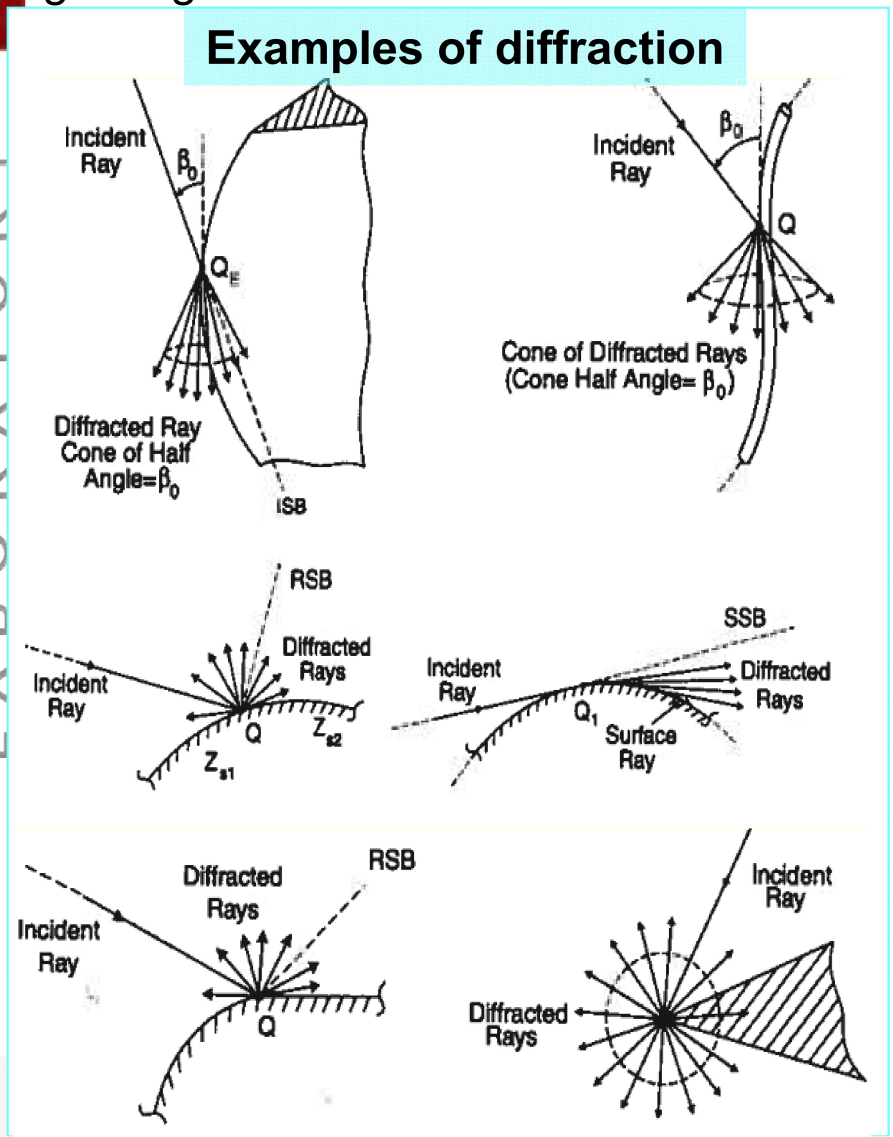

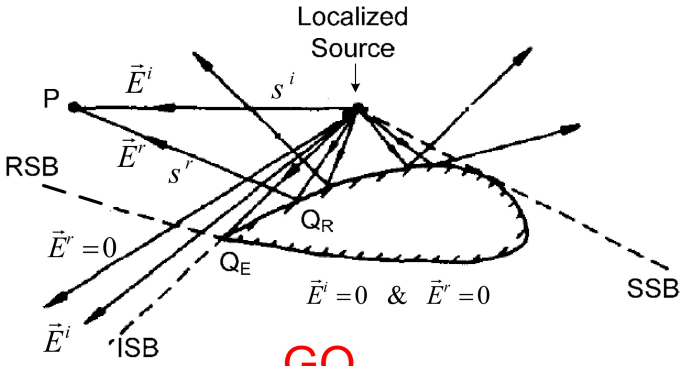

GO

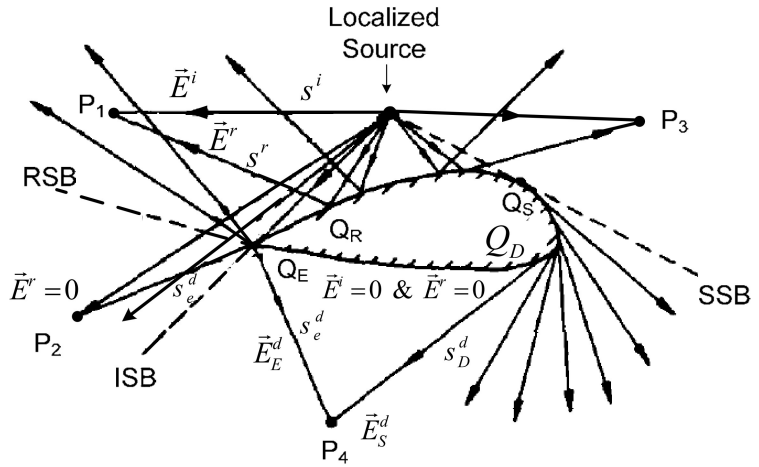

(GO + Diffraction)

$$\vec{E}_e^d(P_2,P_4) \sim \vec{E}^i(Q_E)\cdot\overline{\overline{D}}_E f(s_e^d)e^{-jks_e^d}$$

$$\vec{E}_S^d(P_4) \sim \vec{E}^i(Q_S)\cdot\overline{\overline{T}}(Q_S,Q_D) f(s_D^d)e^{-jks_D^d}$$

RAY METHODS & SOME APPLICATIONS (cont.)

- To find $\overline{\overline{D}}$ and $\overline{\overline{T}}$, etc, in diffraction problems, one may:

  (a) Solve appropriate, simpler canonical problems which model the LOCAL geometrical and electrical properties of the original surface in the neighborhood of diffraction points.

  (b) An exact (or sometimes approximate) solution to a canonical problem is first expressed as an integral containing an exponent κD

$$\kappa = \text{wave number} = 2\pi/\lambda$$

$$D = \text{characteristic dimension}$$

  (c) Canonical integral is then evaluated asymptotically, generally in closed form, as parameter κD becomes large (i.e. at HF).

  (d) $\overline{\overline{D}}$ and $\overline{\overline{T}}$ are then typically found from (c) by inspection.

  (e) Canonical $\overline{\overline{D}}$ and $\overline{\overline{T}}$ generalized to arbitrary shapes by invoking principle of locality of HF waves.

- Keller's original GTD is not valid at and near ISB, RSB, SSB (i.e. in SB transition regions).
- UTD developed to patch Keller's original theory within the SB transition regions.
- GTD corrects GO, and GTD = GO + diffraction
- UTD corrects GTD, but usually UTD → GTD outside SB transition regions.

RAY METHODS & SOME APPLICATIONS (cont.)

- **Additional Comments :**

(a) Ufimtsev's Physical Theory of Diffraction (PTD) (1950s) corrects Physical Optics (PO). PO contains incomplete diffraction.

(b) PTD generally requires numerical integration on the radiating/scattering objects, hence, loses efficiency as frequency increases.

(c) PTD does not describe creeping/surface wave diffraction on smooth convex objects; hence, does not accurately predict patterns in shadow zone of antennas on such complex objects.

(d) Conventional numerical CEM methods become rapidly inefficient with increase in frequency.

(e) In contrast, UTD ray paths remain independent of frequency.

(f) UTD offers an analytical (generally closed form) solution to many complex problems that can not otherwise be solved in an analytical fashion.

RAY METHODS & SOME APPLICATIONS (cont.)

- *In many practical applications of UTD, the following diffraction ray mechanisms dominate*

(a) PEC Wedge Diffraction

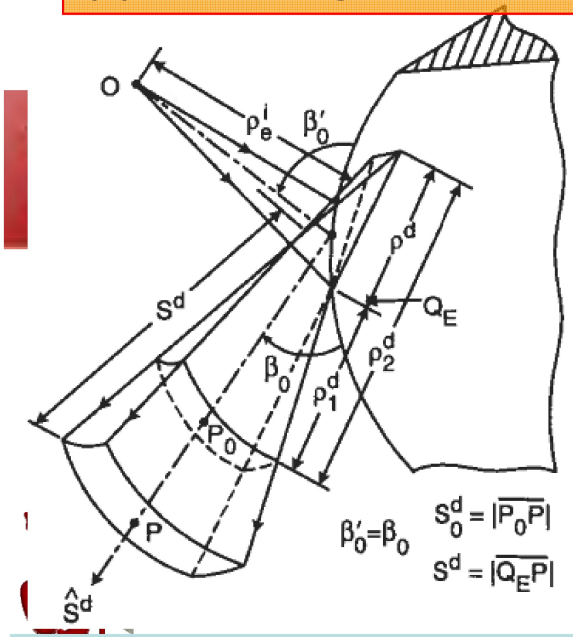

[1] R. G. Kouyoumjian and P. H. Pathak, "A uniform geometrical theory of diffraction for an edge in a perfectly conducting surface," *Proc. EEE,* vol. 62, pp. 1448-1461, Nov. 1974.

Alternative ray solutions (UAT)

[2] S. W. Lee and G. A. Deschamps, "A Uniform Asymptotic theory of EM diffraction by a curved *wedge,"IEEE Trans. Antennas Propagat.,* vol. AP-24, pp. 25-34, Jan. 1976.

[3] Borovikov, V.A.and Kinber B.Ye, "Some problems in the asymptotic theory of diffraction", *IEEE Proceeding*, volume 62, pp. 1416-1437, Nov. 1974.

(b) PEC Convex Surface Diffraction

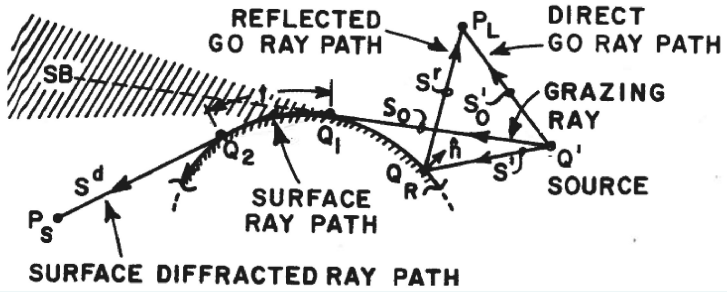

[1] P.H Pathak, "An asymptotic analysis of the scattering of plane waves by a smooth convex cylinder," *Radio Science*, Vol 14 pp419-435, 1979

[2] P.H Pathak et al, "A uniform GTD analysis of the diffraction of EM waves by a smooth convex surface," *IEEE Trans Ant and Propa*. Vol 8 Sept 1980.

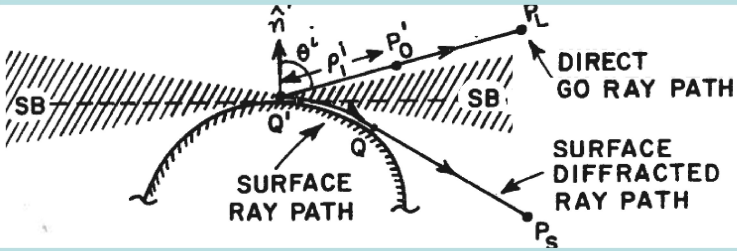

[1] P.H Pathak et al,"A uniform GTD solution for the radiation from sources on a convex surface," *IEEE Trans Ant and Propa*. Vol 29 July 1981.

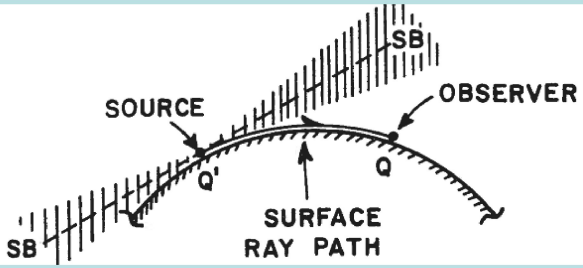

[1] P.H Pathak and N. Wang,"Ray analysis of mutual coupling between antennas on a convex surface," *IEEE Trans Ant and Propa*. Vol 29 Nov 1981.

(Alt. Soln. by S.W. Lee in IEEE AP-S)

(c) PEC Corner Diffraction

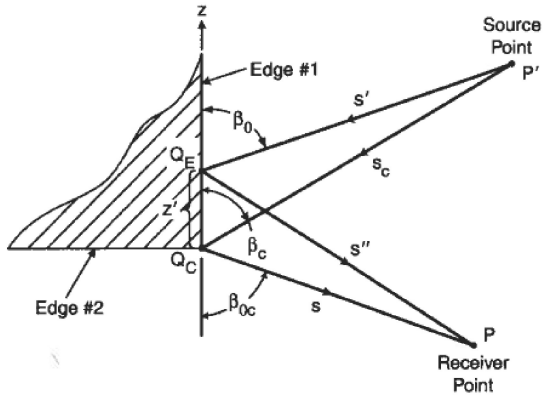

[1] K.C Hill and P.H Pathak, "A UTD solution for EM diffraction by a corner in a plane angular sector," IEEE Ant. Prop. Symp. June 1991.

[2] K. C. Hill, "A UTD solution to the EM scattering by the vertex of a perfectly conducting plane angular sector," Ph.D dissertation, The Ohio State University, 1990.

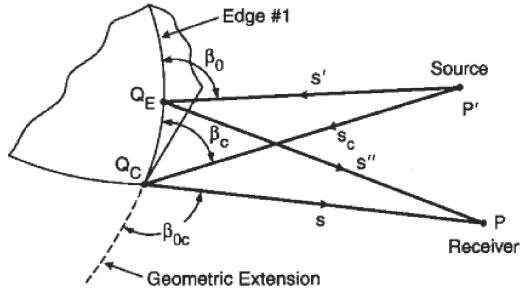

[1] G. Carluccio, "A UTD Diffraction Coefficient for a Corner Formed by Truncation of Edges in an Otherwise Smooth Curved Surface," IEEE Ant. Prop. Symp. June 2009.

Some UTD code developments in USA during 1980's – 1990's

The Ohio State Univ. (OSU) ElectroScience Lab. (ESL) UTD based codes:

(a)OSU-ESL NEWAIR code

(b)OSU-ESL BSC code

• Complex radiating and scattering objects modeled by simpler shapes consisting of ellipsoids, spheroids, cylinders, cone frustrums, flat plates, etc.

- **In many practical applications of UTD, the following diffraction ray mechanisms dominate**

(a) PEC Wedge Diffraction

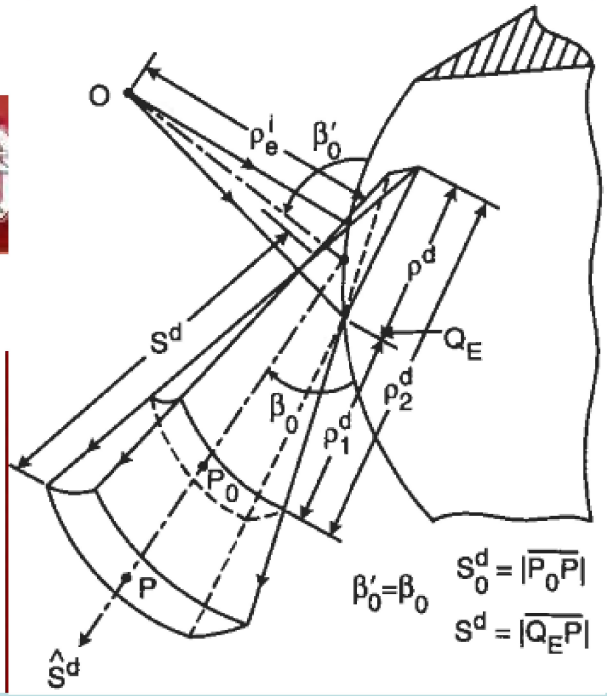

$$\overline{E}^d(P) \simeq \overline{E}^d(P_0)\cdot\sqrt{\frac{\rho_1^d\rho_2^d}{\left(\rho_1^d+s_0^d\right)\left(\rho_2^d+s_0^d\right)}}\cdot e^{-jks_0^d}$$

$$s_0^d = |P_0P|$$

$$\lim_{\substack{P_0\to Q_E\\ \rho_1^d\to 0}} \overline{E}^d(P_0)\cdot\sqrt{\rho_1^d} = \overline{E}^i(Q_E)\cdot\overline{\overline{D}}_e;\begin{Bmatrix}\rho_2^d\to\rho^d\\ s_0^d\to s^d\end{Bmatrix}$$

$$\overline{\overline{D}}_e = -\hat{\beta}_0'\hat{\beta}_0 D_{es}(\phi,\phi',\beta_0) - \hat{\phi}'\hat{\phi} D_{eh}(\phi,\phi',\beta_0)$$

$$\overline{E}^d(P) \simeq \overline{E}^i(Q_E)\cdot\overline{\overline{D}}_e\sqrt{\frac{\rho^d s^d}{\rho^d+s^d}}\cdot\frac{e^{-jks^d}}{s^d}$$

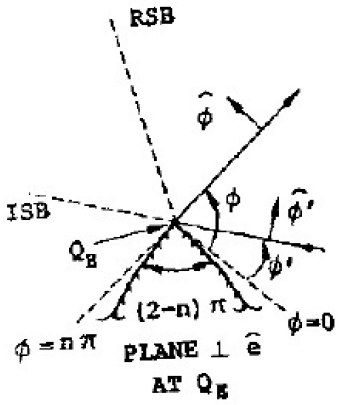

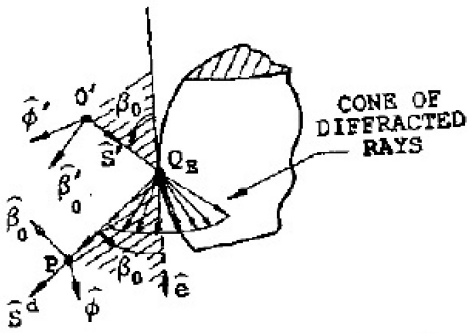

$\overline{\overline{D}}_e$ contains 4 terms which are a product of $\cot\left(\frac{\pi\pm(\phi\mp\phi')}{2n}\right)$ and $F\left(kLa(\phi\mp\phi')\right)$

$$F(x) = 2j\sqrt{x}e^{jx}\int_{\sqrt{x}}^{\infty} d\tau e^{-j\tau^2}$$

UTD EDGE TRANSITION FUNCTION

[1] R. G. Kouyoumjian and P. H. Pathak, "A uniform geometrical theory of diffraction for an edge in a perfectly conducting surface," *Proc. EEE,* vol. 62, pp. 1448-1461, Nov. 1974.

Alternative ray solutions (UAT)

[2] S. W. Lee and G. A. Deschamps, "A Uniform Asymptotic theory of EM diffraction by a curved *wedge,"IEEE Trans. Antennas Propagat.,* vol. AP-24, pp. 25-34, Jan. 1976.

[3] Borovikov, V.A.and Kinber B.Ye, "Some problems in the asymptotic theory of diffraction", *IEEE Proceeding*, volume 62, pp. 1416-1437, Nov. 1974.

$$\overline{E}(P) = \int\int_{S_a} \overline{\overline{\Gamma}}_m(P|Q') \cdot [\overline{M}_S(Q')]\, ds'$$

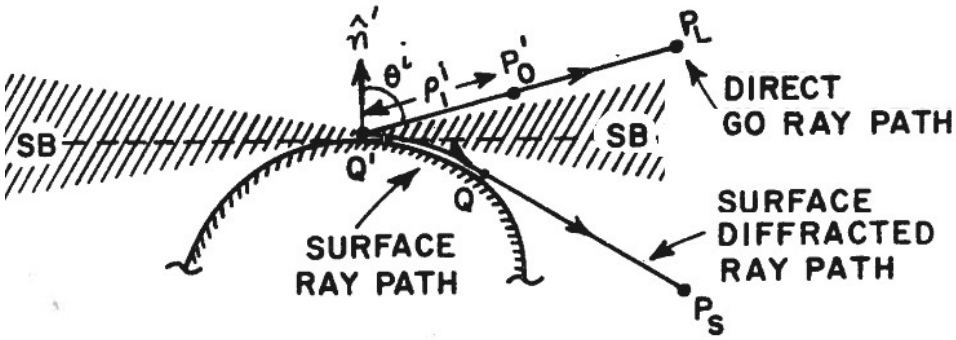

[1] P.H Pathak et al,"A uniform GTD solution for the radiation from sources on a convex surface," *IEEE Trans Ant and Propa*. Vol 29 July 1981.

where $\overline{M}_S(Q') = \overline{E}_a(Q') \times \hat{n}'$ is the equivalent magnetic current in terms of the transmiting electric field $\overline{E}_a(Q')$ in the slot aperture of area S_a; this $\overline{M}_S$ replaces the aperture S_a which is now short circuited. Likewise, the radiation from a short thin monopole of height *h* and transmiting current $I(l')$ fed at the base *Q'* on a convex surface can be found as

$$\overline{E}(P) \approx \begin{cases} \overline{\overline{\Gamma}}_i(P|Q') \cdot \hat{n}' \int_0^h I(l') \\ \qquad \cdot \cos(kl' \cos\theta) dl', & \text{if } P = P_L \\ \overline{\overline{\Gamma}}_i(P|Q') \cdot \hat{n}' \int_0^h I(l') dl', & \text{if } P = P_S. \end{cases}$$

The UTD solution can predict complex surface dependent polarization effects resulting form surface ray torsion (see terms T_1, T_2, T_3, T_4, T_5, T_6).

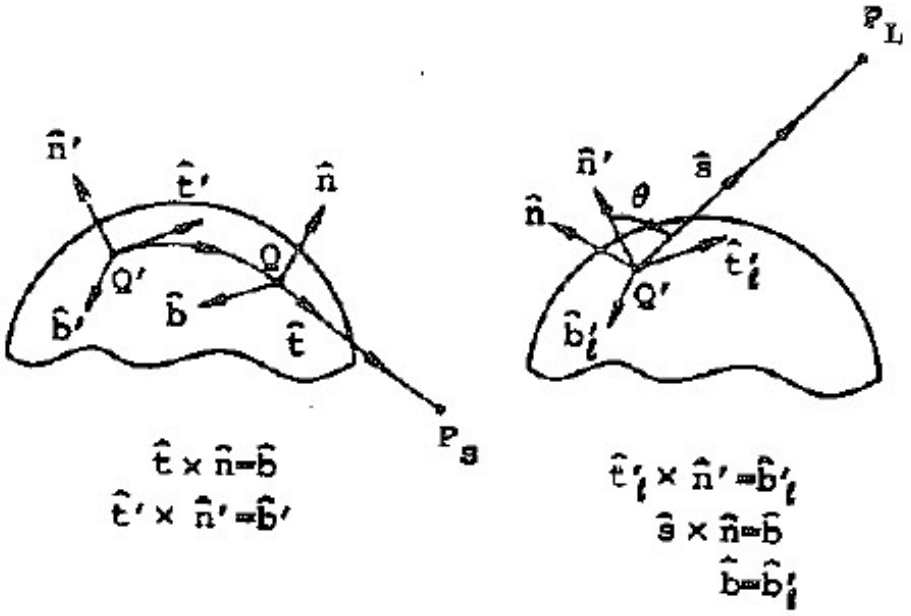

$$\overline{E}(P)=\begin{cases}\overline{\overline{\Gamma}}_i(P|Q')\cdot\hat{p}, & \text{if } \hat{p}=\hat{i}\\ \overline{\overline{\Gamma}}_m(P|Q')\cdot\hat{p}, & \text{if } \hat{p}=\hat{m}\end{cases}$$

The $\overline{\overline{\Gamma}}_{i,m}$ is obtained from uniform asymptotic solutions to problems of radiation by p on conducting cylinders and spheres.

$$\overline{\overline{\Gamma}}_m\sim\begin{cases}(-jk/4\pi)\left(\hat{b}_l'\hat{n}A+\hat{t}_l'\hat{b}B+\hat{b}_l'\hat{b}C+\hat{t}_l'\hat{n}D\right)(e^{(-jks)}/s)\\ \quad\text{for } P=P_L\\ (-jk/4\pi)\left(\hat{b}'\hat{n}T_1H+\hat{t}'\hat{b}T_2S+\hat{b}'\hat{b}T_3S+\hat{t}'\hat{n}T_4H\right)\\ \cdot e^{-jkt}\sqrt{(d\psi_o/d\eta(Q))}[\rho_g(Q)/\rho_g(Q')]^{1/6}\\ \cdot\sqrt{\rho^d/(s^d(\rho^d+s^d))}\exp(-jks^d),\\ \quad\text{for } P=P_S\end{cases}$$

and

$$\overline{\overline{\Gamma}}_i\sim\begin{cases}(-jkZ_o/4\pi)\left(\hat{n}'\hat{n}M+\hat{n}'\hat{b}N\right)(e^{-jks}/s),\\ \quad\text{for } P=P_L\\ (-jkZ_o/4\pi)\left(\hat{n}'\hat{n}T_5H+\hat{n}'\hat{b}T_6S\right)\\ \cdot e^{-jkt}\sqrt{(d\psi_o/d\eta(Q))}[(\rho_g(Q)/\rho_g(Q'))]^{1/6}\\ \cdot\sqrt{\rho^d/(s^d(\rho^d+s^d))}\exp(-jks^d),\\ \quad\text{for } P=P_S.\end{cases}$$

UTD Transition functions in A, B, C, D, H, S, n and N are the radiation Fock fcns.

$$g(\delta)=\frac{1}{\sqrt{\pi}}\int_{\infty e^{-j(2\pi/3)}}^{\infty}d\tau e^{-j\delta\tau}[W_2'(\tau)]^{-1}$$

$$\tilde{g}(\delta)=\frac{1}{\sqrt{\pi}}\int_{\infty e^{-j(2\pi 3)}}^{\infty}d\tau e^{-j\delta\tau}[W_2(\tau)]^{-1}.$$

$\delta>0$ at P_S

$\delta<0$ at P_L

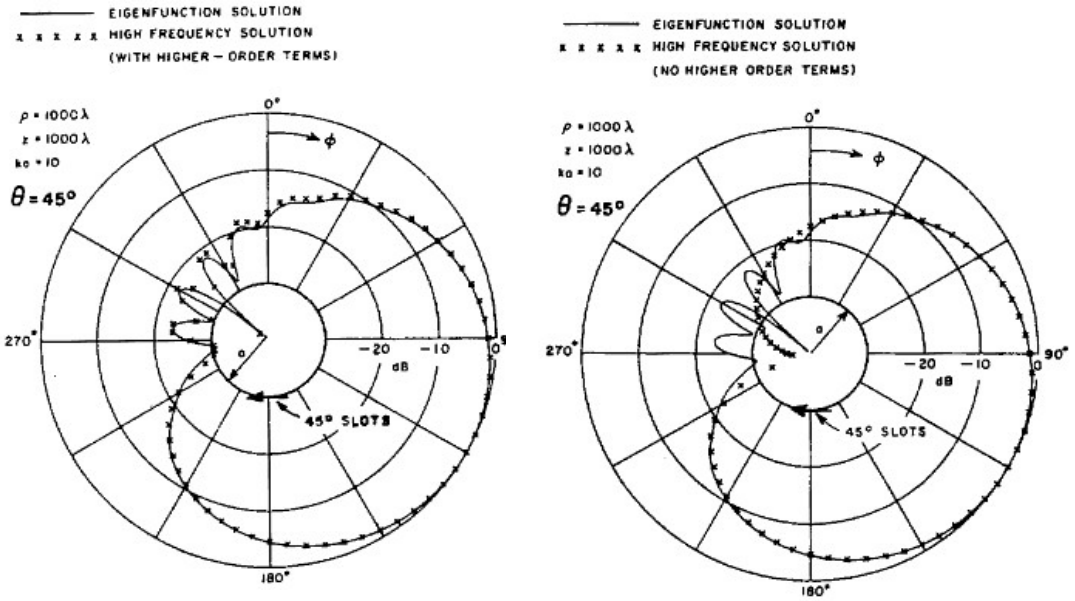

Fig. 8. $|E_\phi|$ radiation pattern of a 45° (tilted) slot in a circular cylinder.

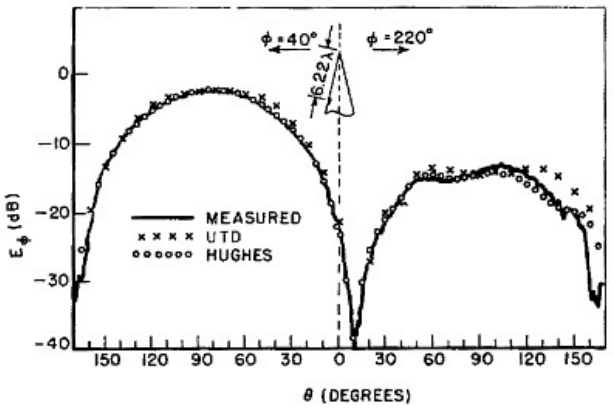

Fig. 9. $|E_\phi|$ radiation pattern of a radial slot in a cone (see cone geometry in Fig. 10).

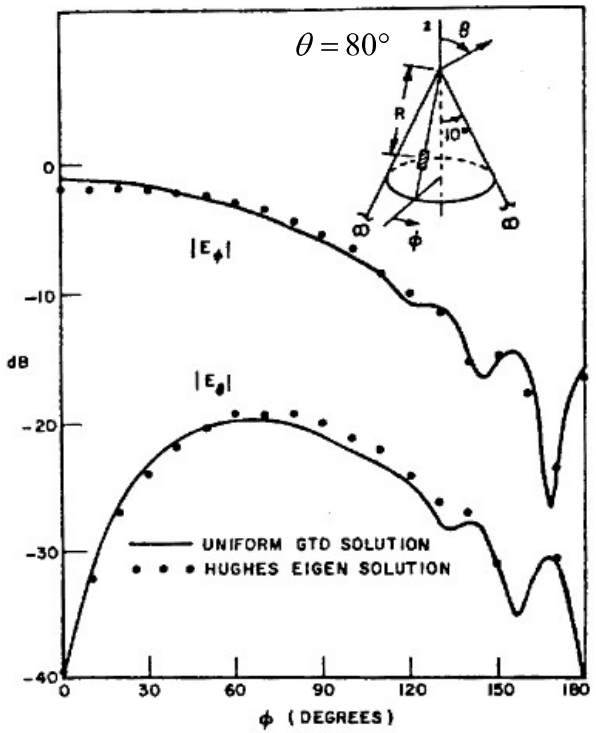

Fig. 10. Radiation patterns of a radial slot in a cone.

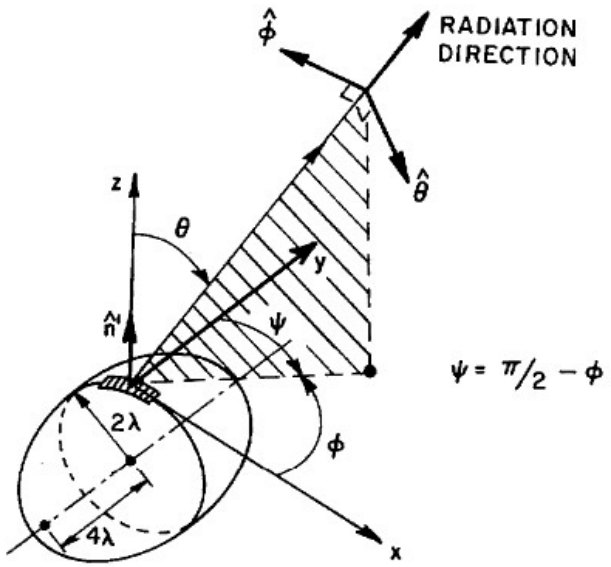

Fig. 11. Prolate spheroidal geometry.

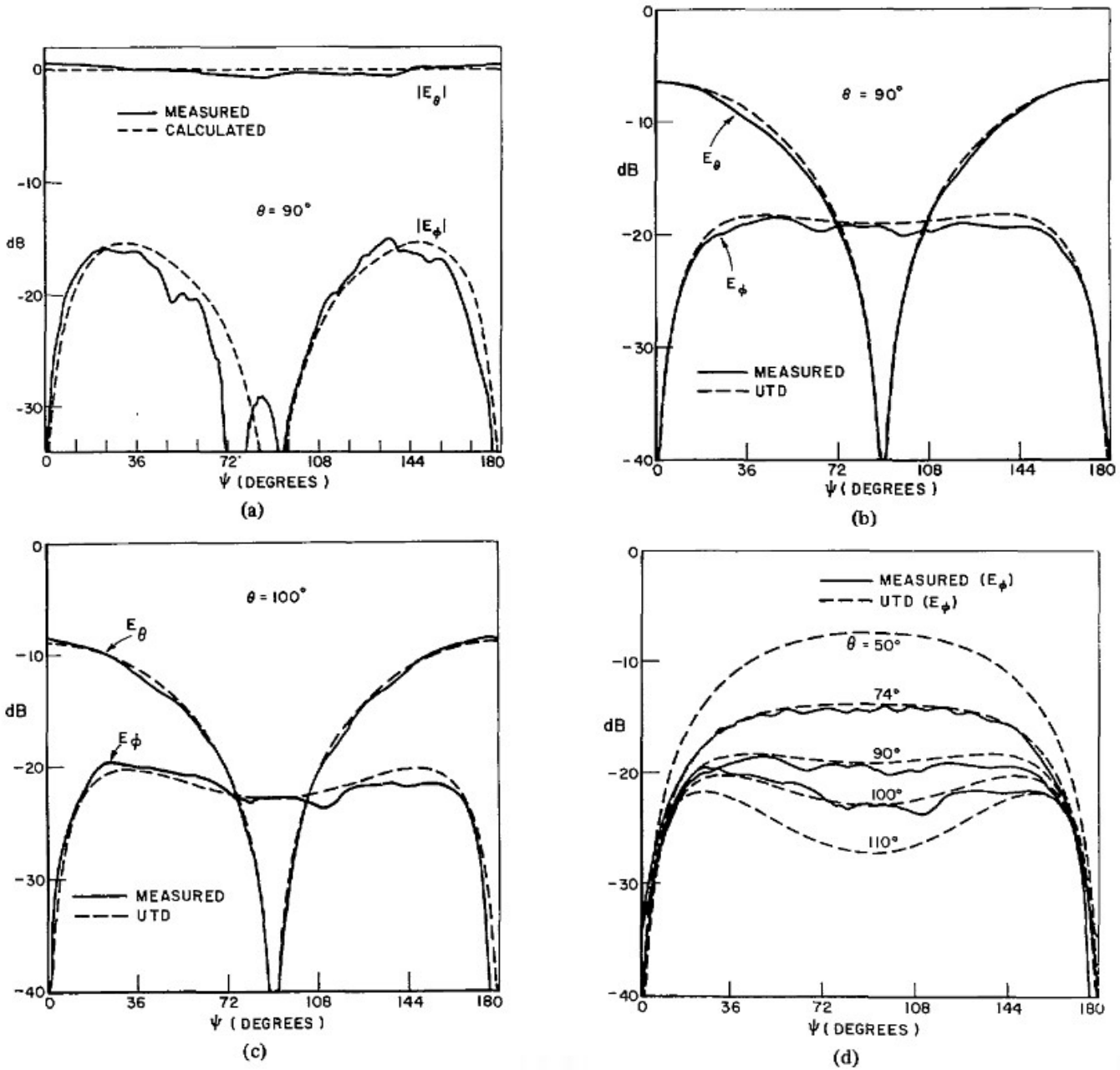

Fig. 12. Radiation patterns of antennas on a prolate spheroid. (a) Pertains to the pattern of a $\hat{n}'$ directed monopole antenna (at the source location in Fig. 11) (b), (c), and (d) Pertains to the patterns of an $\hat{x}$-directed rectangular slot (at the source location in Fig. 11) on a spheroid.

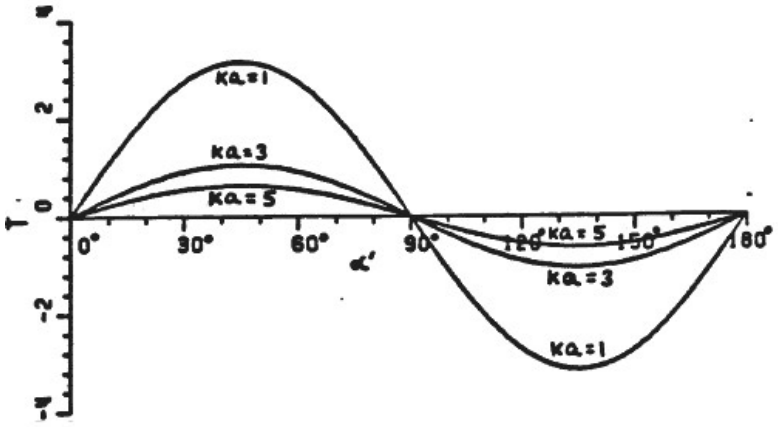

T(Q') as a function of a' for a circular cylinder

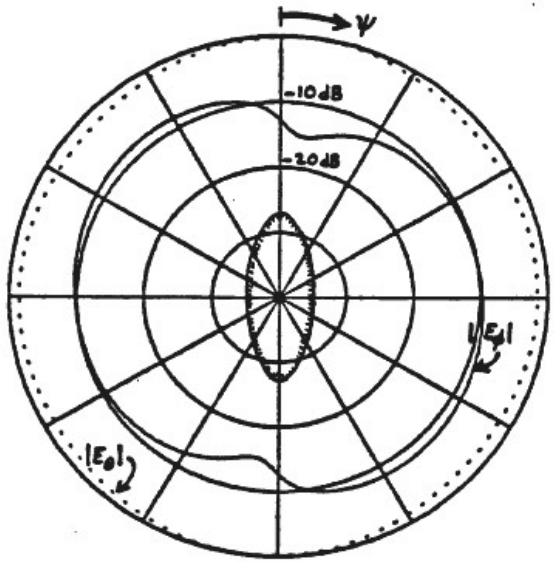

Radiation patterns of a Lindberg crossed slot antenna (phased 90° apart) on a prolate spheroid. $\theta = 75°$

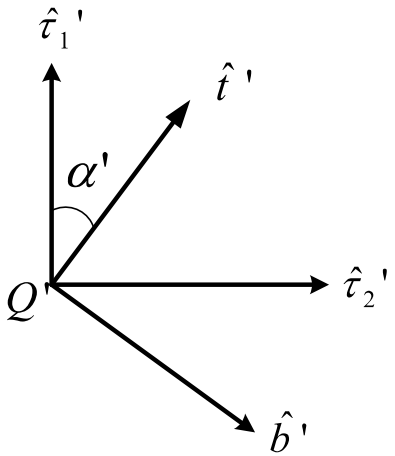

$\hat{\tau}_1'$ and $\hat{\tau}_2'$ denote principal surface directions at Q'.

R_1 and R_2 are principal radii of curvature.

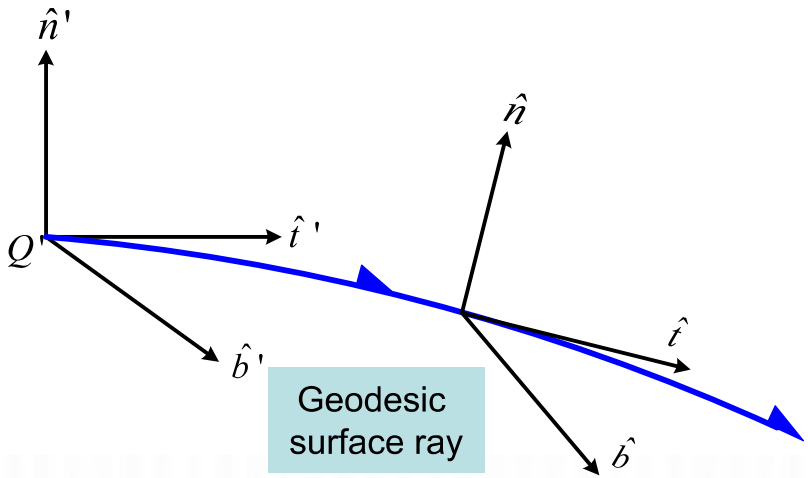

$$T_g(Q') = T(Q')\rho_g(Q'); \qquad T = \text{Torsion}$$

$$T(Q') = \frac{\sin 2\alpha'}{2}\left(\frac{1}{R_2} - \frac{1}{R_1}\right) \quad ; R_2 \le R_1 \text{ at } Q'$$

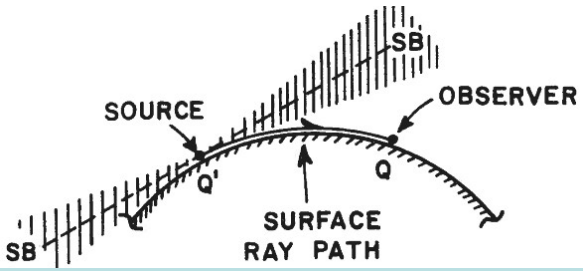

[1] P.H Pathak and N. Wang,"Ray analysis of mutual coupling between antennas on a convex surface," *IEEE Trans Ant and Propa*. Vol 29 Nov 1981.

(Alt. Soln. by S.W. Lee in IEEE AP-S)

$$\left\{ \begin{matrix} \overline{E}(Q) \\ \overline{H}(Q) \end{matrix} \right\} \sim \left\{ \begin{matrix} \overline{\overline{\Gamma}}_{ee}(Q|Q') \\ \overline{\overline{\Gamma}}_{he}(Q|Q') \end{matrix} \right\} \cdot \hat{n}' \int_0^h I(l')dl' , \qquad \text{for a monopole}$$

$$\left\{ \begin{matrix} \overline{E}(Q) \\ \overline{H}(Q) \end{matrix} \right\} \sim \int\int_{Sa} \left\{ \begin{matrix} \overline{\overline{\Gamma}}_{eh}(Q|Q') \\ \overline{\overline{\Gamma}}_{hh}(Q|Q') \end{matrix} \right\} \cdot [\overline{E}_a(Q') \times \hat{n}']ds' , \qquad \text{for a slot antenna}$$

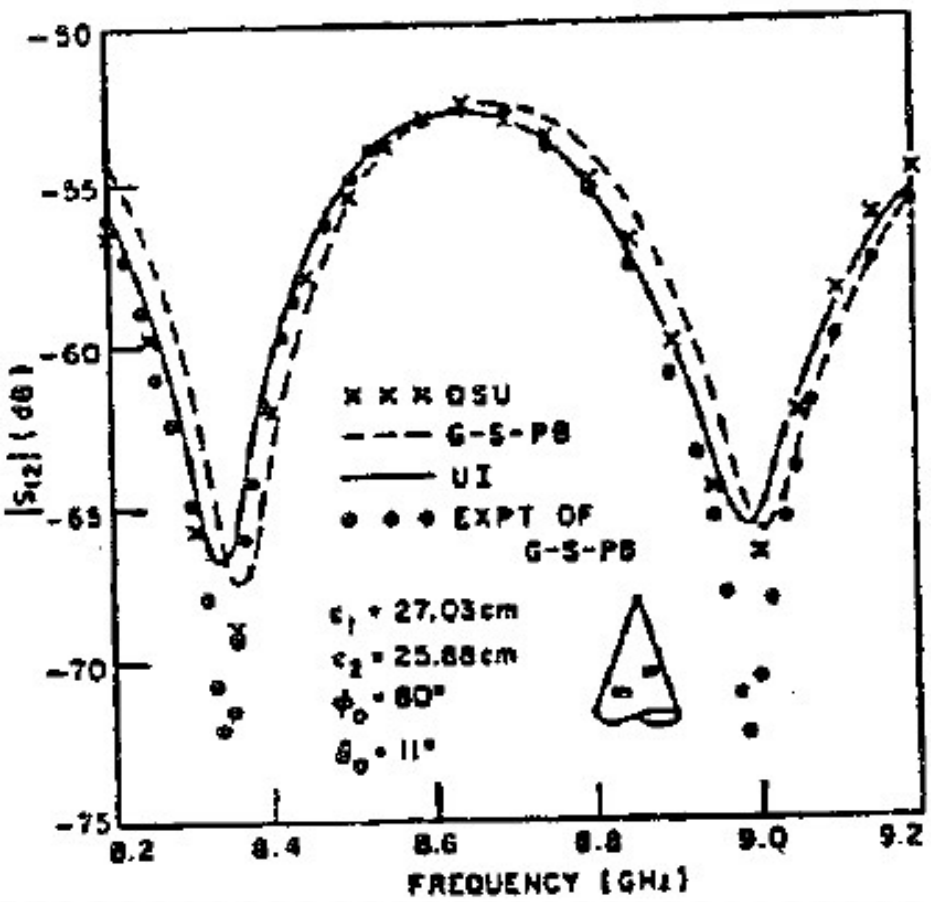

$\overline{\overline{\Gamma}}_{ee}, \overline{\overline{\Gamma}}_{he}, \overline{\overline{\Gamma}}_{eh}$ and $\overline{\overline{\Gamma}}_{hh}$ **contain the UTD transition functions corresponding to surface Fock fcns.**

$$\tilde{U}(\xi) = \left[\frac{kt}{2m(Q')m(Q)\xi}\right]^{3/2} \cdot \frac{\xi^{3/2}e^{j(3\pi/4)}}{2\sqrt{\pi}} \cdot \int_{\infty e^{-j(2\pi/3)}}^{\infty} d\tau e^{-j\xi\tau} \frac{W_2'(\tau)}{W_2(\tau)}$$

$$\tilde{V}(\xi) = \left[\frac{kt}{2m(Q')m(Q)\xi}\right]^{1/2} \cdot \frac{\xi^{1/2}e^{j\pi/4}}{2\sqrt{\pi}} \int_{\infty e^{-j(2\pi/3)}}^{\infty} d\tau e^{-j\xi\tau} \frac{W_2(\tau)}{W_2'(\tau)}.$$

C. L. Yu, W. D. Burnside, and M. C. Gilreath, "Volumetric pattern analysis of airborne antennas," *IEEE Trans. AP*, Sep. 1978.

Modeling of Boeing 737 aircraft

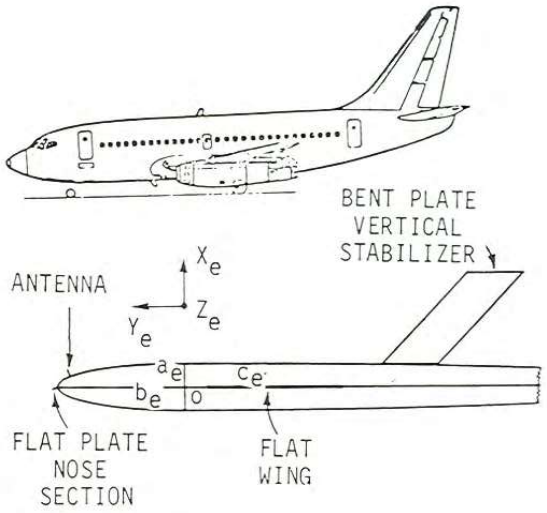

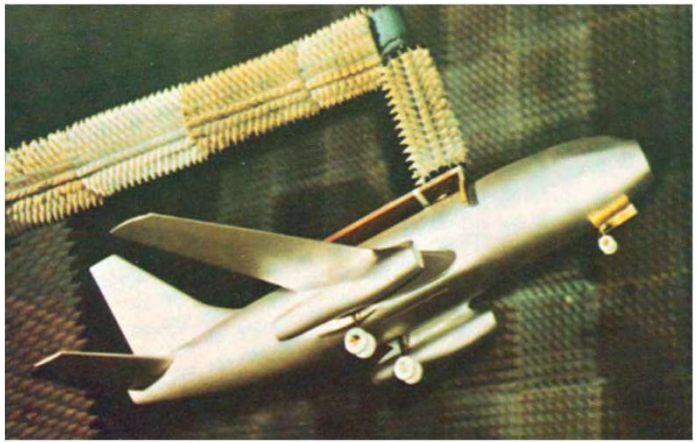

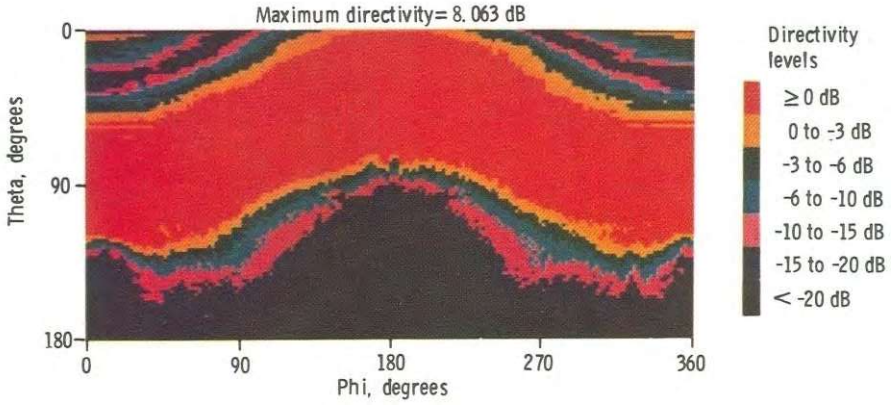

Measured

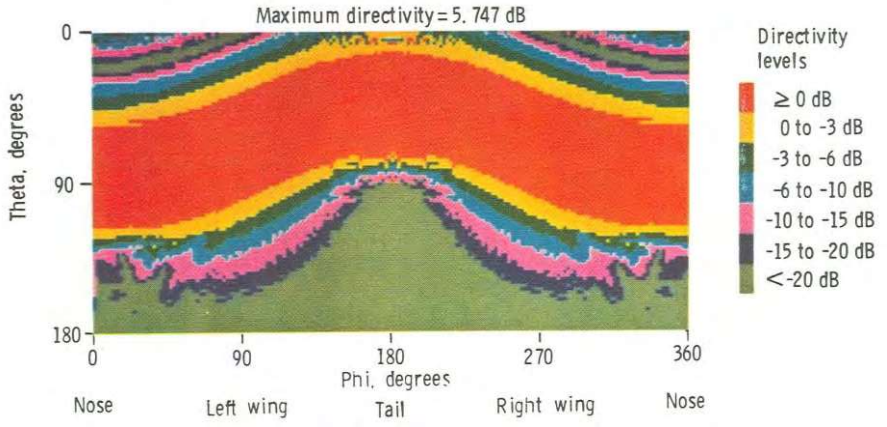

Calculated

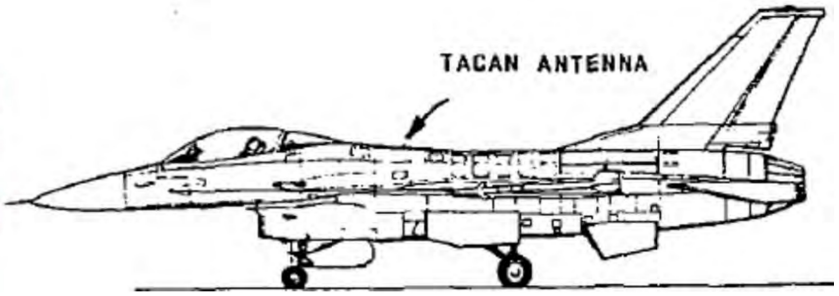

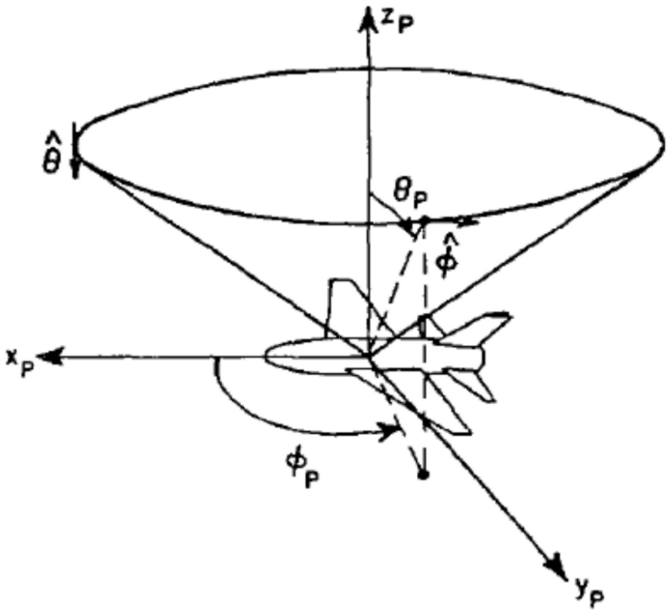

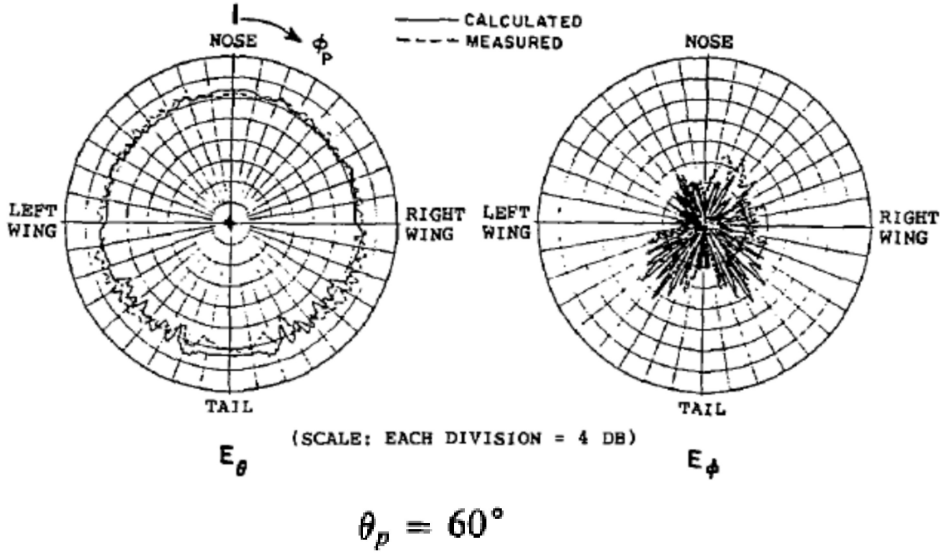

$\theta_p = 60°$

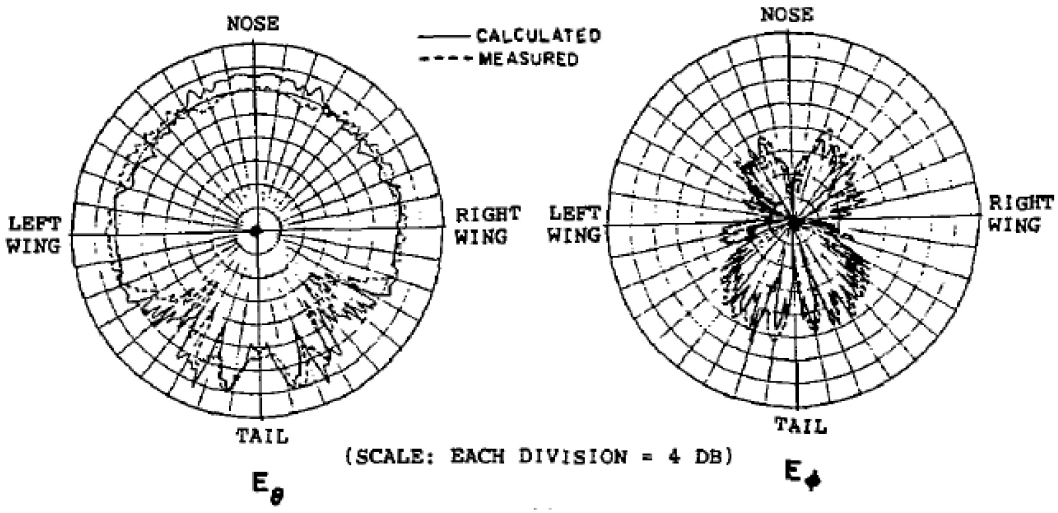

$\theta_p = 80°$

• J. J. Kim and W. D. Burnside, “Simulation and Analysis of Antennas Radiating in a Complex Environment”, IEEE Trans. AP, April 1986.

Comparison of Measured (NRL) and Calculated (NEC-BSC) Antenna Isolation with Receiver Moving above Center of Fuselage

wings not present
includes double diffraction
Computed by Dr. R. J. Marhefka at OSU-ESL. This work was supported by **Gary Roan at NRL**

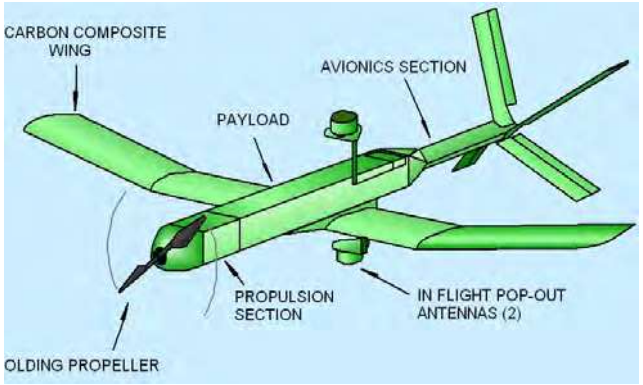

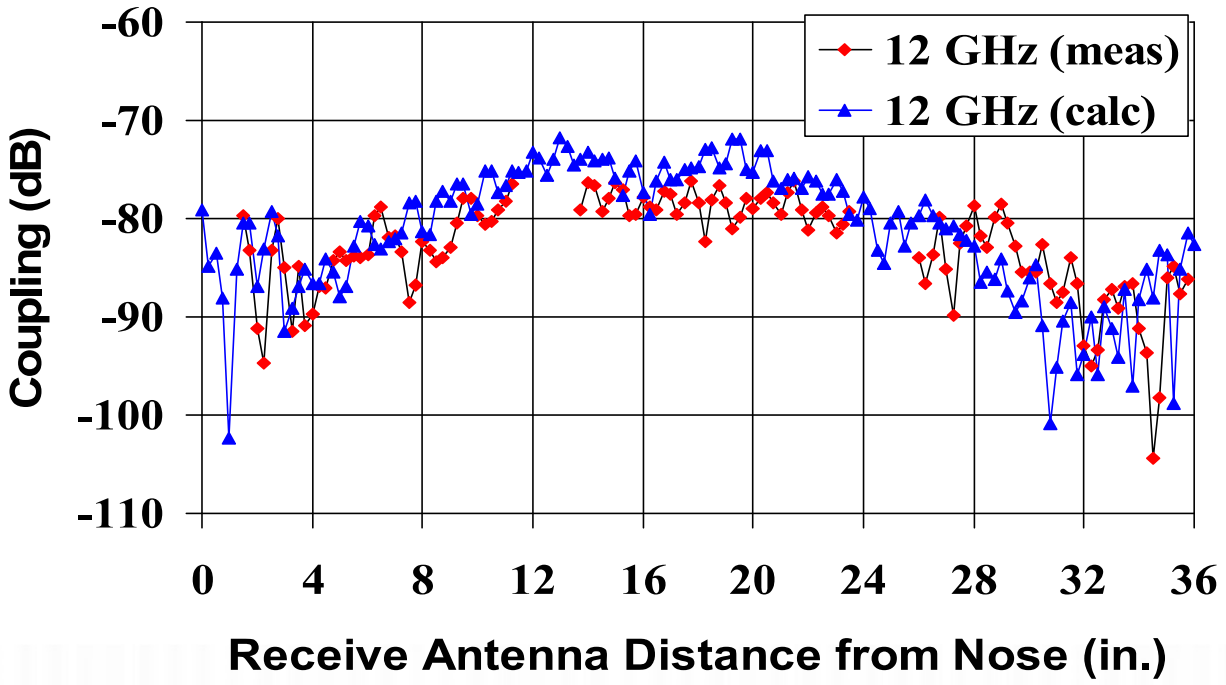

Limitations of Existing UTD Codes

- Existing UTD codes such as NEC-BSC and NEW-AIR have proven to be successful over the past two decades.
- However, these codes are based on the approximation of the electrically large airborne platform in terms of canonical shapes, which is a complicated task.
- Moreover, a canonical shape representation may lead to inaccuracies.
- Very limited capability to analyze material coatings

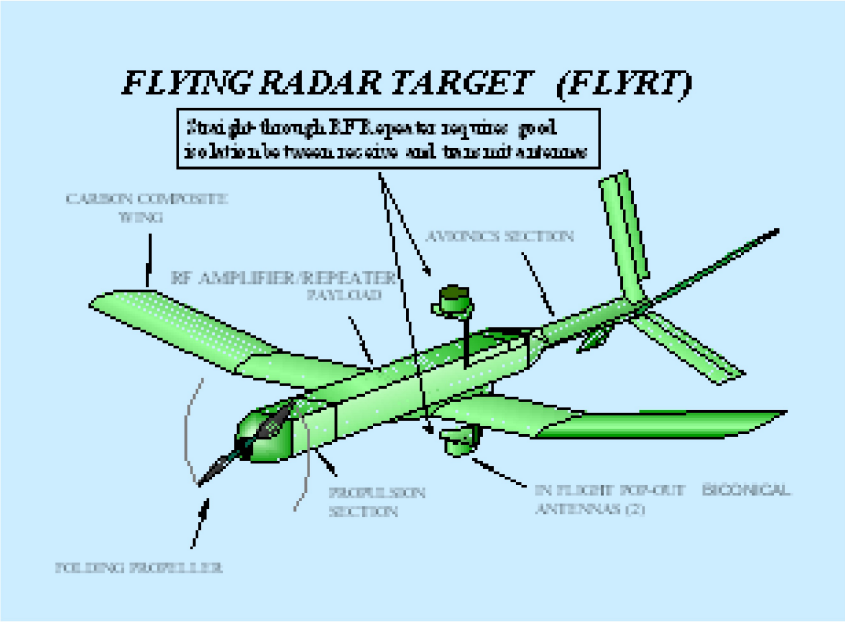

Canonical representation for NEC-BSC

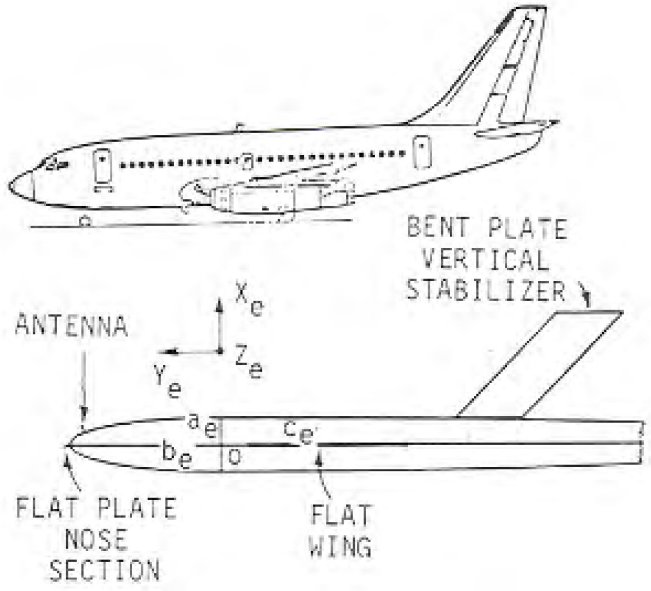

Canonical representation for NEW-AIR

New UTD code development

•Radiating object modeled with better fidelity via facets based on CAD geometry data.

•UTD rays tracked in presence of facets. UTD ray parameters obtained by mapping facets back to the original geometry (via bi-quadratic surfaces or splines, etc).

•Does not require an expert user.

•Will eventually incorporate thin material coating on metallic (or PEC) platform.

ElectroScience LABORATORY

New code (Applied EM)

Quarter wavelength monopole on a KC-130 at 500 MHz ($18.3\lambda_0$ height, $69.2\lambda_0$ wingspan, $49.7\lambda_0$ length at 500 MHz).

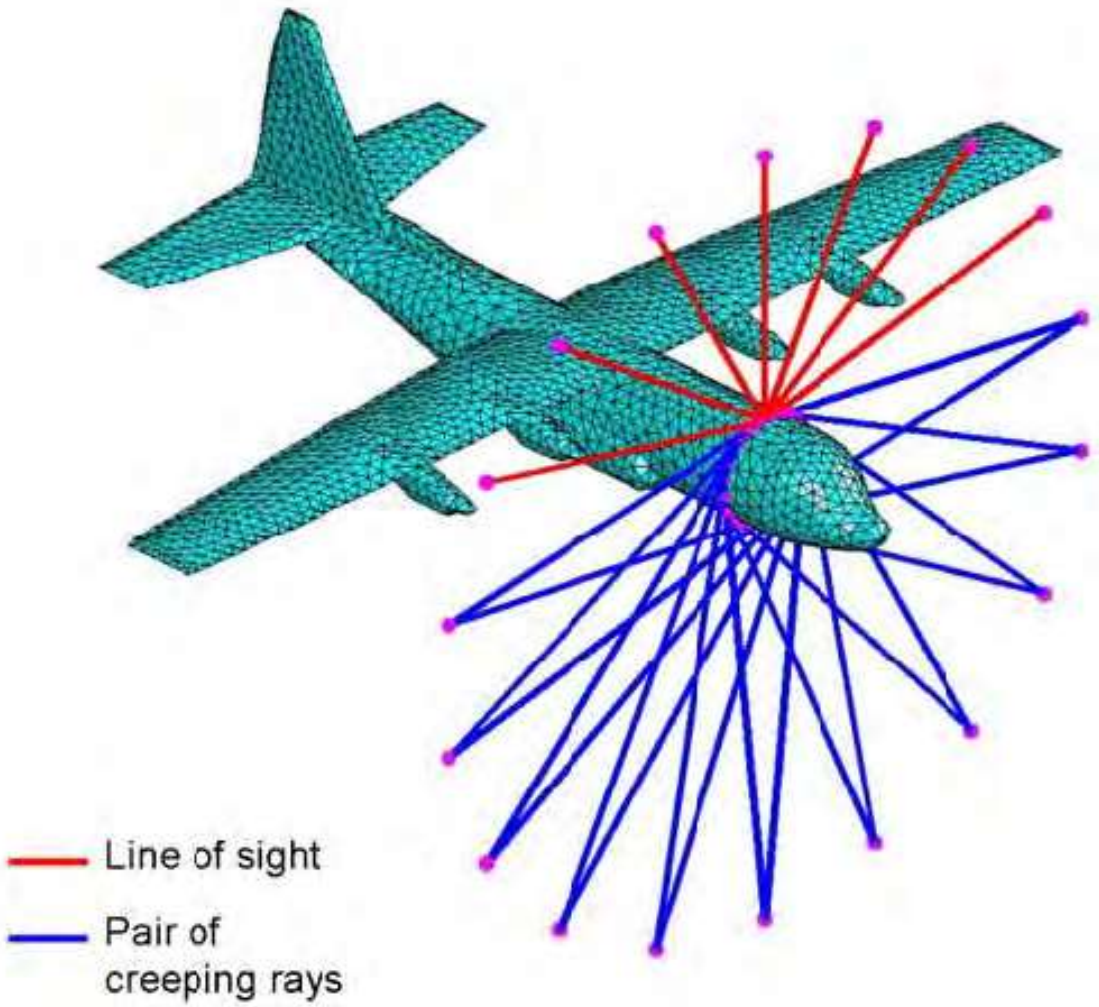

ElectroScience LABORATORY

Preliminary Validation

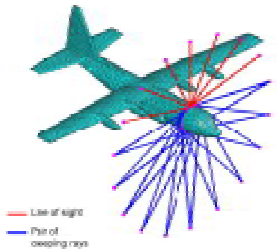

Quarter wavelength monopole on a KC-130 at 500 MHz
($18.3\lambda_0$ height, $69.2\lambda_0$ wingspan, $49.7\lambda_0$ length at 500 MHz).

Near Field

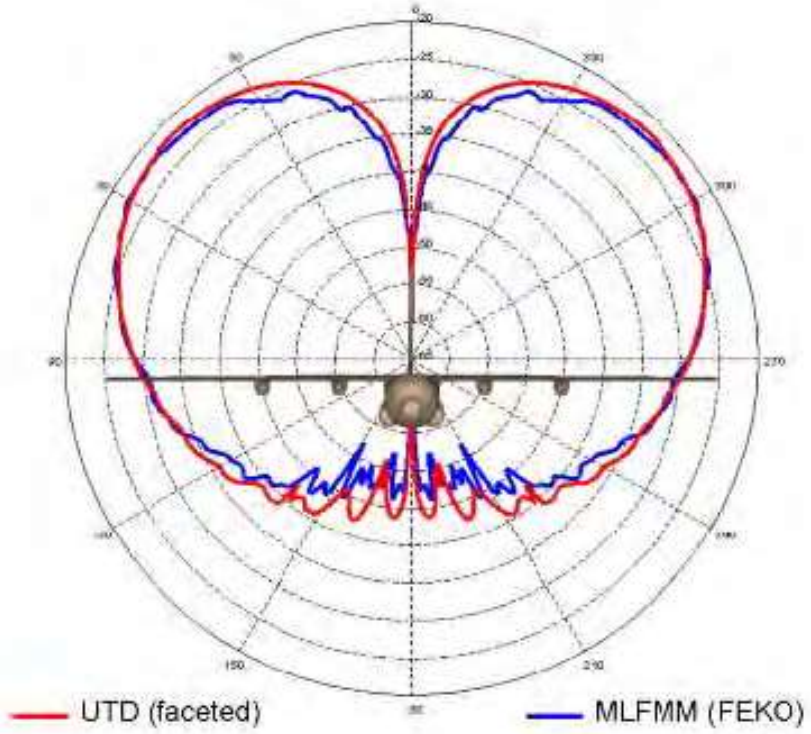

Far Field

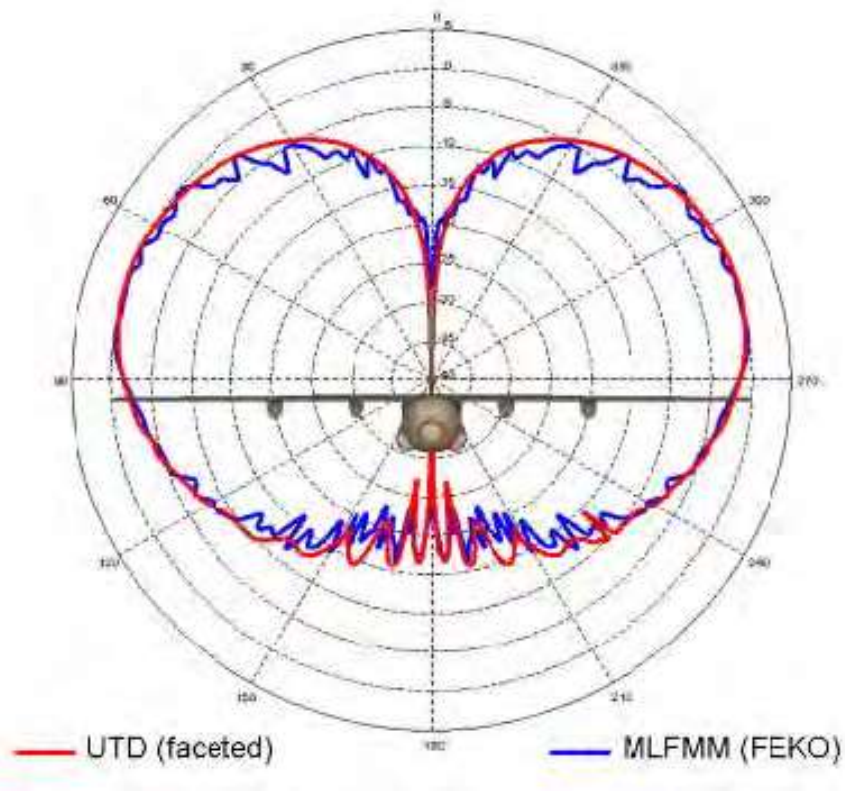

Mesh Geometry	Frequency (GHz)	# of facets for UTD	CPU time for UTD	# of facets for MLFMM	CPU time for MLFMM
KC-135	0.500	6,496	3.57 sec	420,466	1 h 28 min

Monopole under a C-130 Aircraft

Monopole under the fuselage:

- **Frequency: 500 MHz.**
- **Monopole size: $\lambda_0/4$.**
- **Height: $18.3\lambda_0$.**
- **Wingspan: $69.2\lambda_0$.**
- **Length: $49.7\lambda_0$.**

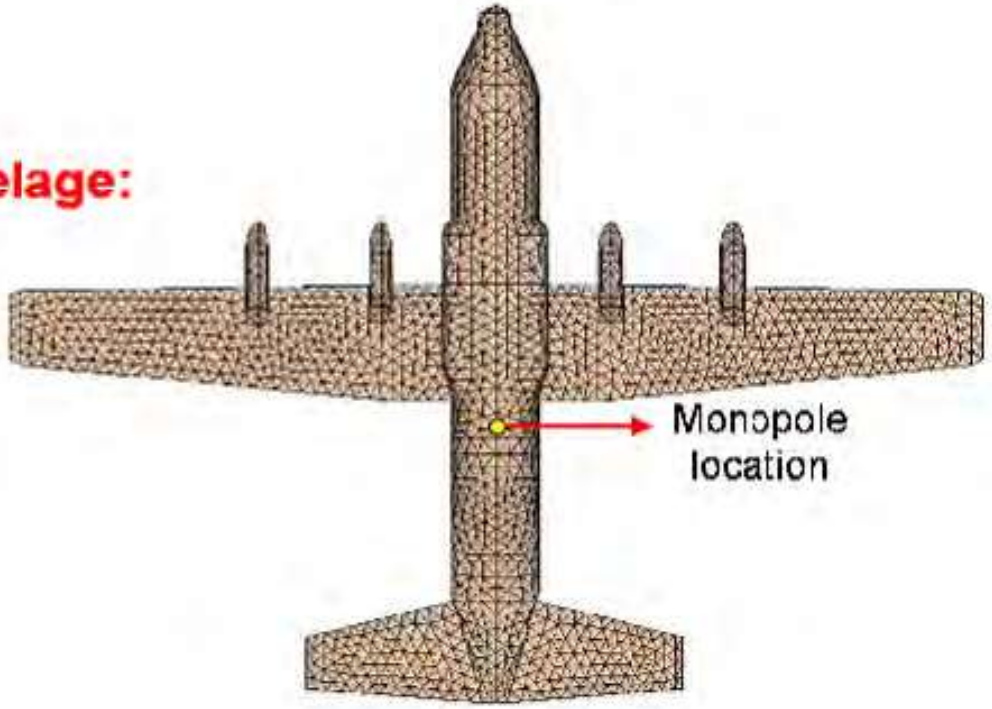

Near Field Ray Interactions

Front view

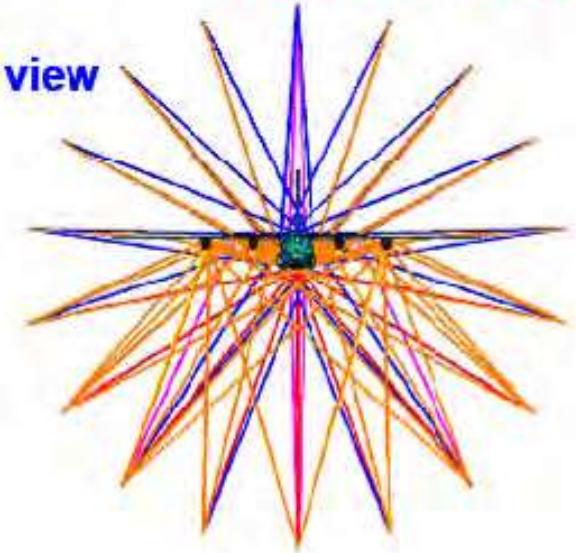

Side view

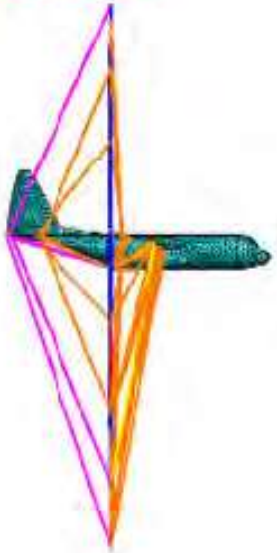

Top view

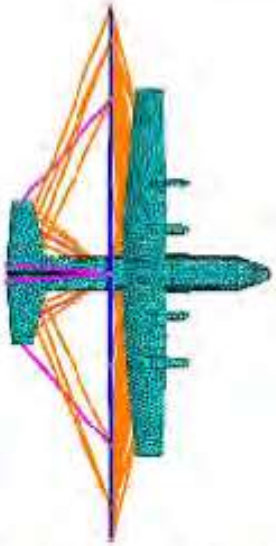

Bottom view

Preliminary Validation

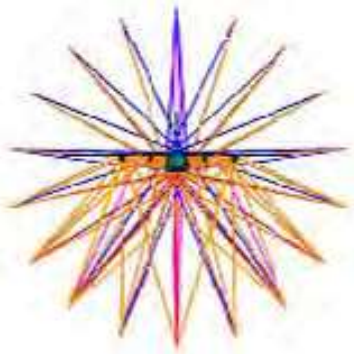

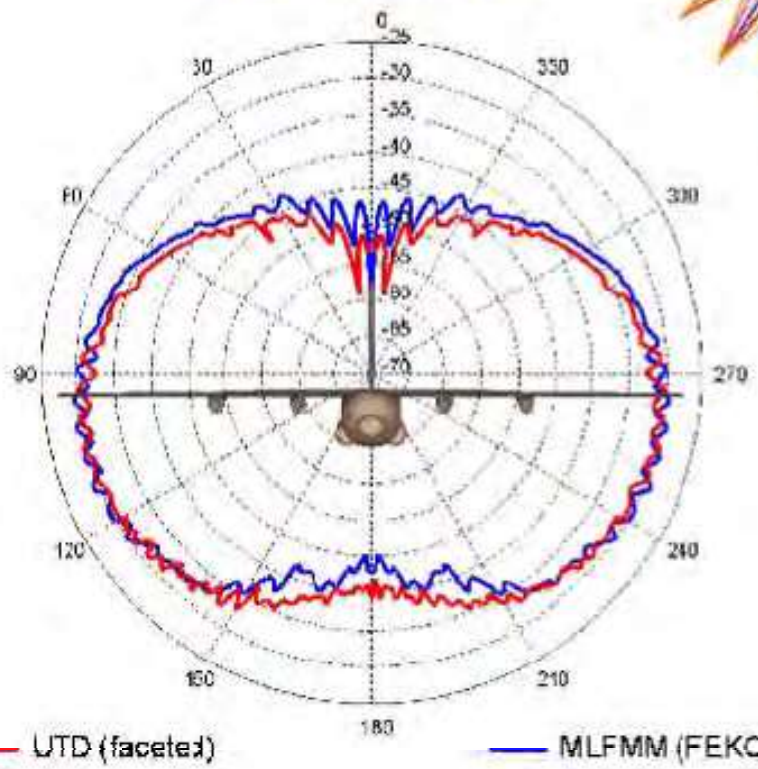

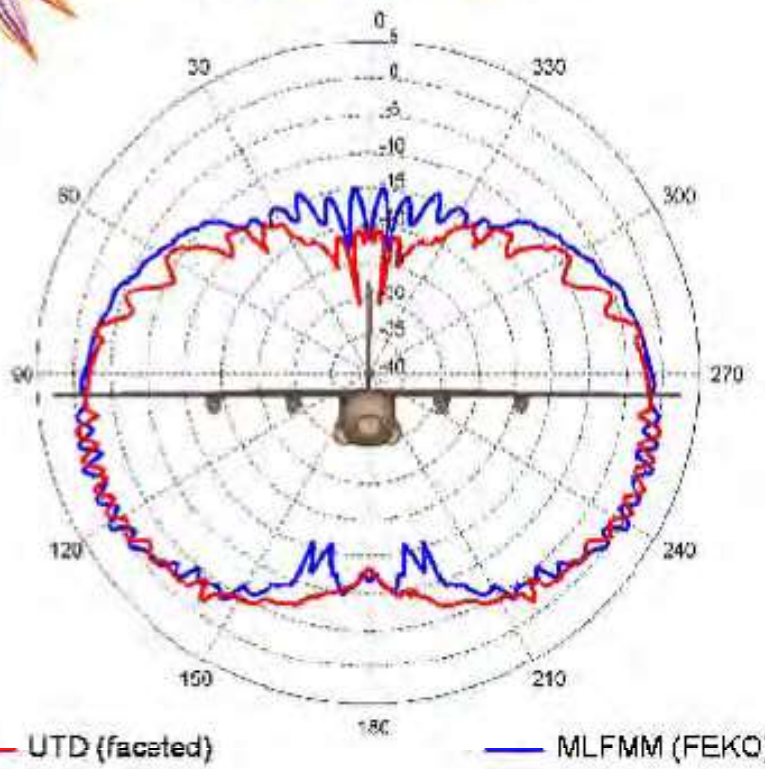

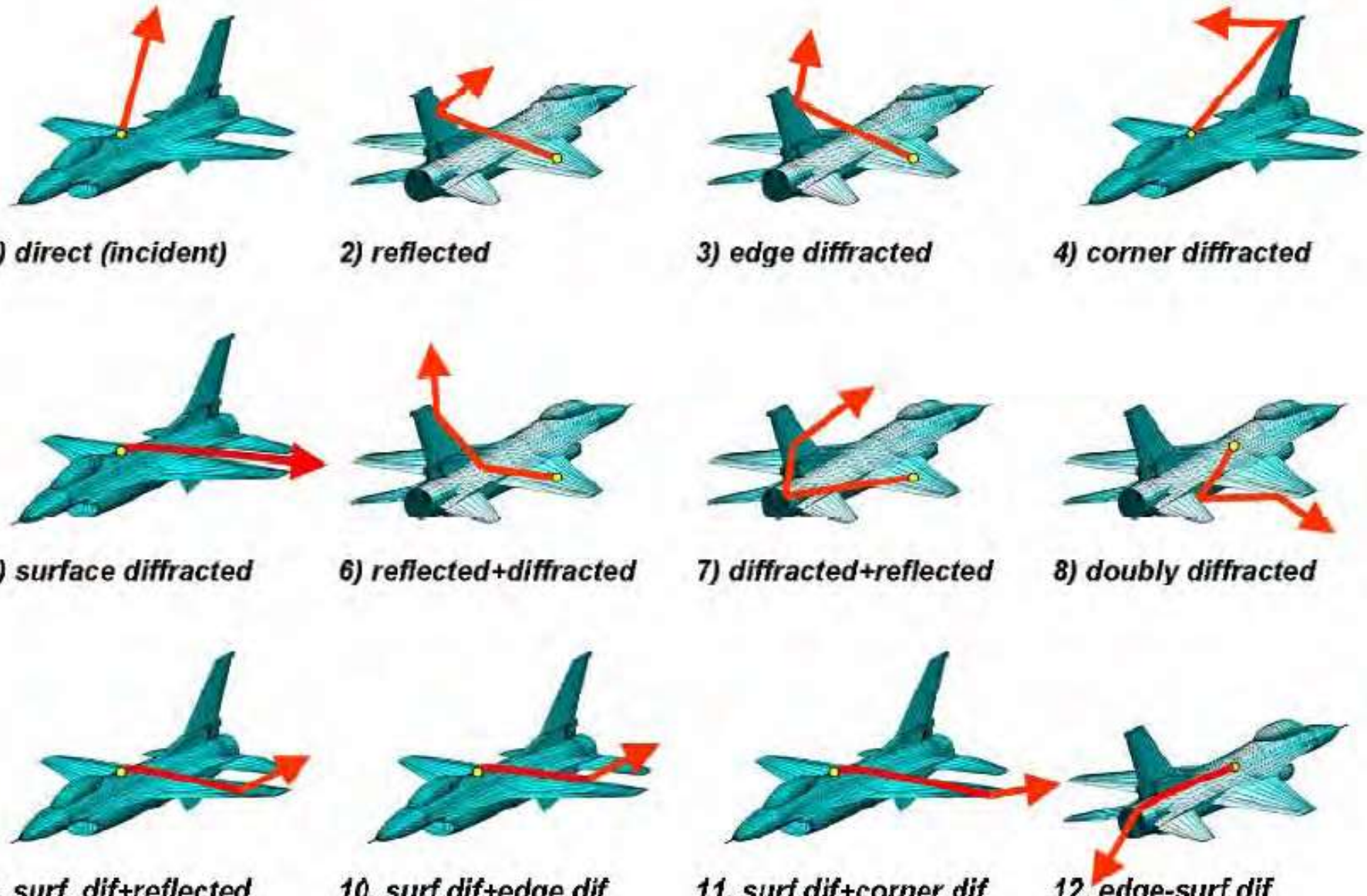

ElectroScience LABORATORY

New UTD analytical development

ElectroScience LABORATORY

- UTD + slope for PEC planar faced wedges with thin material coating in form useful and accurate for engineering applications.
- UTD + slope for curved PEC wedges with thin material coating.
- UTD for PEC corners in curved edges and surfaces with thin material coating.
- UTD for PEC edge excited surface (or creeping) rays (and its reciprocal problem) in a form useful for engineering applications.

Previous Work on Thin Material Coated Metallic Wedge Structures

- Material coatings are generally replaced by approximate boundary conditions (e.g. Impedance Boundary Condition [IBC])
- Solutions to canonical problems with "approx." boundary conditions formulated exactly via Wiener-Hopf (W-H) or Maliuzhinets (MZ) methods for surfaces made up of planar structures. Ray solutions extracted analytically from them via asymptotic procedures.
- W-H method:
  - J. L. Volakis and T. B. A. Senior, "Diffraction by a Thin Dielectric Half-Plane", IEEE Trans. AP, Dec.1987
  - R. G. Rojas, "Wiener-Hopf Analysis of the EM Diffraction by an Impedance Discontinuity in a Planar Surface and by an Impedance Half-Plane", IEEE Trans. AP, Jan. 1988.
  - R. G. Rojas and P. H. Pathak, "Diffraction of EM Waves by a Dielectric/Ferrite Half-Plane and Related Configurations", IEEE Trans. AP, June 1989.
  - J. L. Volakis and T. B. A. Senior, "Application of a Class of Generalized Boundary Conditions to Scattering by a Metal-Backed Dielectric Half Plane", Proc. IEEE, May 1989.
  - V. G. Daniele and G. Lombardi, "Wiener-Hopf Solution for Impedance Wedges at Skew Incidence", IEEE Trans. AP, Sep. 2006 .
- MZ method:
  - G. D. Maliuzhinets, "Excitation, Reflection and Emission of Surface Waves from a Wedge with Given Face Impedance", Sov. Phys.-Dokl., 1958.
  - R. G. Rojas, "Electromagnetic Diffraction of an Obliquely Incident Plane Wave Field by a Wedge with Impedance Faces", IEEE AP, July 1988.
  - R. Tiberio and G. Pelosi and G. Manara and P. H. Pathak, "High-Frequency Scattering from a Wedge with Impedance Faces Illuminating by a Line Source, Part I: Diffraction", IEEE Trans. AP, Feb. 1989, see also IEEE Trans. AP, July 1993.
  - M. A. Lyalinov and N.Y. Zhu, "Diffraction of a Skew Incident Plane Electromagnetic Wave by an Impedance Wedge", Wave Motion, 2006.
- Approx. skew incidence solution (MZ) for imp. wedges based on modifying the HP solution:
  - H. Syed and J. L. Volakis, "Skew incidence diffraction by an impedance wedge with arbitrary face impedances", Electromagnetics, Vol. 15, No.3, 1995.

An Approximate UTD Ray Solution for Skew Incidence Diffraction by Material Coated Wedges of Arbitrary Angle

T Lertwiriyaprapa, P. H. Pathak and J. L. Volakis

ElectroScience Laboratory

Department of Electrical and Computer Engineering

The Ohio State University

URSI, Chicago 2008

- **Present solution based on spectral synthesis.**
- **Solution useful and accurate for engineering applications.**

Numerical Results

(3-D Junction Planar Material Slabs on a PEC Ground Plane)

•Comparison of UTD-MZ, UTD and MZ at $r=5\lambda$, $\phi'=45°$, $\beta'0=65°$, $\tau=\lambda/20$, $\varepsilon r0=2$, $\mu r0=4$, $\varepsilon rn=5$, and $\mu rn=1$.

• MZ is R. G. Rojas, "Electromagnetic Diffraction of an Obliquely Incident Plane Wave Field by a Wedge with Impedance Faces", IEEE AP, July 1988.

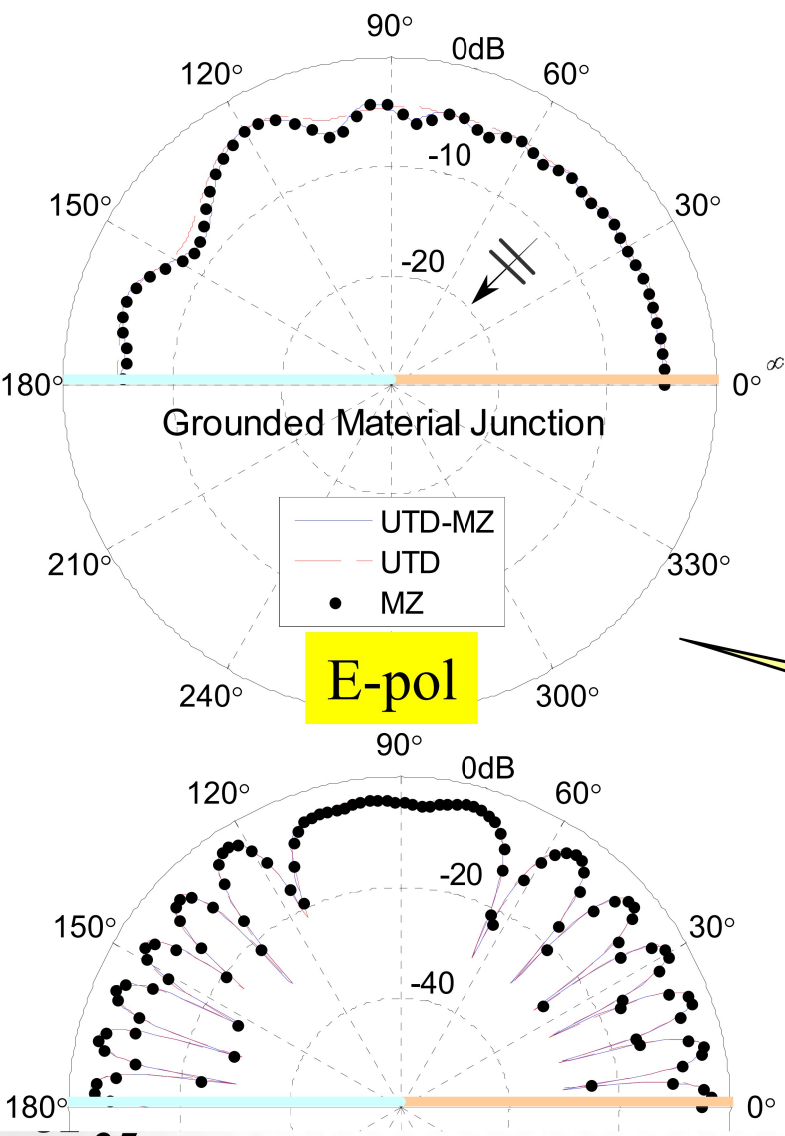

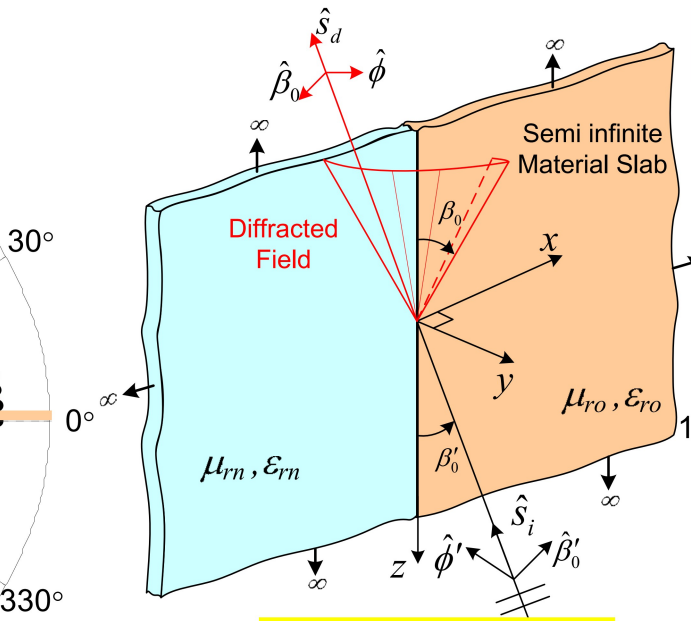

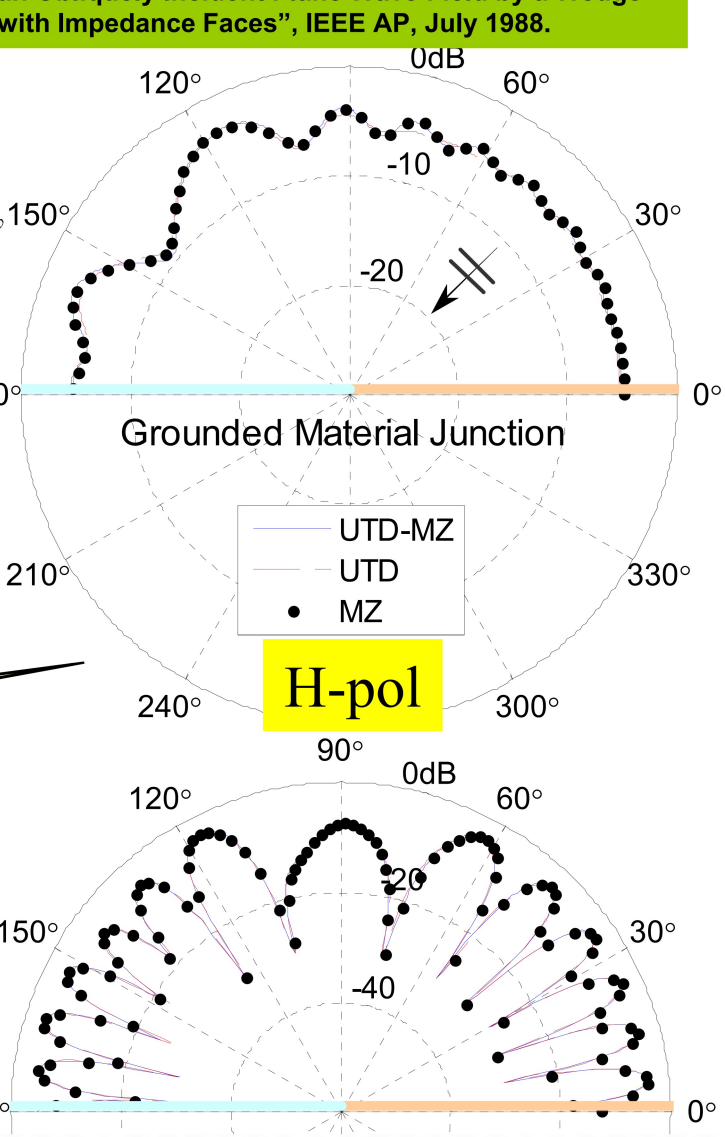

Scatt. Field

Total Field

Numerical Results

(3-D Material Coated PEC Right-Angled Wedge)

•Comparison of UTD-MZ and MZ at $r=10\lambda$, $\phi'=45°$, $\beta'o=65°$, $\tau=\lambda/20$, $\varepsilon rn=2$, and $\mu rn=5$.

• MZ is R. G. Rojas, "Electromagnetic Diffraction of an Obliquely Incident Plane Wave Field by a Wedge with Impedance Faces", IEEE AP, July 1988.

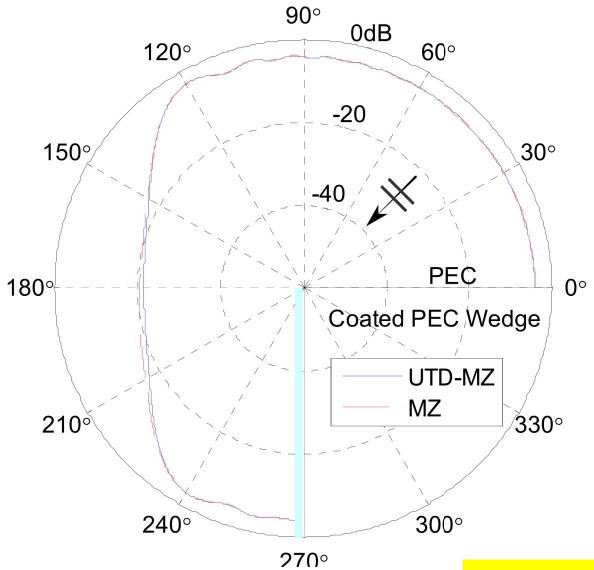

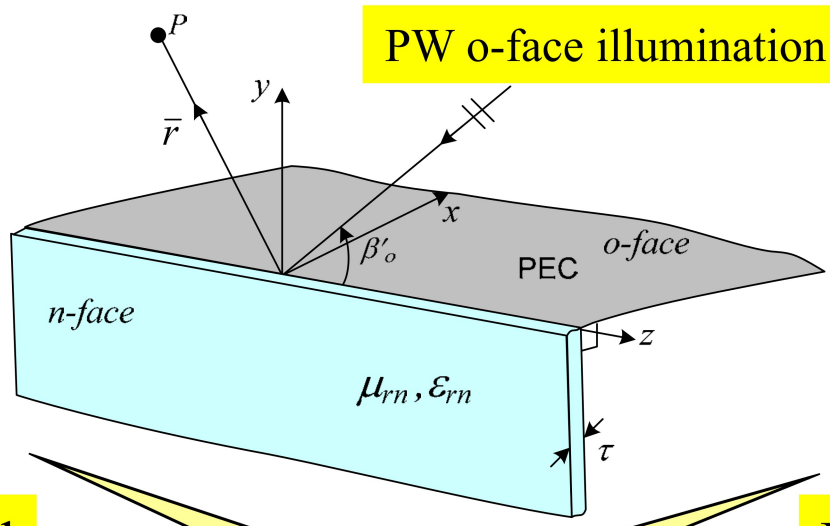

PW o-face illumination

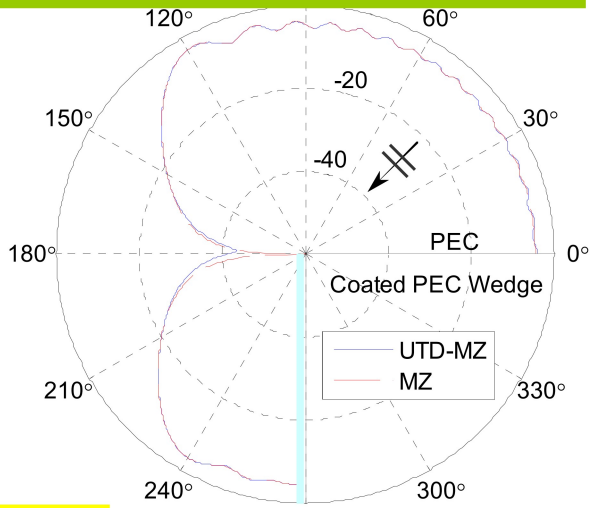

E-pol

H-pol

Scatt. Field

Total Field

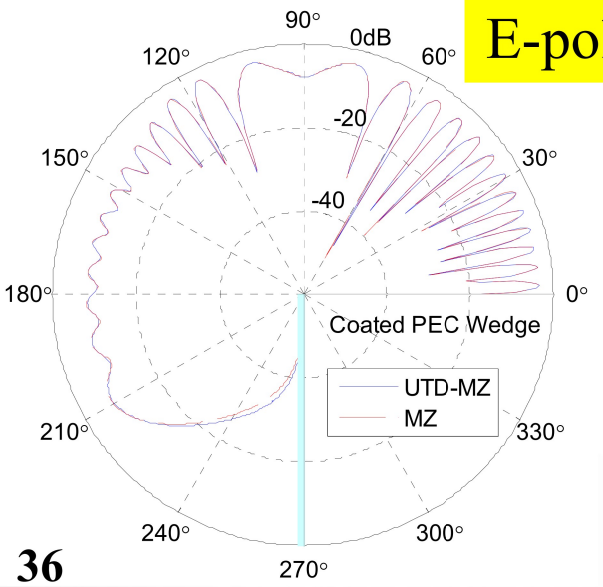

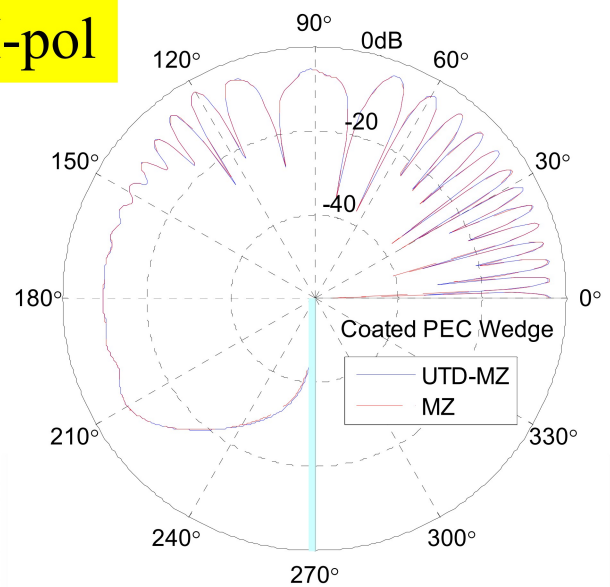

Numerical Results

(3-D Junction Planar Material Slabs on a PEC Ground Plane)

•Comparison of UTD-MZ and MZ at $r=10\lambda$, $\phi'=45°$, $\beta'0=65°$, $\tau=\lambda/20$, $\varepsilon r0=4$, $\mu r0=2$, $\varepsilon rn=2$, and $\mu rn=5$.

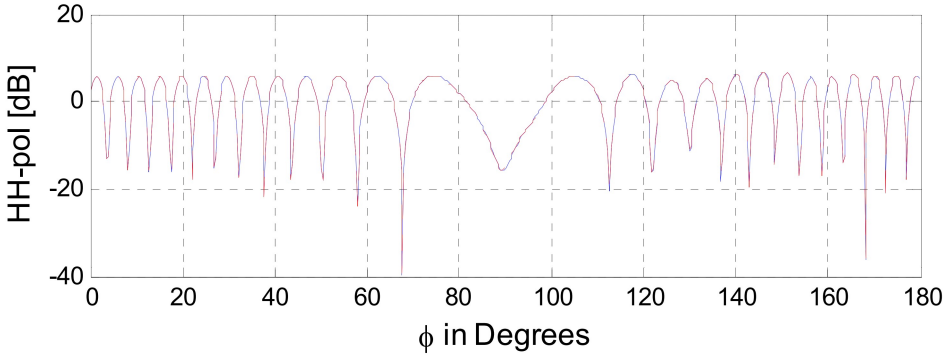

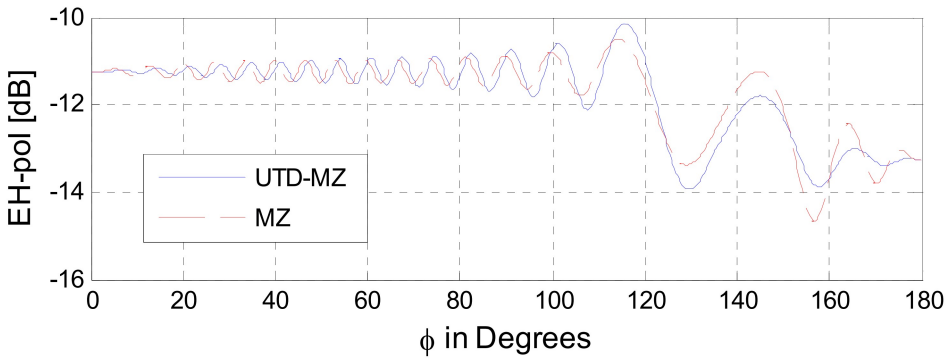

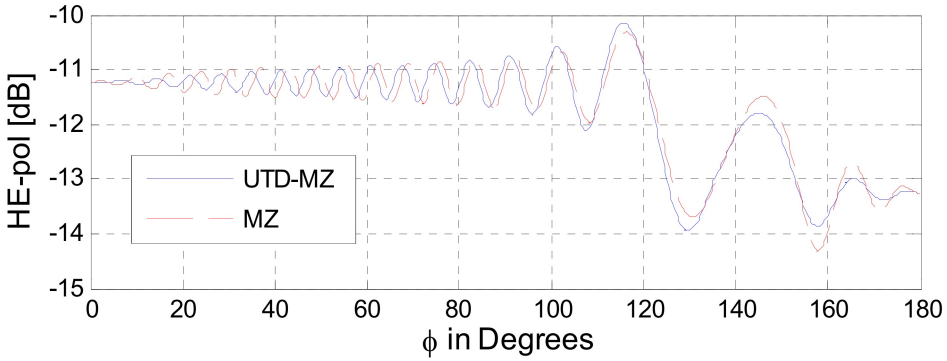

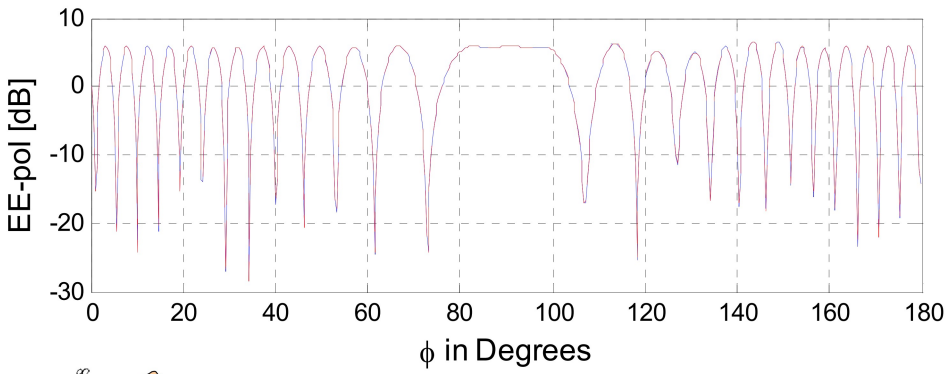

Total Field

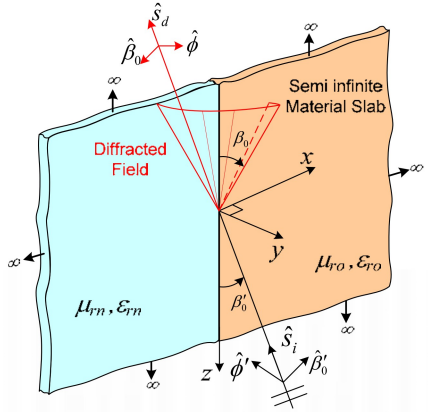

• MZ is R. G. Rojas, "Electromagnetic Diffraction of an Obliquely Incident Plane Wave Field by a Wedge with Impedance Faces", IEEE AP, July 1988.

Numerical Results

(3-D Material Coated PEC Half Plane)

- Comparison of UTD-MZ and MZ at $r=10\lambda$, $\phi'=45°$, $\beta'o=65°$, $\tau=\lambda/20$, $\varepsilon ro=4$, $\mu ro=2$, $\varepsilon rn=2$, and $\mu rn=5$.

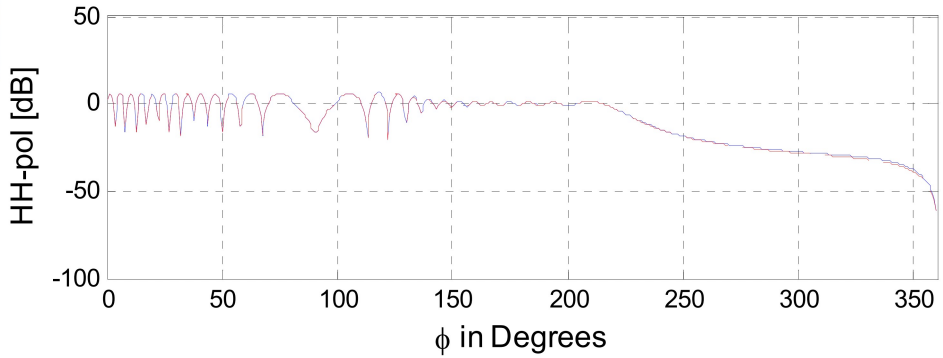

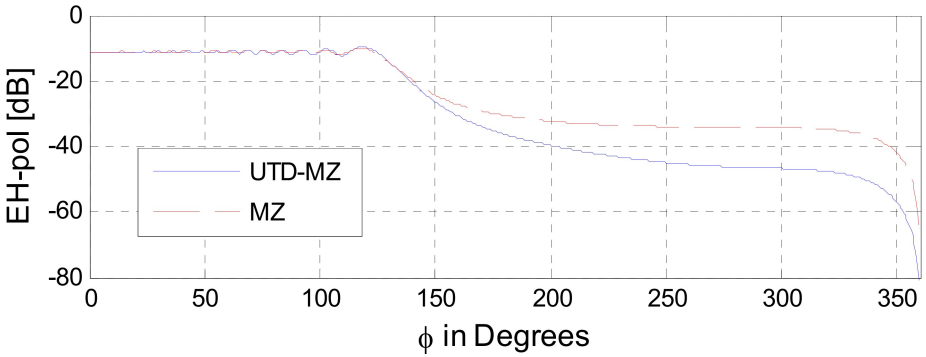

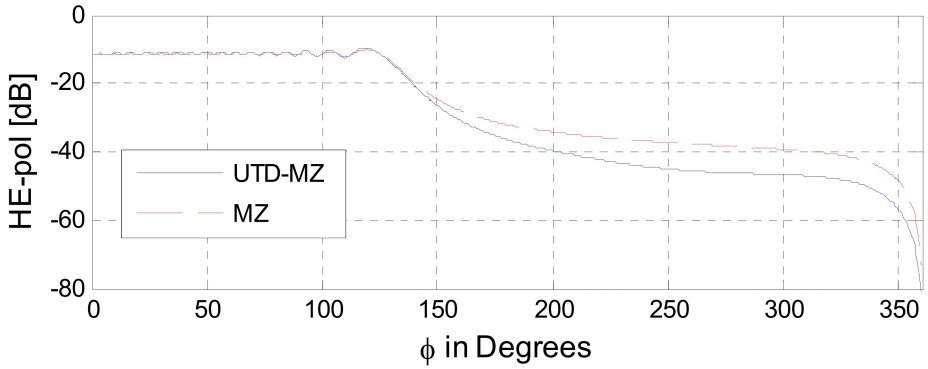

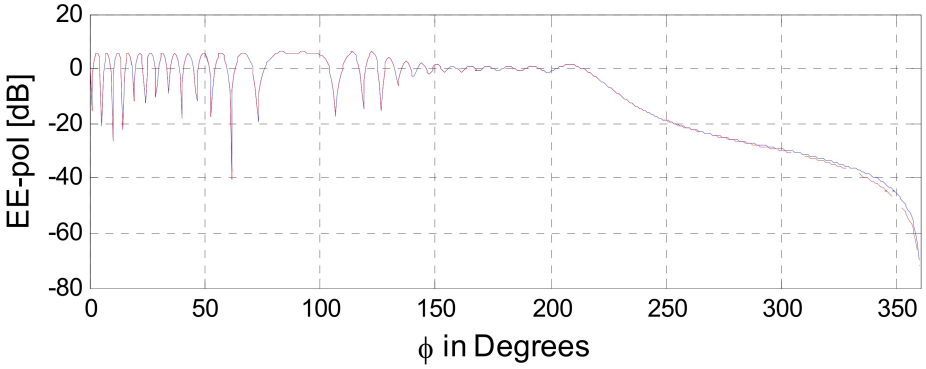

Total Field

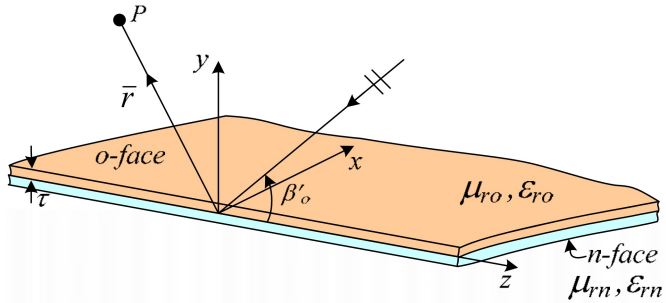

• MZ is R. G. Rojas, "Electromagnetic Diffraction of an Obliquely Incident Plane Wave Field by a Wedge with Impedance Faces", IEEE AP, July 1988.

Numerical Results

(3-D Material Coated PEC Right-Angled Wedge)

• Comparison of UTD-MZ and MZ at $r=10\lambda$, $\phi'=45°$, $\beta'o=65°$, $\tau=\lambda/20$, $\varepsilon ro=4$, $\mu ro=2$, $\varepsilon rn=2$, and $\mu rn=5$.

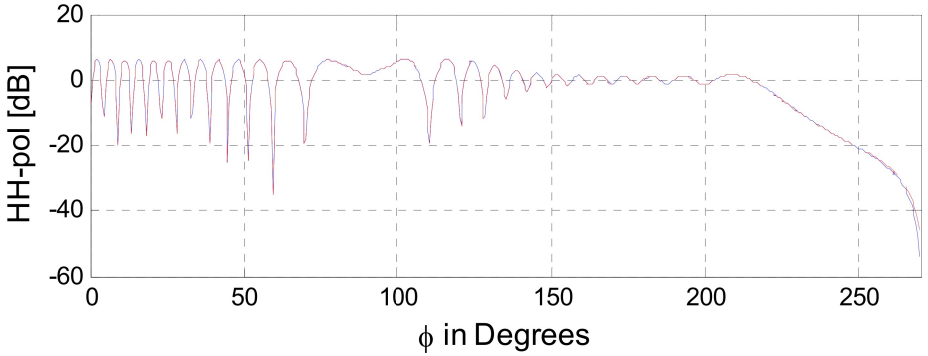

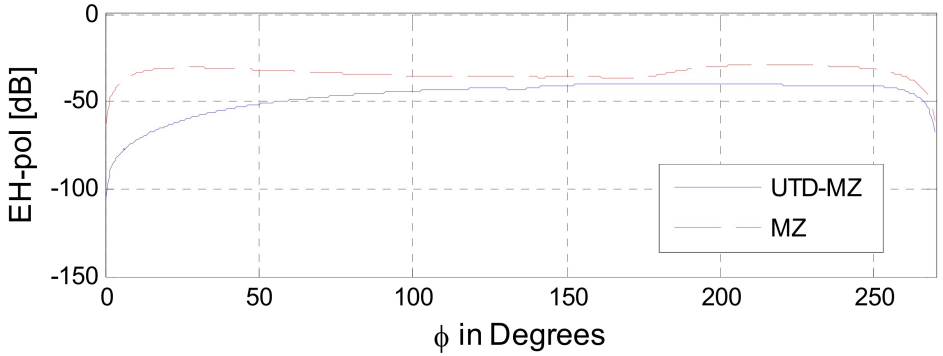

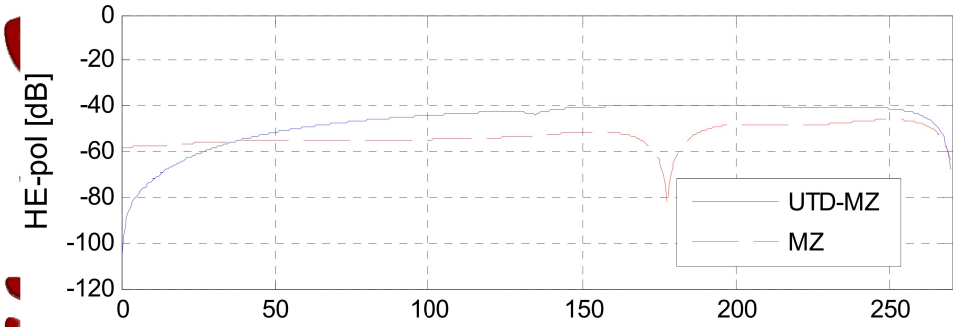

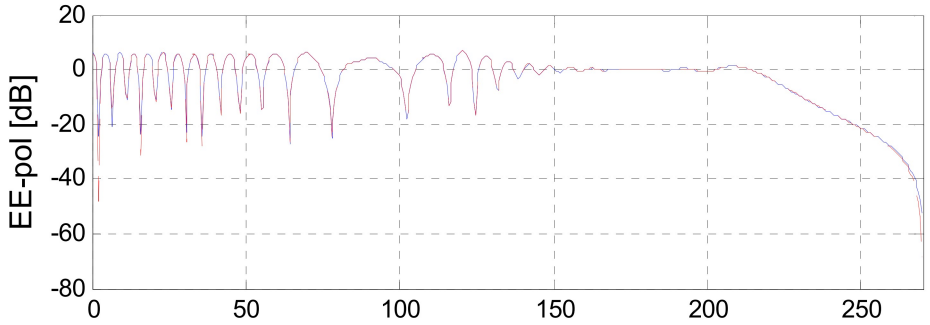

Total Field

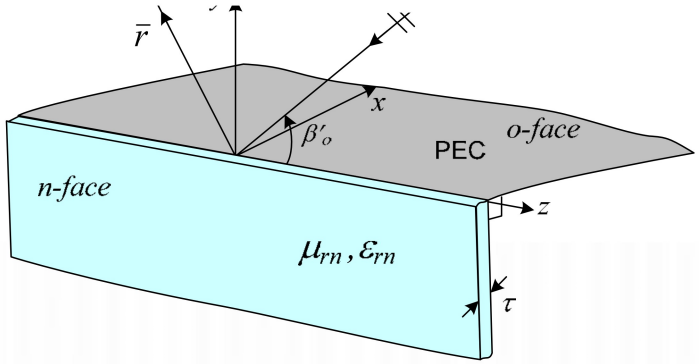

• MZ is R. G. Rojas, "Electromagnetic Diffraction of an Obliquely Incident Plane Wave Field by a Wedge with Impedance Faces", IEEE AP, July 1988.

Numerical Results

(3-D Material Coated PEC Wedge, WA = 540)

- $r'=5\lambda$, $\phi'=117°$, $\beta'=66°$, $r=5\lambda$, $\tau=\lambda/20$, $\varepsilon rn=2.4$, and $\mu rn=8$.

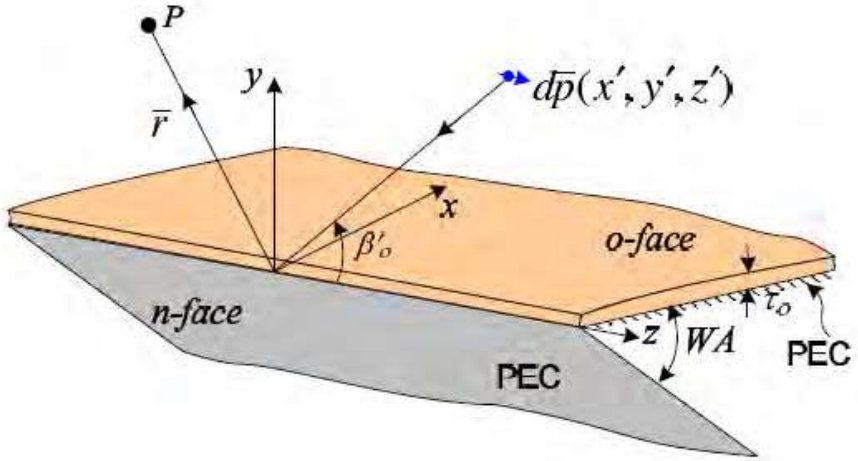

z-directed current moment excitation

Scatt. Field

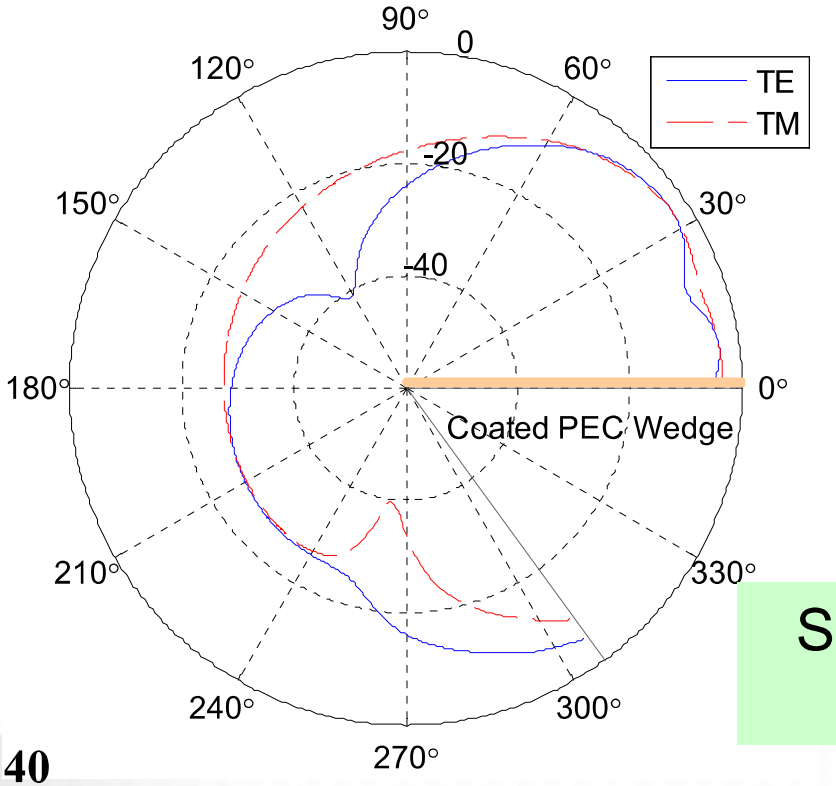

Total Field

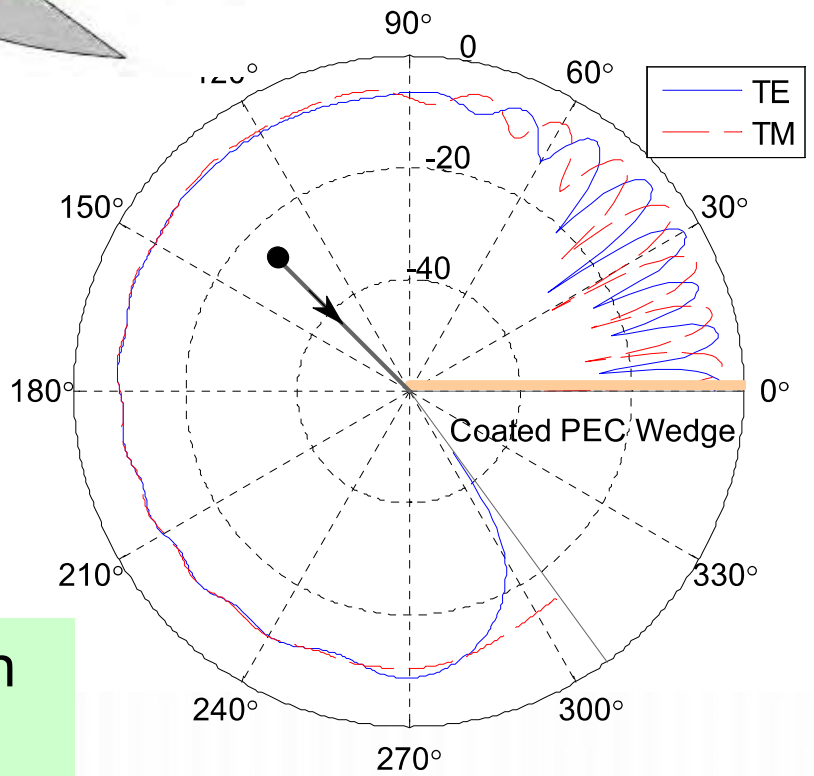

Slope diffraction is included

ANTENNAS ON CONVEX COATED STRUCTURES

Kittisak Phaebua and Prabhakar Pathak

- **A Uniform Geometrical Theory of Diffraction (UTD) Ray Solution is developed to predict the radiation by antennas on smooth convex metallic surfaces with thin material coating.**

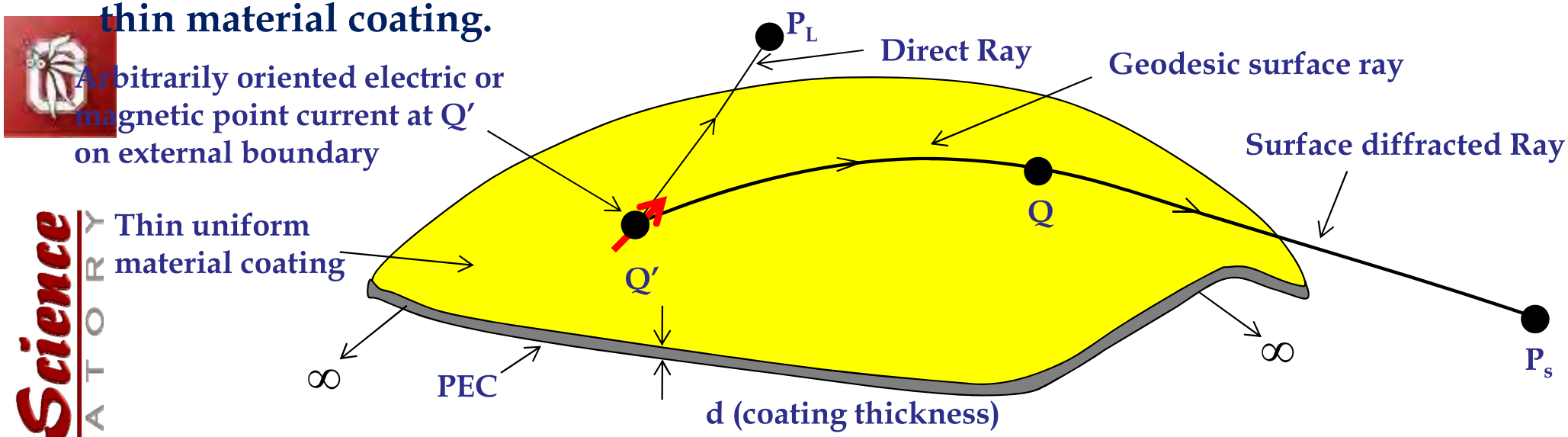

- **Metallic surface is assumed to be a perfect electric conductor (PEC).**
- **Thin coating** $\longrightarrow$ $kd \ll k\rho_g$; $k = \frac{2\pi}{\lambda}$; ρ_g **= surface radii of curvature**

  Also, $kd < 1$
- **For sufficiently thin material** (ε_r, μ_r) **coating, one can approximate the actual boundary on the external surface by a surface impedance** Z_s

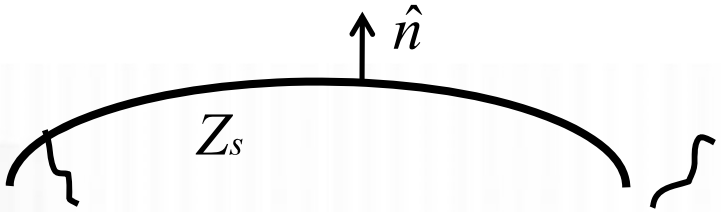

$$\hat{n} \times \hat{n} \times \overline{E} = -Z_s \, \hat{n} \times \overline{H}$$

$$Z_s \approx -jZ_o kd \left[\frac{1-\varepsilon_r \mu_r}{\varepsilon_r}\right]\left[1+\frac{(kd)^2}{2}(1-\varepsilon_r \mu_r)\right]^{-1}$$

MOTIVATION

- **UTD Ray Analysis can be applied to analyze radiation by conformal antennas and antenna arrays in the presence of a smooth PEC convex surface with thin material coating.**

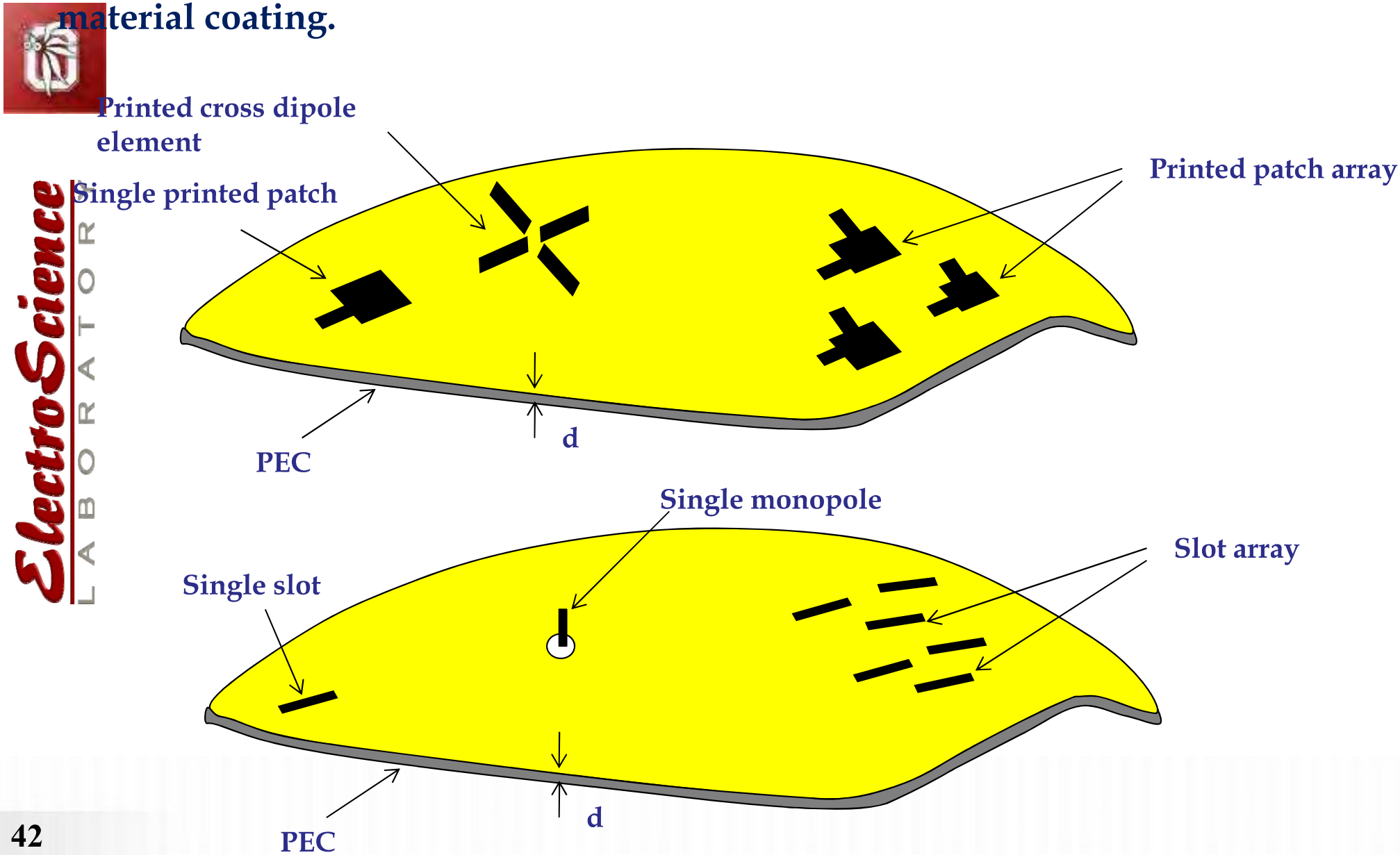

SOME PREVIOUS RELATED WORK

[1] P. Munk and P. H. Pathak, "A UTD Analysis of the Radiation and Mutual Coupling Associated with Antennas on a Smooth Perfectly Conducting Arbitrary Convex Surface with a Uniform Material Coating," Antennas and Propagation Society International Symposium, vol. 1, pp. 696 - 699, Jul. 1996.

- UTD ray solution not in form convenient for applications. Also, not all UTD transition functions computed.

[2] N. A. Logan and K. S. Lee, "A Mathematical Model for Diffraction by Convex Surface," In Electromagnetic waves. R. ranger, Ed, Univ. Wisconsin Press, 1962.

- No specific ray solution for radiation available.

[3] Wait, J. R., Electromagnetic Waves in Stratified Media, A Pergamon Press Book, McMillan Co., New York, 1962.

- Propagation of waves around the earth, spherical surface analyzed. No UTD ray solution presented

- Similar to work by V. A. Fock, Electromagnetic Diffraction and Propagation Problems, New York, Pergamon Press, 1965 (Original work in Russian was published in 1940s)

[4] L. W. Pearson, "A scheme for automatic computation of Fock-type integrals," IEEE Trans. Antennas Propagat.,vol. AP-35, pp. 1111–1118, Oct. 1987.

- Solution presented for only the scattering into shadow region of a coated circular cylinder.

[5] C. Tokgöz, P. H. Pathak and R. J. Marhefka," An Asymptotic Solution for the Surface Magnetic Field Within the Paraxial Region of a Circular Cylinder With an Impedance Boundary Condition", IEEE Trans. Antennas Propagat., vol. 53, no. 4, April 2005.

- Mostly restricted to surface fields on cylinders due to point magnetic currents on the same surface.

[6] P. H. Pathak, N. Wang, W. D. Burnside and R. G. Kouyoumjian, "A uniform GTD solution for the radiation from sources on a convex surface", IEEE Trans. Antennas Propagat., vol. AP-29, no. 4, pp. 609-622, July 1981.

- UTD analysis restricted to smooth convex PEC surfaces.

[7] P. H. Pathak, R. J. Burkholder, Y. Kim and J. Lee, "A Hybrid Numerical-Ray Based Analysis of Large Convex Conformal Antenna Array on Large Platforms," Presented at ACES conference in Finland, April, 2010.

- Hybrid numerical UTD solution restricted to complex antennas on locally smooth convex PEC surfaces.

ElectroScience LABORATORY

ANALYTICAL FORMULATION

- **A UTD solution for radiation by an arbitrarily oriented $d\overline{p}_e$ or $d\overline{p}_m$ on an arbitrary smooth convex surface with a uniform surface impedance boundary condition (IBC) is developed from canonical solutions.**

(Prabhakar Pathak & Kittisak Phaebua)

- **Canonical problems to be solved pertain to $d\overline{p}_e(Q')$ (or $d\overline{p}_m(Q')$) with arbitrary orientation on circular cylinders and spheres with IBC.**

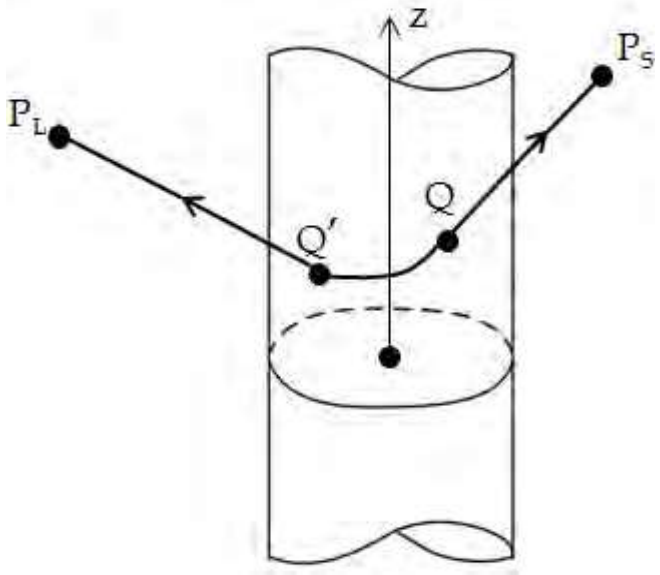

(a) Canonical circular cylinder problem geometry

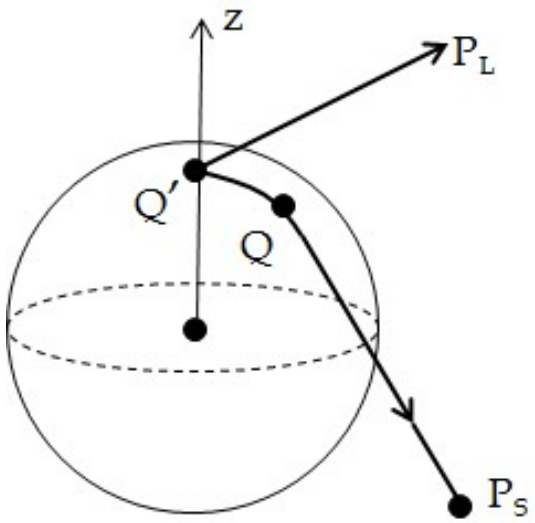

(b) Canonical spherical problem geometry

- **Generalization of canonical solutions to arbitrary convex surface performed heuristically based on the principal of locality of HF wave phenomena**

NUMERICAL RESULTS (CYL)

Radius of cylinder $= 4\lambda$

Thickness of dielectric coating $= 0.02\lambda$

Length of cylinder $= 50\lambda$

Frequency of operation = 10 GHz

$\varepsilon_r = 2.1$ (Teflon)

$\mu_r = 1$

Normal electric current source, $J_\rho(\bar{J}.\hat{n}')$

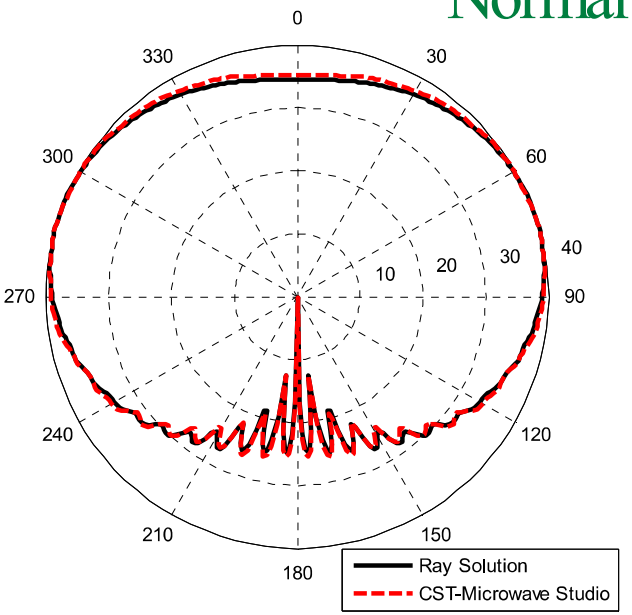

E_ϕ at $\theta = 60^o$

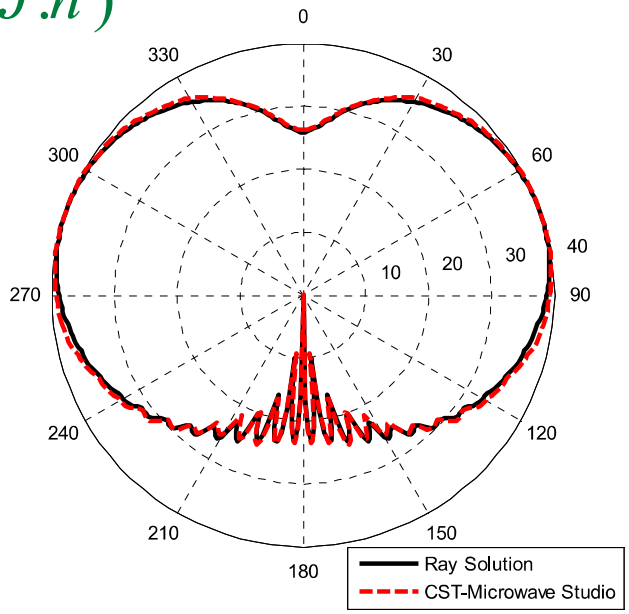

E_ϕ at $\theta = 80^o$

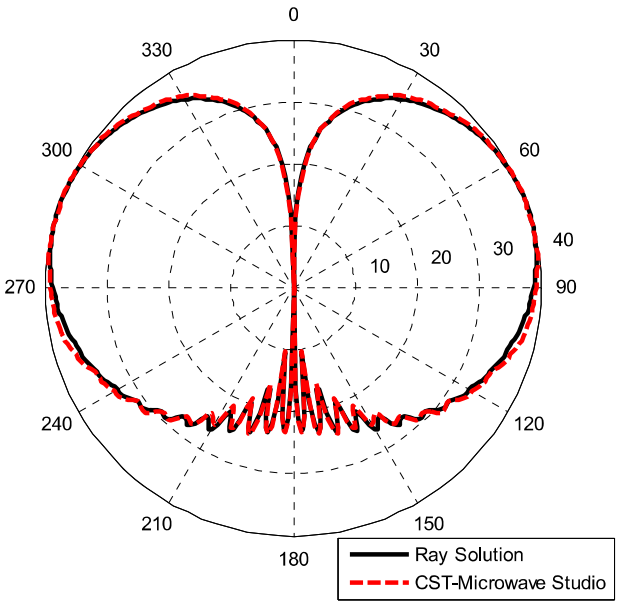

E_ϕ at $\theta = 90^o$

NUMERICAL RESULTS (CYL)

Radius of cylinder $= 4\lambda$

Thickness of dielectric coating $= 0.02\lambda$

Length of cylinder $= 50\lambda$

Frequency of operation = 10 GHz

$\varepsilon_r = 2.1$ (Teflon)

$\mu_r = 1$

Tangential magnetic current source, $M_t(\bar{M}.\hat{b}')$

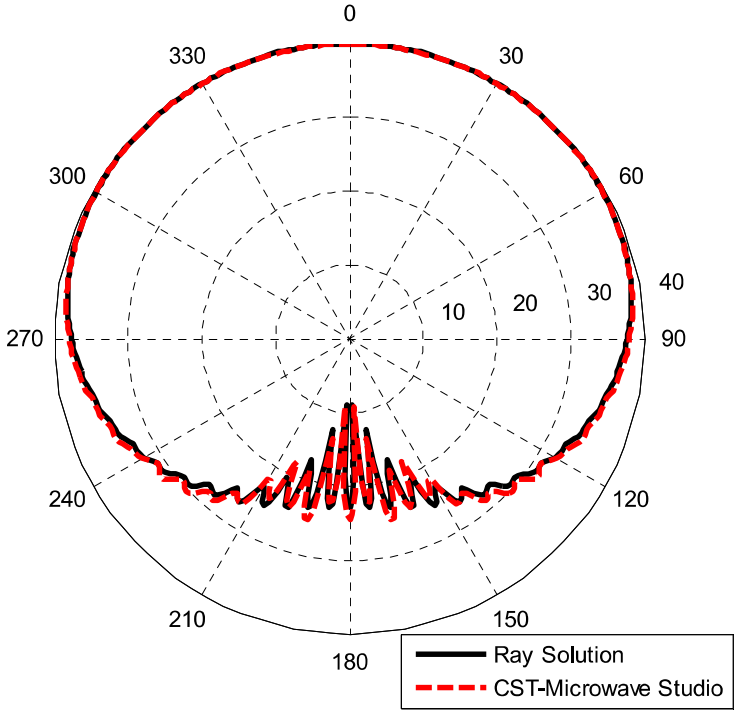

E_ϕ at $\theta = 90^o$

NUMERICAL RESULTS (SPH)

Radius of sphere $= 4\lambda$

Thickness of dielectric coating $= 0.02\lambda$

Frequency of operation = 10 GHz

$\varepsilon_r = 2.1$ (Teflon) ; $\mu_r = 1$

Normal electric current source, $J_r(\bar{J}.\hat{n}')$

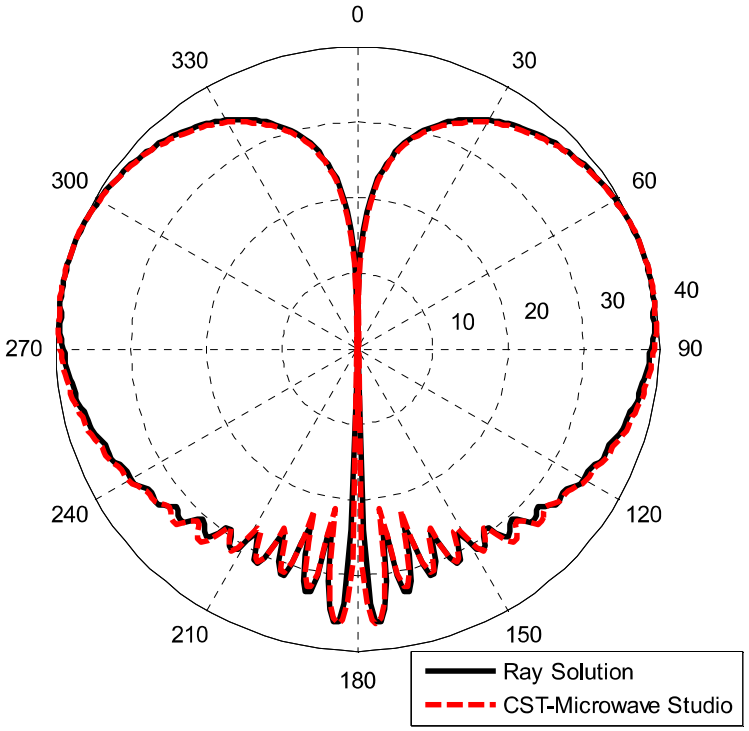

$E_\theta = E_n$

Tangential magnetic current source, $M_t(\bar{M}.\hat{b}')$

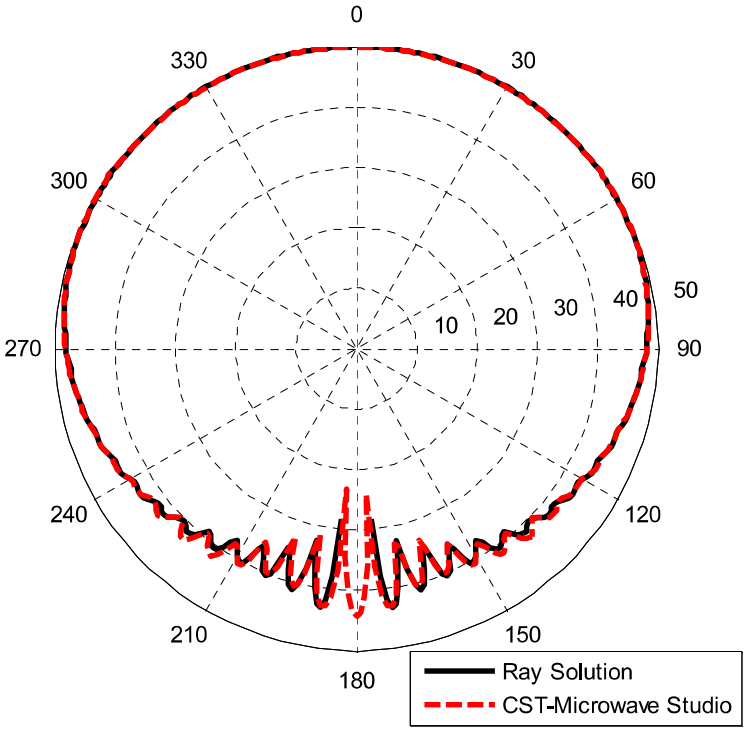

$E_\theta = E_n$

A UTD Diffraction Coefficient for a Corner Formed by Truncation of Edges in an Otherwise Smooth Curved Surface

Giorgio Carluccio[(1)], Matteo Albani[(1)], and Prabhakar H. Pathak[(2)]

(1) Department of Information Engineering, University of Siena
Via Roma 56, 53100 Siena, Italy, http://www.dii.unisi.it
(2) ElectroScience Laboratory, The Ohio State University
1320 Kinnear Road, 43212 Columbus – OH, USA,
http://electroscience.osu.edu

IEEE International Symposium on Antennas and Propagation
and USNC/URSI NationalRadio Science Meeting

June 01-05, 2009

UTD Vertex Diffraction Coefficient

Shadow Boundary Cones (SBCs) and Shadow Boundary Planes (SBPs):

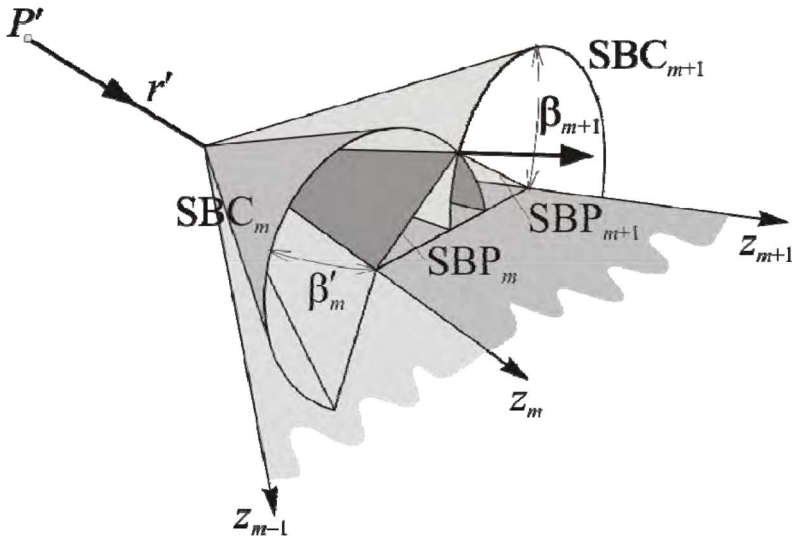

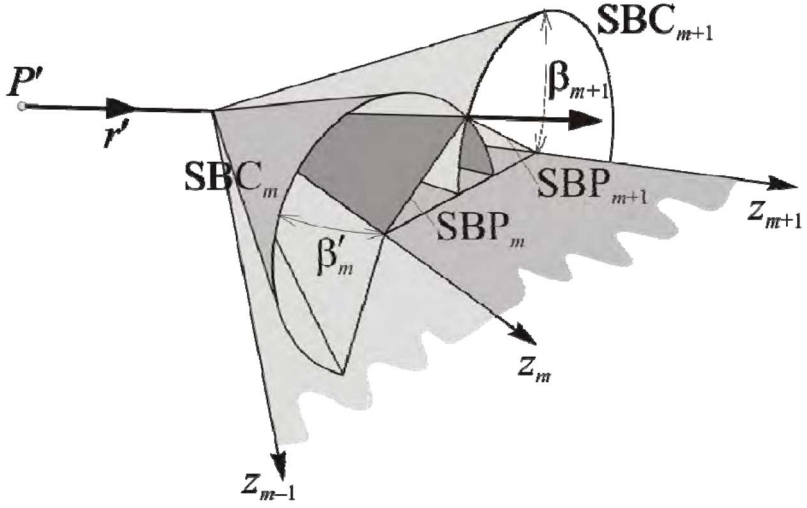

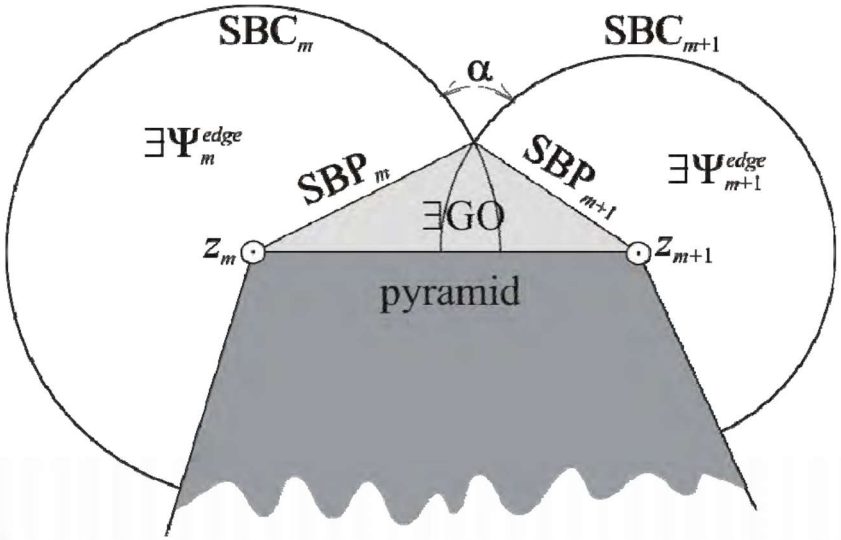

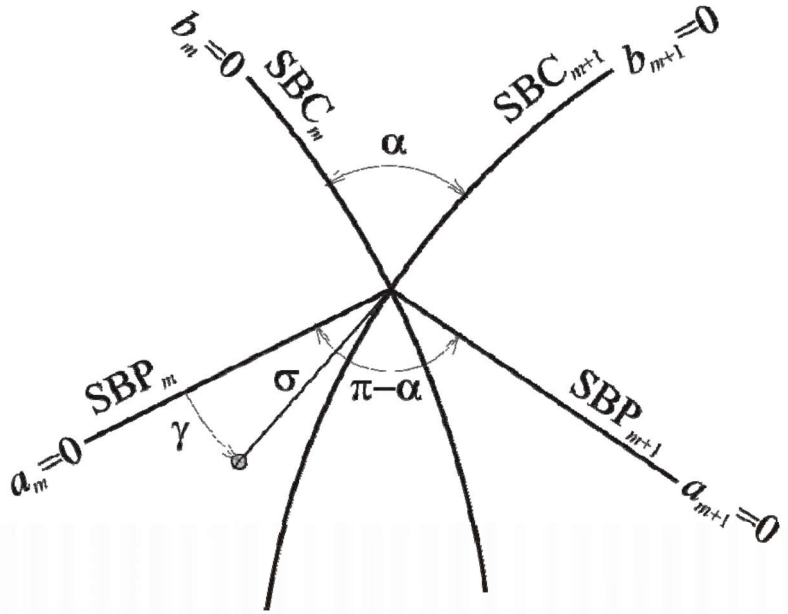

III Example: Vertex Double Transition

We consider a smooth convex parabolic surface illuminated by an electric point source

Scan Center on the Vertex A

$$r = 3\lambda, \varphi = 45°, -180° < \vartheta < 0°$$

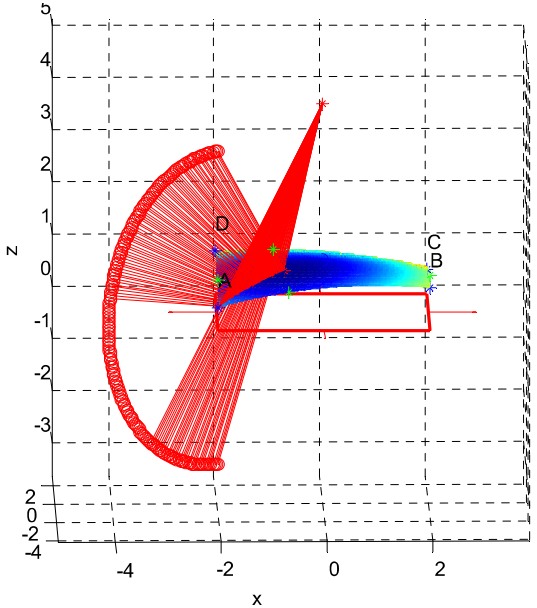

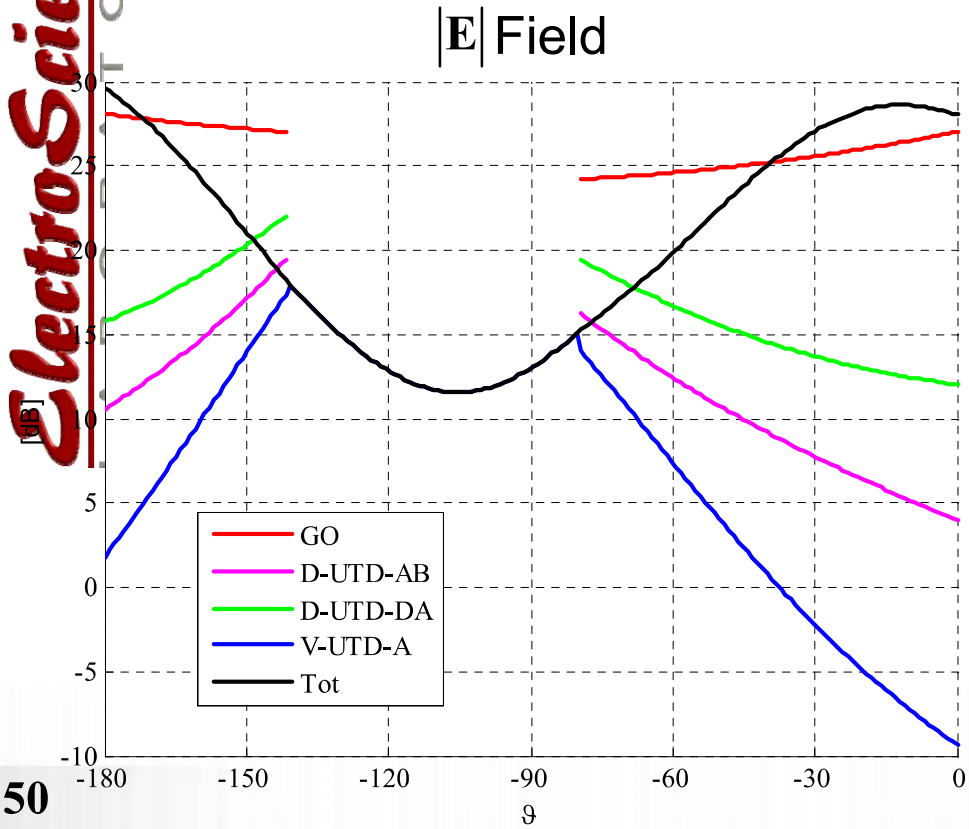

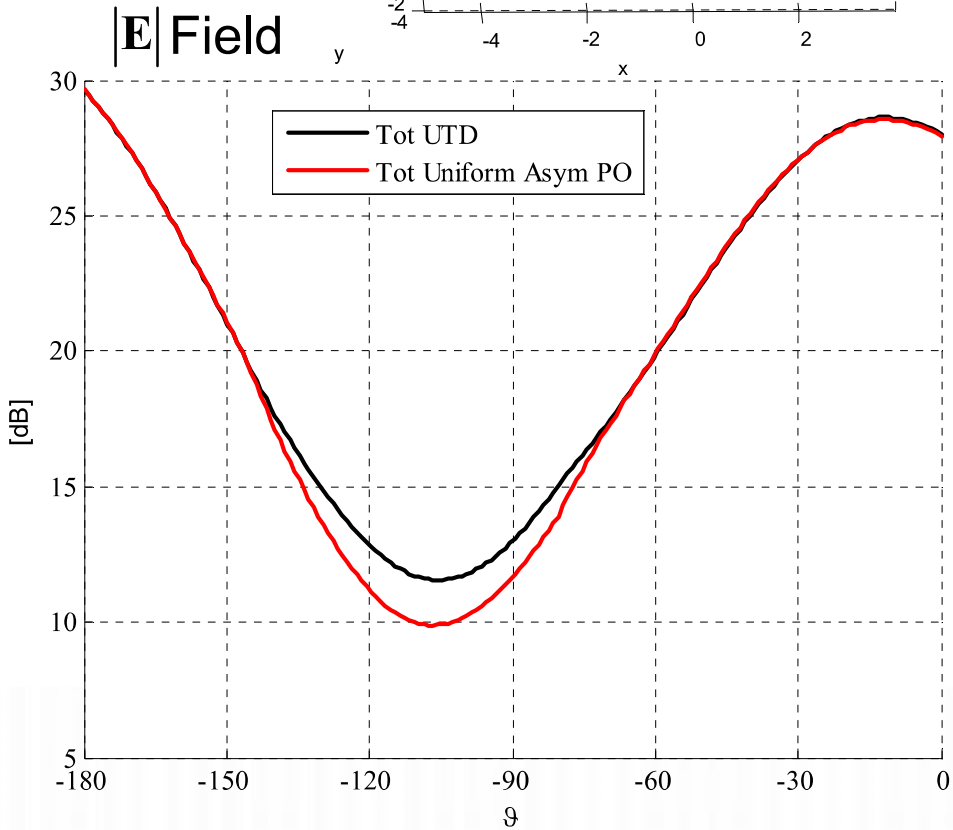

Remarks

ElectroScience LABORATORY

- A UTD diffraction coefficient for a corner formed by truncation of edges in a smooth curved surface was presented.

- A PO diffraction coefficient is derived by asymptotical evaluation of the PO integral, to understand how the surface curvature affects the diffracted field transitional behavior.

- The UTD diffraction coefficient was obtained by heuristically modifying the UTD diffraction coefficient for a corner in a flat surface, on the basis of the previous PO result.

- Numerical examples show how the proposed diffracted coefficient smoothly compensates for the abrupt discontinuity occurring when the GO field or the singly diffracted at edges abruptly vanish.

- Valid for astigmatic ray tube illumination.

- Can be extended to include thin material coating.

A UTD Analysis of the Radiation and Mutual Coupling Associated with Antennas on a Smooth Perfectly Conducting Arbitrary Convex Surface with a Uniform Material Coating

P. Munk* and P.H. Pathak
The Ohio State University ElectroScience Laboratory
1320 Kinnear Road, Columbus, Ohio

1 Introduction

A uniform geometrical theory of diffraction (UTD) solution has been developed for predicting the radiation and mutual coupling associated with conformal antennas placed anywhere within or on a uniform homogeneous material which covers a perfectly conducting convex surface of arbitrary shape. This work is of interest in the design of conformal antennas and arrays for aircraft, spacecraft, missiles and automobiles. The present solution is heuristically constructed, via locality of high frequency fields, from the asymptotic high frequency field solutions pertaining to the canonical problems of the radiation and coupling associated with sources located in or on a material coated circular conducting cylinder and a material coated conducting sphere, respectively. This solution employs the ray coordinates of the geometric theory of diffraction (GTD) illustrated in Figure 1. In the case of the coupling problem the surface field excited by the current source is associated with Keller's surface rays which traverse geodesic paths between the source point Q' and the surface field point Q as in Figure 1(a). In the radiation problem the field propagates along Keller's surface diffracted ray path, from the source at Q' to the observer at P_s in the shadow region as in Figure 1(a), whereas in the lit region the incident field propagates along the geometric optics ray path from Q' to P_l as in Figure 1(b). The fields associated with each of the rays in Figures 1(a), 1(b), and 1(c) may be compactly expressed in terms of a dyadic $\overline{\overline{\Gamma}}^{s}(P|Q')$ which behaves as a transfer function between the source located at Q', and field point. It is further noted that the components of the dyadic $\overline{\overline{\Gamma}}^{s}(P|Q')$ are expressed in terms of generalized Fock type radiation field and surface field integrals.

2 The Form of the Field Solution

In the case of the radiated fields, the electric field $\overline{E}(P)$ radiated by a source $\hat{p}\delta(\overline{r}-\overline{r}_{Q'})$ at Q' can be expressed symbolically as

$$\overline{E}(P) = \overline{\overline{\Gamma}}_p(P|Q')\cdot\hat{p} \quad ; \quad \text{for } \hat{p}=\hat{i} \text{ or } \hat{m} \tag{1}$$

0-7803-3216-4/96$5.00 © 1996 IEEE

where $\hat{i}$ and $\hat{m}$ represent unit strength electric and magnetic point currents at Q' respectively. For the field point $P = P_L$ in the lit region as in Figure 1(b), the dyadic $\overline{\overline{\Gamma}}_p(P|Q')$ is given as

$$\overline{\overline{\Gamma}}_p(P|Q') \sim \frac{-jK_0}{4\pi}\left[\hat{b}'_i\hat{n}A + \hat{t}'_i\hat{b}B + \hat{b}'_i\hat{b}C + \hat{t}'_i\hat{n}D\right]\cdot\frac{e^{-jK_0 s}}{s} \tag{2}$$

and for the field point $P = P_S$ in the shadow region as in Figure 1(c)

$$\overline{\overline{\Gamma}}_p(P|Q') \sim (-jK_0/4\pi)\left[\hat{b}'\hat{n}T_1 + \hat{t}'\hat{b}T_2 + \hat{b}'\hat{b}T_3 + \hat{t}'\hat{n}T_4\right] e^{-jK_0 t}\sqrt{\frac{d\psi_0}{d\eta(Q)}}\left[\frac{\rho_g(Q)}{\rho_g(Q')}\right]^{1/6}\sqrt{\frac{\rho_d}{s^d(\rho_d+s^d)}}\cdot e^{-jK_0 s^d} \tag{3}$$

where the components A, B, C, D, T_1, T_2, T_3, and T_4 are deduced from the asymptotic solutions for the canonical problems and are expressed in terms of generalized Fock radiation type integrals developed here. The quantities ρ^d and s^d are the same as in [1]; also, $d\eta(Q)$ is the width of the surface ray at Q, and $d\psi_0$ and $d\psi$ are the angles subtended by surface ray strip at Q' and Q respectively, also the same as in [1].

In the case of the mutual coupling, the UTD expressions for the EM fields $(\overline{E}(Q), \overline{H}(Q))$ at Q due to a point current element at Q' may be symbolically written as

$$\begin{Bmatrix} \overline{E}(Q) \\ \overline{H}(Q) \end{Bmatrix} = \begin{Bmatrix} \overline{\overline{\Gamma}}_{ep}(Q|Q') \\ \overline{\overline{\Gamma}}_{hp}(Q|Q') \end{Bmatrix}\cdot\hat{p}, \tag{4}$$

Similar to [2] for the special case of the perfectly conducting convex surface without material coating. $\overline{\overline{\Gamma}}_{ep}$ and $\overline{\overline{\Gamma}}_{hp}$ can be expressed in terms of the unit vectors fixed in the surface ray coordinates as in (2). These $\overline{\overline{\Gamma}}_{ep}$ and $\overline{\overline{\Gamma}}_{hp}$ contain generalized surface type Fock integrals.

3 Numerical Results

An example of the numerical evaluation of a typical radiation type Fock integral is given below. Consider a dielectric coated conducting circular cylinder with inner radius $a = 1.59\lambda_0$, coating thickness $t = .06\lambda_0$, and with a dielectric constant $\epsilon_r = 2.56$. The radiation type of the Fock integral in the circular cross section plane for this geometry is given as

$$g^h(\mathcal{Z}') = \frac{1}{\sqrt{\pi}}\int_{-\infty}^{\infty} d\tau \frac{e^{-j\mathcal{Z}'\tau}}{w_2'(\tau) - q(\tau)\cdot w_2(\tau)} \tag{5}$$

where $q(\tau)$ is a parameter dependent on the material coating, i.e thickness and material parameters, and $w_2(\tau)$ is the Fock type Airy function [1, 2]. A numerically efficient, and accurate method has been developed based on the procedure prescribed by Pearson [5], where this procedure has been extended to treat all classes of the Fock type integrals, namely the radiation and surface, including the U and V type of the latter. Figure 2 clearly illustrates the effectiveness of this newly developed method, where the numerical evaluation of the radiation integral given in Equation (5) (represented by the solid line) agrees extremely well with its closed form asymptotic representation valid for large negative $\mathcal{Z}'$ (corresponding to the lit region of the cylinder geometry) and with its residue series representation valid for large positive $\mathcal{Z}'$ (corresponding to the deep shadow region).

4 Conclusions

The present UTD solution provides a relatively simple yet accurate solution which is ideally suited analyzing conformal antenna and antenna array problems whose electrical size or shape preclude them from being solved by the standard numerical techniques. This solution which is valid for perfectly conducting convex surfaces with a material coating is valid uniformly within shadow boundary transition regions and is expressed in terms of a more general class of Fock functions that may be readily computed via a fast and efficient numerical procedure. In addition, this solution also explicitly shows the effect of surface ray torsion on the radiated fields in the shadow and transition regions.

References

[1] P.H. Pathak, N. Wang, W.D. Burnside, and R.G. Kouyoumjian, "A Uniform GTD Solution for the Radiation from Sources on a Convex Surface," *IEEE Trans. on Antennas and Prop.*, Vol. AP-29, No. 4, July 1981.

[2] P.H. Pathak and N. Wang, "An Analysis of the Mutual Coupling Between Antennas on a Smooth Convex Surface," Final Rep. 784583-7, Oct. 1978, The Ohio State University ElectroScience Lab., Dept. Electrical Engineering.

[3] J.B. Keller, "Geometrical Theory of Diffraction," *J. Opt. Soc. Amer.*, Vol. 52, pp. 116–130, 1962.

[4] V.A. Fock, Electromagnetic Diffraction and Propagation Problems, New York: Pergamon, 1965.

[5] L.W. Pearson, "A Scheme for Automatic Computation of Fock-Type Integrals," *IEEE Trans. Antennas Propagat.*, Vol. AP-35, No. 10, pp. 1111–1118, Oct. 1987.

Edge excited surface rays

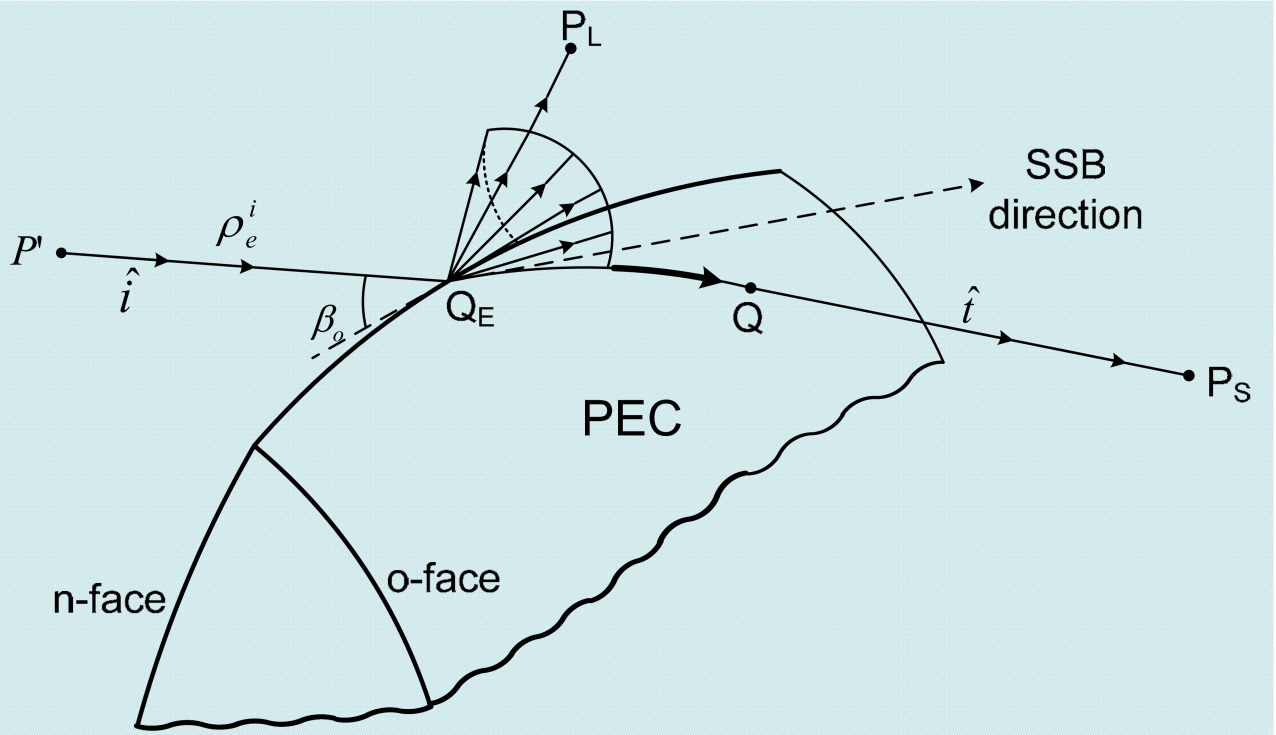

- Presently UTD solution has been obtained for ISB and SSB far apart.

- Work is in progress to obtain an asymptotic solution useful for engineering applications when ISB and SSB regions overlap.

Comments

- Keller's original GTD is not valid at and near ISB, RSB, SSB (i.e. in SB transition regions).
- UTD developed to patch Keller's original theory within the SB transition regions.
- GTD corrects GO, and GTD = GO + diffraction
- UTD corrects GTD, but usually UTD → GTD outside SB transition regions.
- UTD ray paths remain independent of frequency.
- UTD offers an analytical (generally closed form) solution to many complex problems that can not otherwise be solved in an analytical fashion.
- UTD in some cases must be augmented by PO/PTD or ECM

• PO/PTD can give rise to spurious contributions from the shadow boundary line in a smooth body.

• PO/PTD does not incorporate creeping wave effects.

•PO can correct for UTD transport singularities at and near the confluence of edge induced GO ray shadow boundaries and GO/diffracted ray caustics (e.g. forward radiation from parabolic reflector antennas).

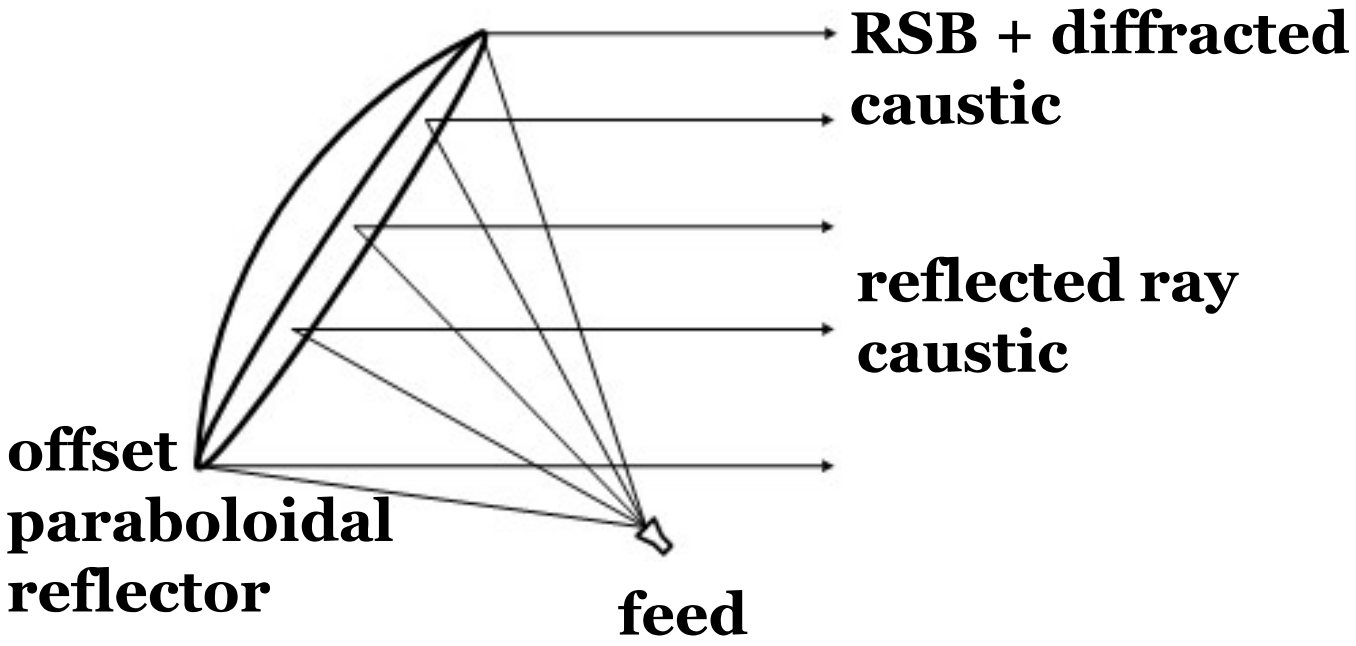

SPECTRAL THEORY OF DIFFRACTION (STD)

- **UTD/GTD requires a RAY OPTICAL incident field**
- **If the incident field is NON-RAY OPTICAL, then it must be represented by:**
  - **a) continuous set of PLANE WAVES (e.g. Plane Wave Spectrum)**
  - **b) discrete set of RAY OPTICAL fields**
- **Each constituent RAY OPTICAL field in the SPECTRAL DECOMPOSITION of a NON-RAY OPTICAL incident wave can be treated by UTD.**
- **The total UTD solution is then a summation of the UTD response to each constituent RAY OPTICAL incident field**

R. Tiberio, G. Manara, G. Pelosi, R. KouyoumJian: ''HF EM scattering of plane waves from double wedges," *IEEE Trans* ***AP-37***, pp. 1172-1180, Sept. 1989

Y. Rahmat-Samii, R. Mittra ''A spectral domain interpretation of HF phenomena," *IEEE Trans* ***AP-25*** pp. **676**-687, Sept. 1977

Equivalent Current Method (ECM)

- **ECM** is useful for patching UTD/GTD at and near **diffracted ray CAUSTICS** far from ISB, RSB

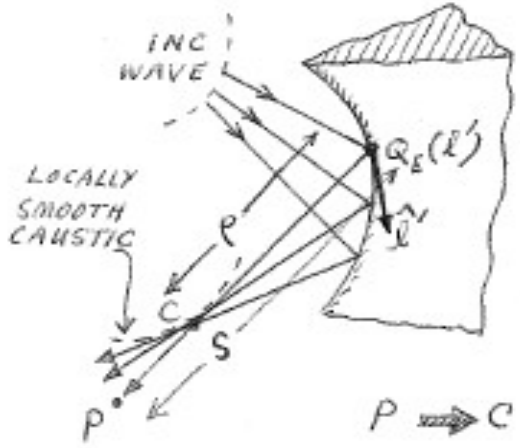

$$\bar{E}^d(P) \sim \bar{E}^i(Q_E) \cdot \bar{\bar{D}}_e \sqrt{\frac{\rho s}{\rho + s}}\, \frac{e^{-jks}}{s}$$

If $s >> \rho$

$$\bar{E}^d(P) \sim \bar{E}^i(Q_E) \cdot \bar{\bar{D}}_e \sqrt{\rho}\, \frac{e^{-jks}}{s}$$ — SPH. WAVE

If $s << \rho$ and $ks >> 1$

$$\bar{E}^d(P) \sim \bar{E}^i(Q_E) \cdot \bar{\bar{D}}_e \frac{e^{-jks}}{\sqrt{s}}$$ — CONICAL WAVE

AT & NEAR CAUSTIC C.

- A conical wave is produced by a TRAVELING WAVE line current. Comparing TW line current fields with $s << \rho$ case, one obtains:

$$\begin{Bmatrix} I(\ell') \\ M(\ell') \end{Bmatrix} = \frac{-e^{-j\frac{\pi}{4}}}{\sqrt{\sin\beta_0 \sin\beta_0'}} \sqrt{\frac{8\pi}{k}} \begin{Bmatrix} Y_0 \\ Z_0 \end{Bmatrix} \hat{\ell}' \cdot \begin{Bmatrix} \bar{E}^i(Q_E(\ell'))\, D_{es}(\phi,\phi';\sqrt{\sin\beta_0 \sin\beta_0'}) \\ \bar{H}^i(Q_E(\ell'))\, D_{eh}(\phi,\phi';\sqrt{\sin\beta_0 \sin\beta_0'}) \end{Bmatrix}$$

$$\bar{E}^d(P) \sim \frac{jkZ_0}{4\pi} \int_{\mathcal{L}} \left[\hat{R}\times\hat{R}\times I(\ell')\hat{\ell}' Y_0 \hat{R}\times M(\ell')\hat{\ell}'\right] \frac{e^{-jkR}}{R}\, d\ell'$$

$$\bar{r} = \overline{OP}\ ; \quad \bar{r}' = \overline{OQ_E(\ell')}$$

$$R = |\bar{r} - \bar{r}'|.$$

Outside the CAUSTIC region ECM → GTD

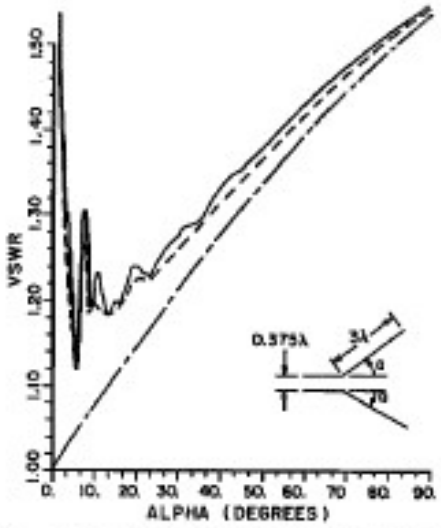

Fig. . The geometry and VSWR of a horn antenna. The dash-dotted curve denotes only throat contribution, the solid curve denotes throat and aperture contributions, and the dashed line denotes moment method calculation.

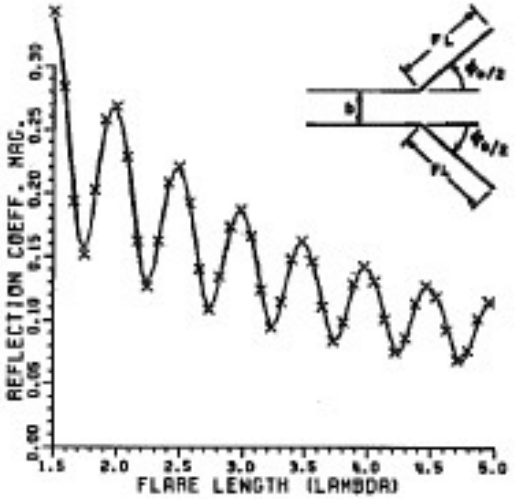

Fig. . Magnitude of the reflection from the two-dimensional E plane sectoral horn as a function of the wavelength. Here, $b = 1.58$ cm, flare length (FL) = 31.92 cm, and $\phi_0 = 33.5°$. The solid curve is from Jull [1972], and the crosses indicate results of the present analysis.

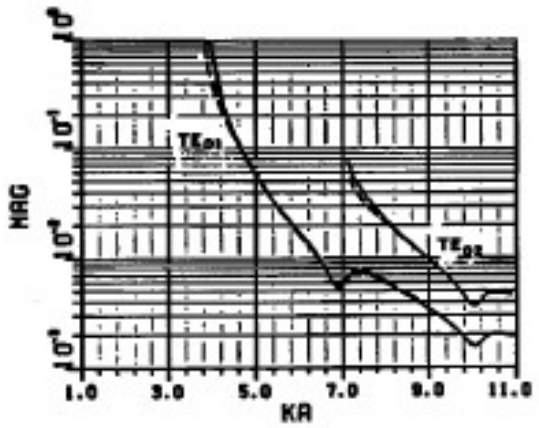

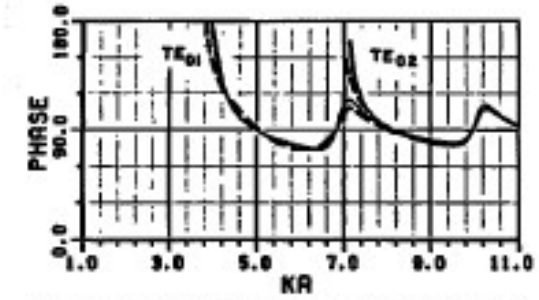

Fig. . Modal reflection coefficients due to an incident TE_{01} mode in an open-ended circular waveguide (a is the radius). The solid line gives the present solution, and the dashed line gives that of the Wiener-Hopf method.

ECM for Interior Waveguide Discontinuities

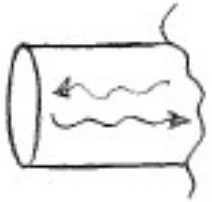

P. H. Pathak and A. Altintas, "An efficient high-frequency analysis of modal reflection and transmission coefficients for a class of waveguide discontinuities," *Radio Sci.*, vol. 23, no. 6, pp. 1107–1119, Nov.–Dec. 1988.

C. W. Chuang and P. H. Pathak, "Ray analysis of modal reflection for three-dimensional open-ended waveguides," *IEEE Trans. Antennas and Propagat.*, vol. 37, pp. 339–346, Mar. 1989.

ElectroScience LABORATORY

Previous related work

R. F. Millar, "An approximate theory of the diffraction of an electromagnetic wave by an aperture in a plane screen," *Proc. Inst. Elect. Eng.*, vol. 103C, pp. 177–185, 1956.

Ryan, C. E., and L. Peters, Jr., Evaluation of edge-diffracted fields including equivalent currents for the caustic regions, *IEEE Trans. Antennas Propag., AP-17*(3), 292–299, 1969.

H. Y. Yee, L. B. Felsen, and J. B. Keller, "Ray theory of reflection from the open end of a waveguide," *SIAM J. Appl. Math.*, vol. 16, pp. 268–300, 1968.
S. W. Lee, "Ray theory of diffraction by open-ended waveguides: Applications," *J. Math. Phys.*, vol. 13, pp. 656–664, 1972.
J. Boersma, "Ray-optical Analysis of Reflections in an open ended parallel plane Waveguide: TM case," *SIAM J. Appl. Math.*, vol. 29, pp. 164–195, 1975.
R. C. Rudduck and L. L. Tsai, "Aperture reflection coefficients for TEM and TE_{10} mode parallel-plate waveguides," *IEEE Trans. Antennas Propagat.*, vol. AP-16, pp. 83–89, 1968.

A. Michaeli, "Elimination of infinities in equivalent edge currents, parts I and II," *IEEE Trans. Antennas Propagat.*, vol. AP-34, pp. 912–918, July 1986 and pp. 1034–1037, Aug. 1986.
K.M. Mitzner, "Incremental length diffraction coefficients," Aircraft Div., Northrop Corp., Tech. Rep. AFAL-TR-73–296, Apr. 1974.
E.F. Knott, "The relationship between Mitzner's ILDC and Michaeli's equivalent currents," *IEEE Trans. Antennas Propagat.*, vol. AP-33, pp. 112–114, Jan. 1985.
R. A. Shore and A. D. Yaghjian, "Incremental diffraction coefficients for planar surfaces," *IEEE Trans. Antennas Propagat.*, vol. 36, pp. 55–70, Jan. 1988.

ADDITIONAL COMMENTS ON ASYMPTOTIC HF METHODS

- Asymptotic HF methods are powerful for analyzing a wide variety of electrically large EM problems.

- Conventional CEM numerical solution methods based on self consistent wave formulations become rapidly inefficient, or even intractable, for solving large ''EM problems''.

ElectroScience LABORATORY

- UTD is more developed, especially for handling smooth convex boundary diffraction.

- HF wave optical methods (PO, PTD, ITD, SBR) have not directly incorporated creeping waves.

- Ray optical methods require ray tracing. More efficient but less robust. Ray paths independent of frequency.

- Wave optical methods require numerical integration on the large object. Less efficient but more robust. Does not scale with frequency.

Pathak (younger version)

Kouyoumjian

Keller

Kouyoumjian

Tiberio

Manara

Nepa

ElectroScience LABORATORY

Beam Methods & Some Applications

- Beams provide useful basis functions for representing EM fields.
- Ray methods fail at caustics (focii) of ray systems. Caustics are formed by intersection or envelopes associated with the same class of rays. Beams remain valid in regions of real ray caustics

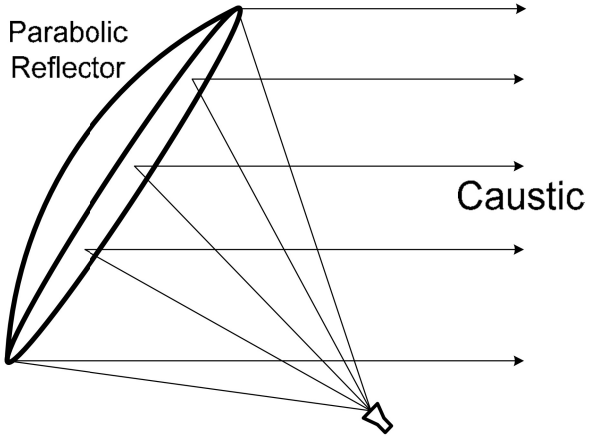

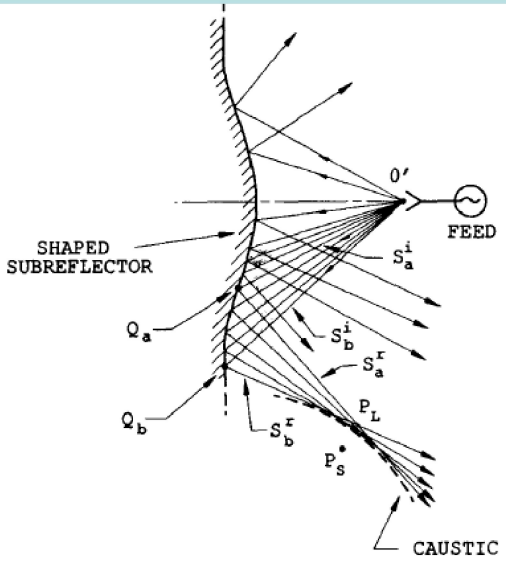

- Beams can be used to treat large reflector systems and radome problems efficiently.
- Beams can be used to improve the speed of conventional Moment Method (MoM) solution of governing EM integral equation (IE) for the radiating object.
- Beams can also be used for Near Field→ Far Field transformations required in near field measurements.

Complex Source Beam (CSB) Diffraction by a Wedge

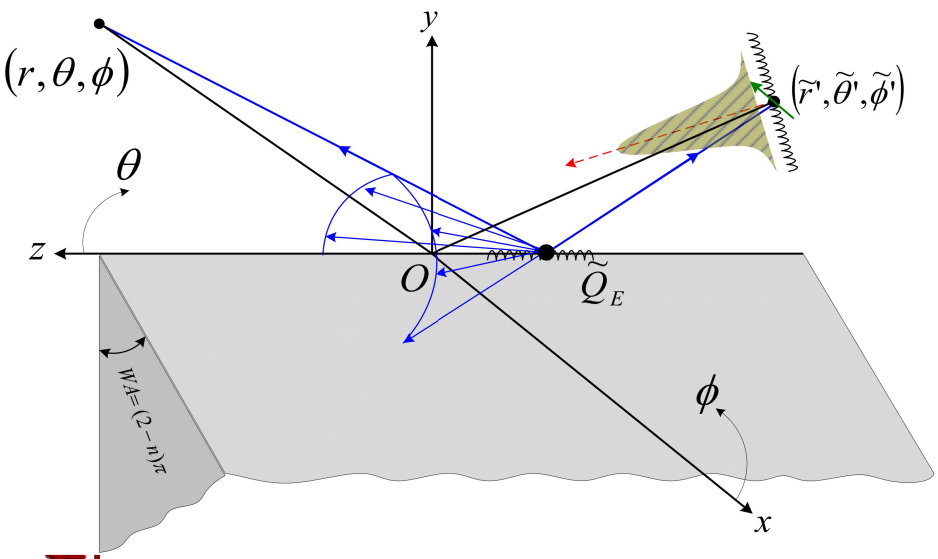

• UTD for real source excitation of wedge developed via first order Pauli-Clemmow method (PCM) [1-4] for asymptotic solution of canonical wedge diffraction integral along a steepest descent path (SDP)

•First order PCM not strictly valid (for poles crossing the SDP away from saddle point); hence analytic continuation of UTD for complex source location without further study is questionable!

•First order Van der Waerden method (VWM) [1-4] is valid even where PCM fails.

ElectroScience LABORATORY

• However, one can show that the first order VWM method, upon using a key rearrangement (and combination) of terms, yields:

Key Step ⇒ $\mathrm{VWM} = \mathrm{PCM} + \Delta \equiv \mathrm{EPCM}$ (Extended PCM)

• Next, for the special wedge case of interest, it is shown analytically (and verified numerically) that $\Delta \approx 0$.

Note :

$\mathrm{PCM} \rightarrow$ UTD for wedge

$\mathrm{VWM} \equiv \mathrm{EPCM} \rightarrow$ EUTD for wedge

Therefore, analytic continuation of UTD for a wedge is OK for complex waves

For a wedge ⇒ $\mathrm{EUTD} = \mathrm{UTD} + \Delta \approx \mathrm{UTD}$ (since Δ is negligible)

1. T. B. A. Senior and J. L. Volakis, "Approximate Boundary Conditions in Electromagnetics," The Institute of Electrical Engineerings, London, 1995.
2. L. B. Felsen and N. Marcuvitz, "Radiation and Scattering of Waves," Englewood Cliffs, NJ: Prentice-Hall, 1973.
3. C. Gennarelli and L. Palumbo, "A uniform asymptotic expansion of typical diffraction integrals with many coalescing simple pole singularities and a first-order saddle point," *IEEE Trans. Antennas and Propagat.*, vol. AP-32, pp. 1122-1124, Oct. 1984.
4. R. G. Rojas, "Comparison between two asymptotic methods," *IEEE Trans. Antenn- as and Propagation*, vol. 35, no. 12, pp 1492-1493, Dec 1987.

Complex Source Beam (CSB) Diffraction by a Wedge (cont.)

Numerical Result 1

$WA = 30°$
$r' = 5\lambda$
$\theta' = 140°$
$\phi' = 50°$
$b = 10\lambda$
$\theta_b = 60.6°$
$\phi_b = 217.4°$
$r = 2\lambda$
$\theta = 45°$
$\hat{p}^{i,r} = \pm\hat{z}$

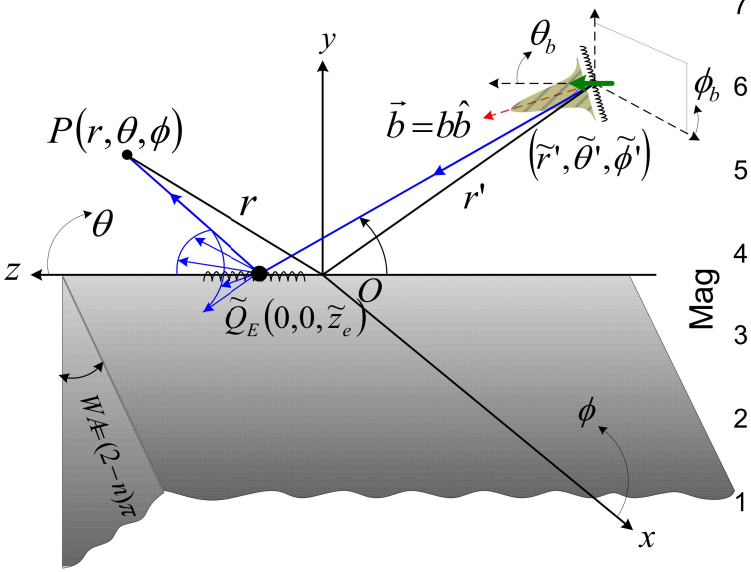

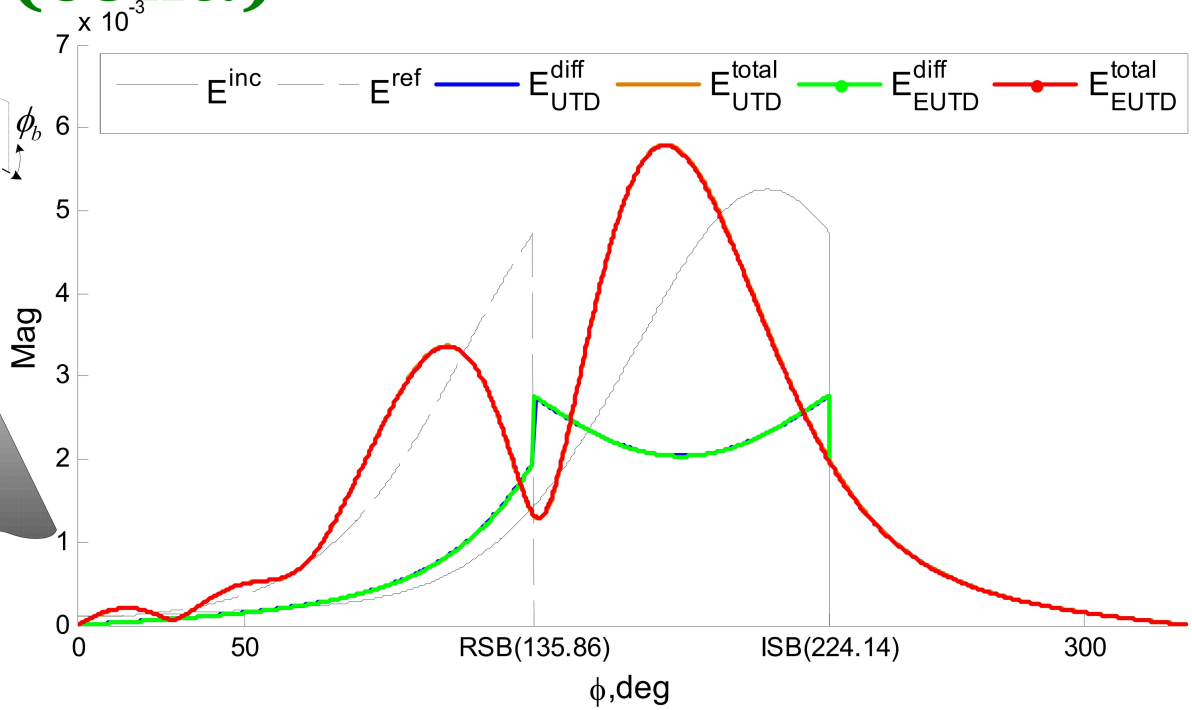

• **Trajectories of** $\mathrm{Im}(\alpha_p^{i,r})$

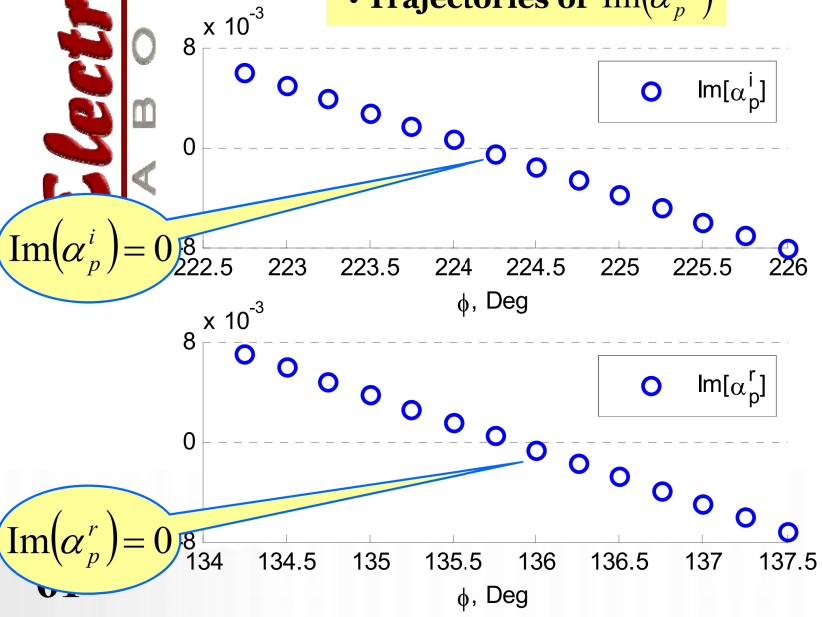

$$V^a_{2,4}\left(\xi_p^-\left(\tilde{\beta}^{\mp}\right)\right) = -\frac{n\gamma_p^-\left(\tilde{\beta}^{\mp}\right)}{\cos\left(\xi_p^-\left(\tilde{\beta}^{\mp}\right)/2\right)} \times\left(\tilde{s}+\tilde{s}'\right)+\cot\left(\frac{\pi\pm\tilde{\beta}^{\mp}}{2n}\right)$$

$$V^b_{2,4}\left(\xi_p^-\left(\tilde{\beta}^{\mp}\right)\right) = 1-F\left(\pm\sqrt{k\tilde{\alpha}^-\left(\tilde{\beta}^{\mp}\right)}\right)$$

• **Additional term in EUTD solution**

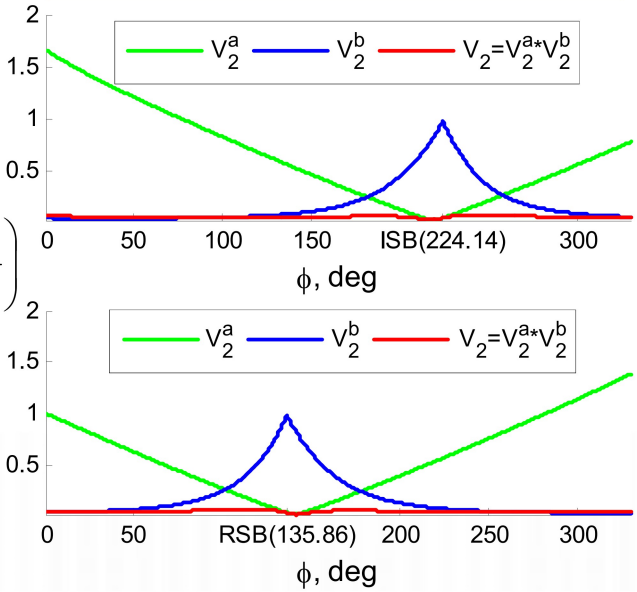

Complex Source Beam (CSB) Diffraction by a Wedge (cont.)

Numerical Result 2

$WA = 45°$
$r' = 20\lambda$
$\theta' = 100°$
$\phi' = 70°$
$b = 10\lambda$
$\theta_b = 78.57°$
$\phi_b = 258.57°$
$r = 12\lambda$
$\theta = 40°$
$\hat{p}^{i,r} = \pm\hat{z}$

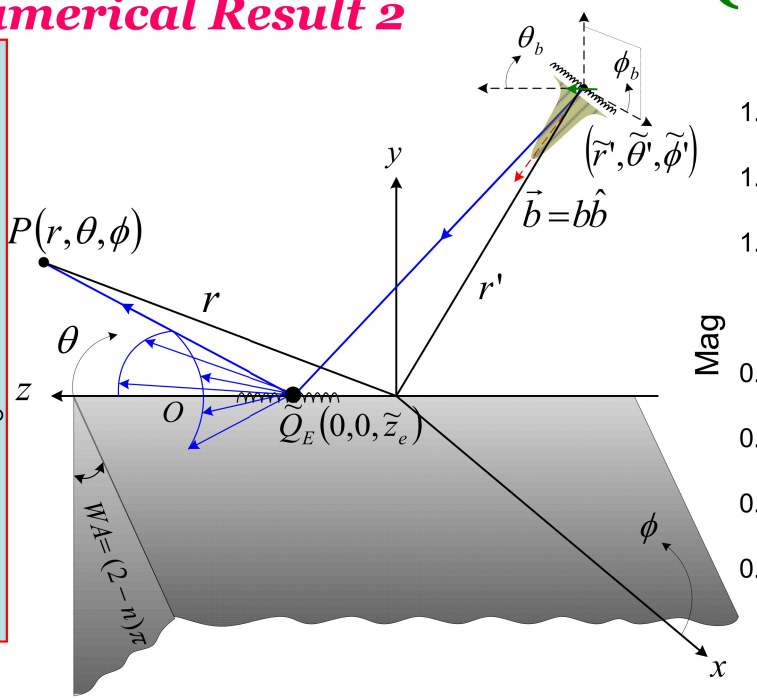

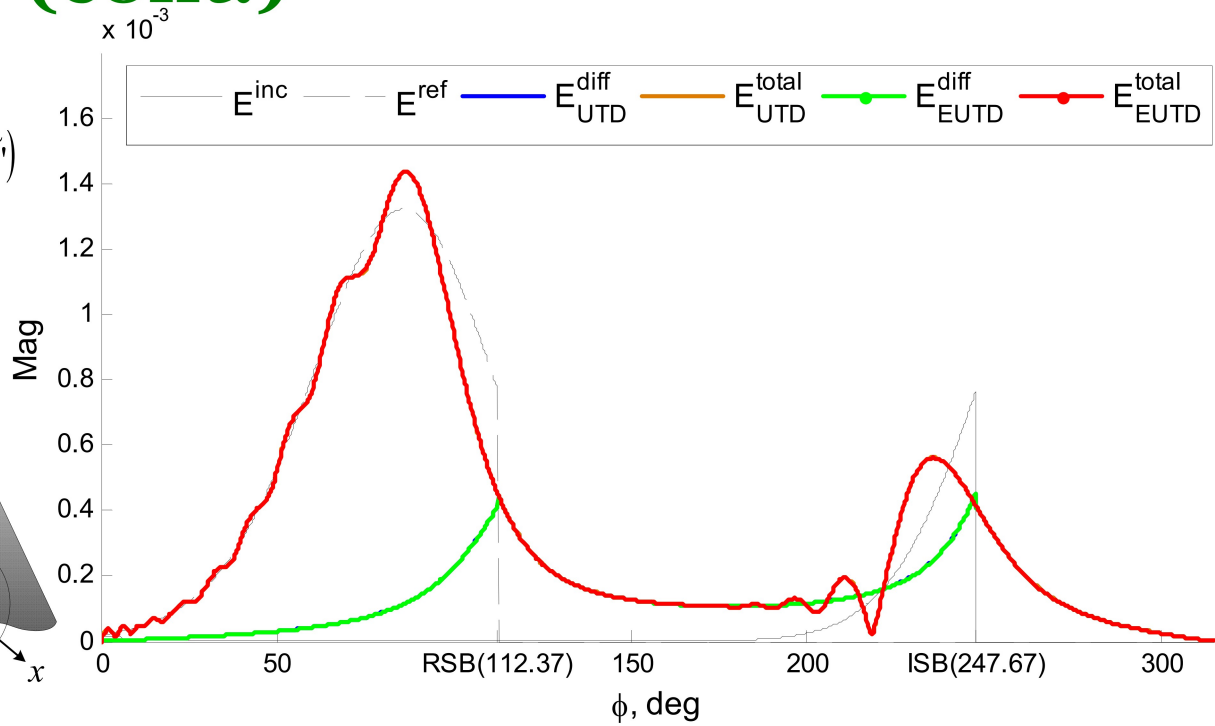

• **Trajectories of** $\mathrm{Im}(\alpha_p^{i,r})$

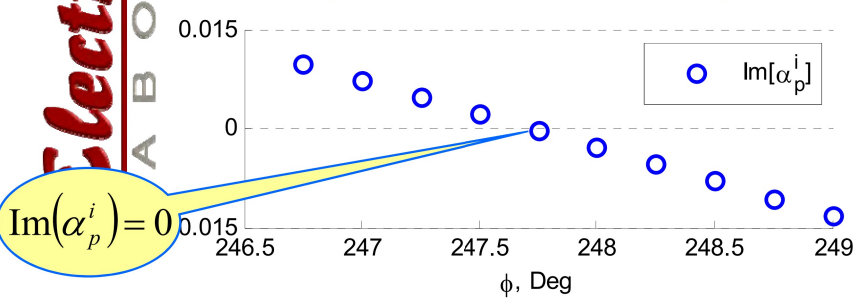

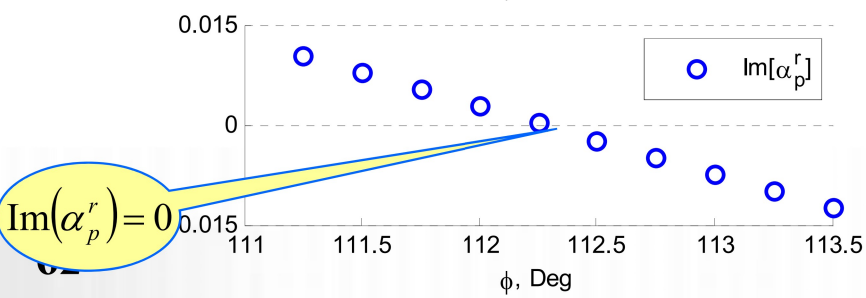

$$V_{2,4}^a\left(\xi_p^-\left(\tilde{\beta}^{\mp}\right)\right) = -\frac{n\gamma_p^-\left(\tilde{\beta}^{\mp}\right)}{\cos\left(\xi_p^-\left(\tilde{\beta}^{\mp}\right)/2\right)} \times\left(\tilde{s}+\tilde{s}'\right)+\cot\left(\frac{\pi \pm \tilde{\beta}^{\mp}}{2n}\right)$$

$$V_{2,4}^b\left(\xi_p^-\left(\tilde{\beta}^{\mp}\right)\right) = 1 - F\left(\pm\sqrt{k\tilde{\alpha}^-\left(\tilde{\beta}^{\mp}\right)}\right)$$

• **Additional term in EUTD solution**

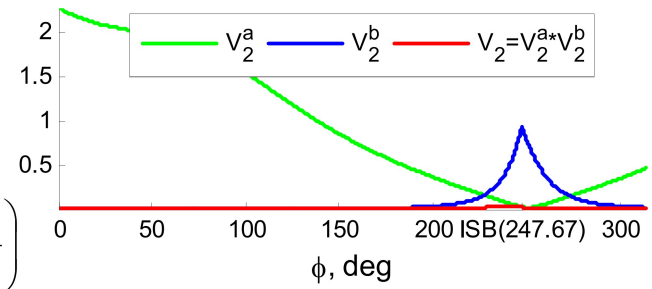

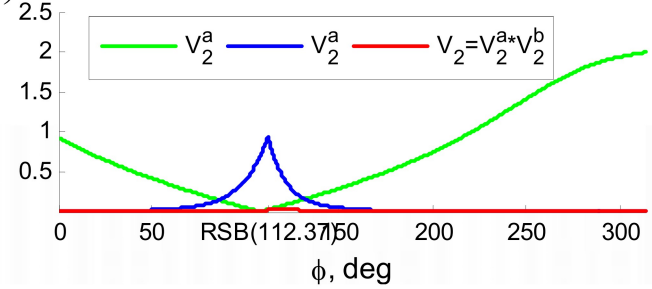

Other Complex Waves

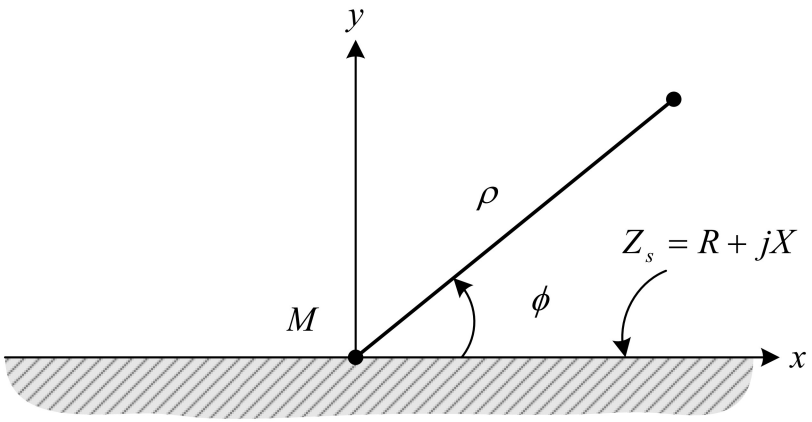

$$\alpha_{p1,p2} = -\sqrt{2}e^{-j\frac{\pi}{4}} \sin\frac{\xi_{p1,p2} - \phi}{2}$$

Shadow boundaries are determined when

$$\mathrm{Im}\,\alpha_{p1,p2} = 0$$

Leaky Wave
$(Z_S = -327.94 - j17.79)$

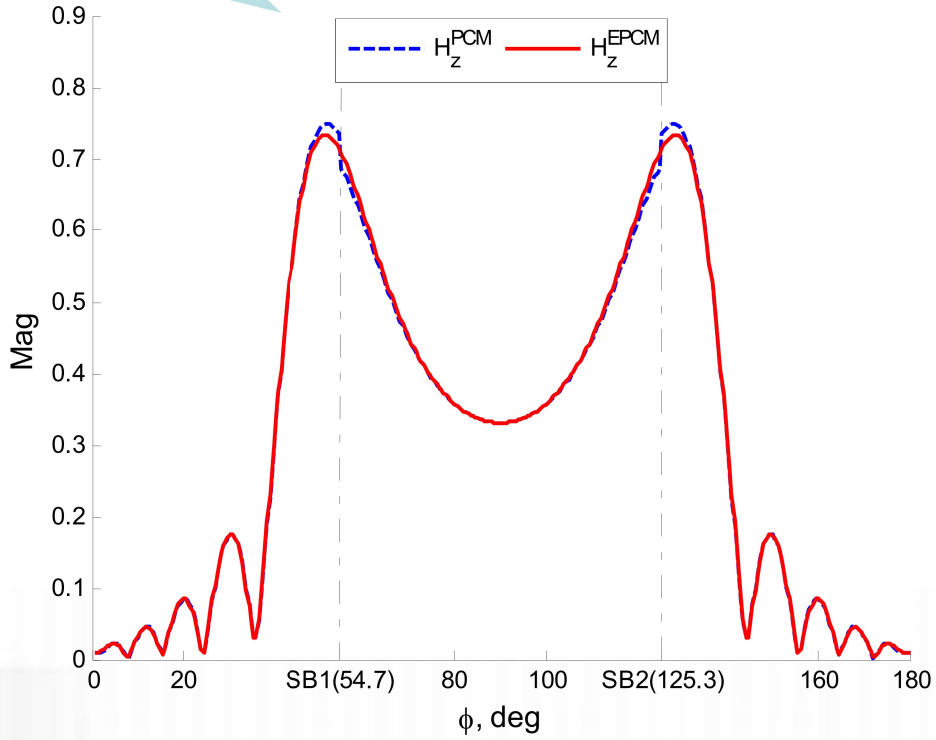

Surface Wave
$(Z_S = j35.58)$

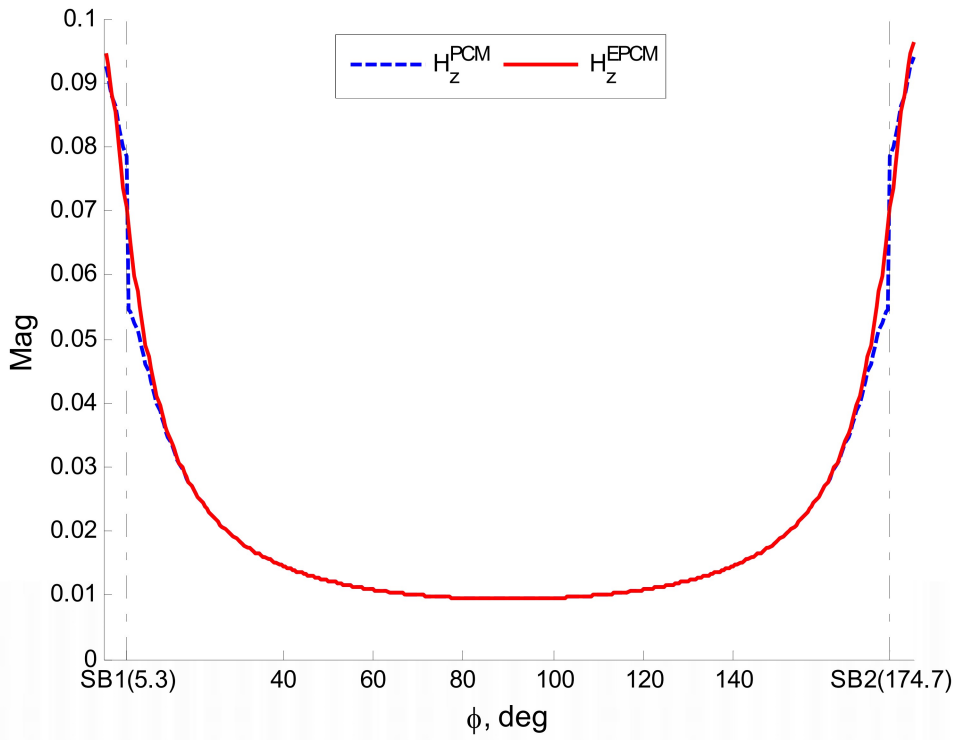

Keller Cone of Edge Diffraction

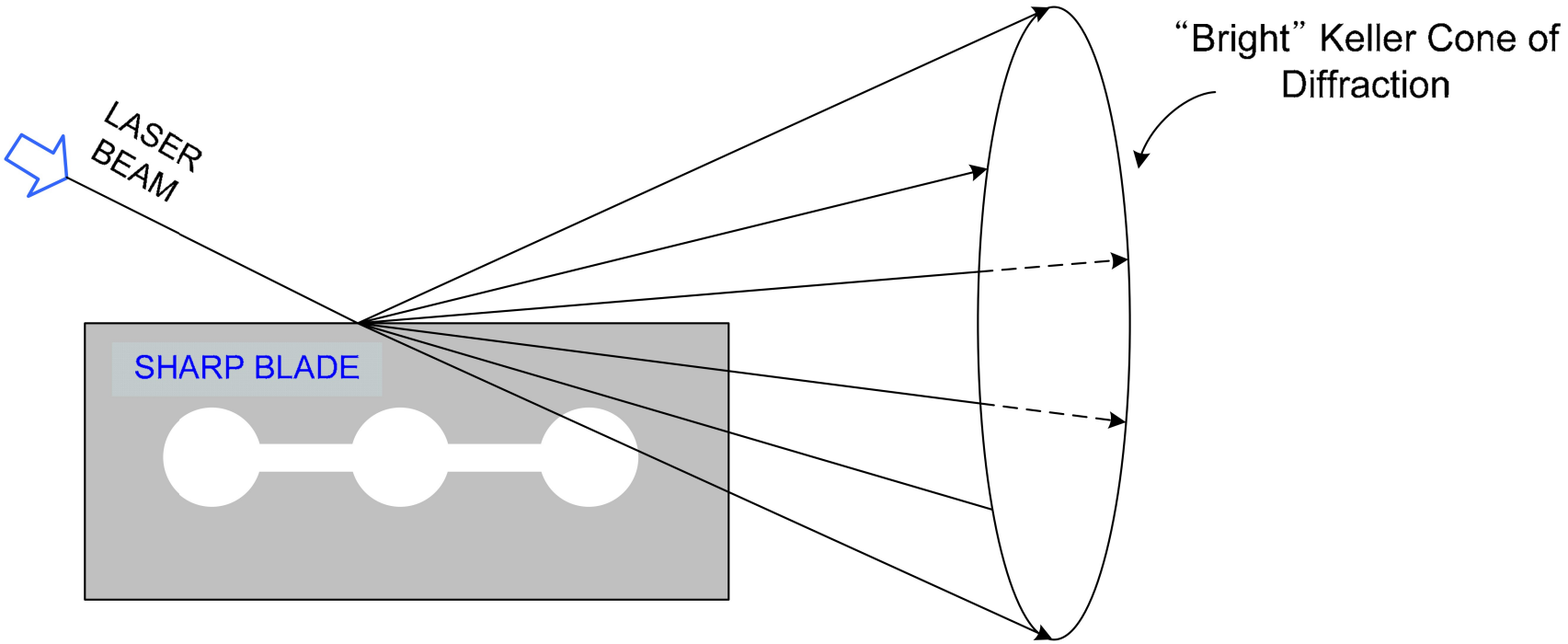

Laser beam incident in the plane of the sharp blade

Large Antenna Applications

Fast analysis of the reflector antennas.

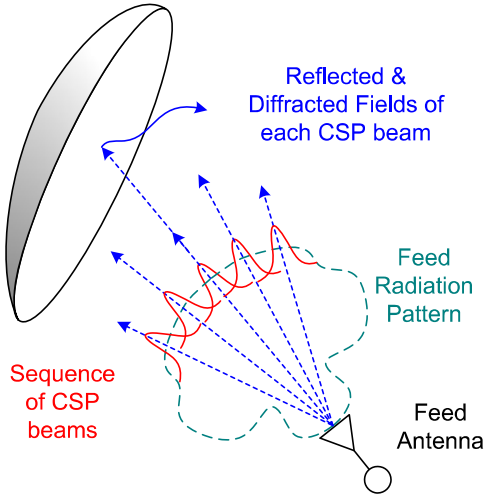

- A GB -UTD (PO based) method was previously reported in [1].
- With the CSP method, feed pattern is expanded into a set of CSBs.
- Each CSP beam field is scattered from the reflector by using complex extension of UTD.
- A 2-D case for a single beam illumination was reported in [2].
- This new fully 3-D CSP-UTD approach (UTD for beams) is expected to be more accurate then [1].

Antenna radiation in the presence of radomes.

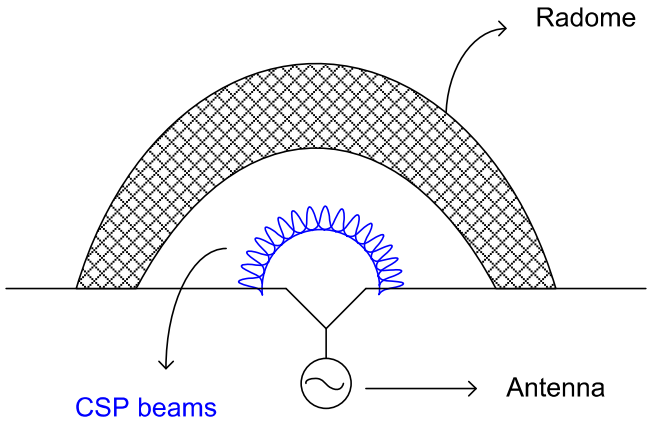

- The field of the antenna is first expanded into a set of CSP beams.
- Each beam is next tracked through the radome.
- The transmitted beams are summed up at the observer location.
- Complex ray tracing can be employed for beam tracking through the radome [3,4].

[1] H. T. Chou, P. H. Pathak and R. J. Burkholder, "Novel Gaussian Beam Method for the Rapid Analysis of Large Reflector Antennas", IEEE Trans. Antennas Propagat., 2001

[2] G.A.Suedan and E.V. Jull, "Beam diffraction by planar and parabolic reflectors," IEEE Trans. Antennas Propagat., 1991.

[3] X. J. Gao and L. B. Felsen, "Complex ray analysis of beam transmission through two-dimensional radomes", IEEE Trans. Antennas Propagat., 1985

[4] J. J. Maciel and L. B. Felsen, "Gaussian beam analysis of propagation from an extended plane aperture distribution through dielectric layers, part 1 - plane layer," IEEE Trans. Antennas Propagat., 1990.

CSB-UTD Diffraction by a Curved Wedge

$$z = \frac{x^2 + y^2}{4 f_m}$$

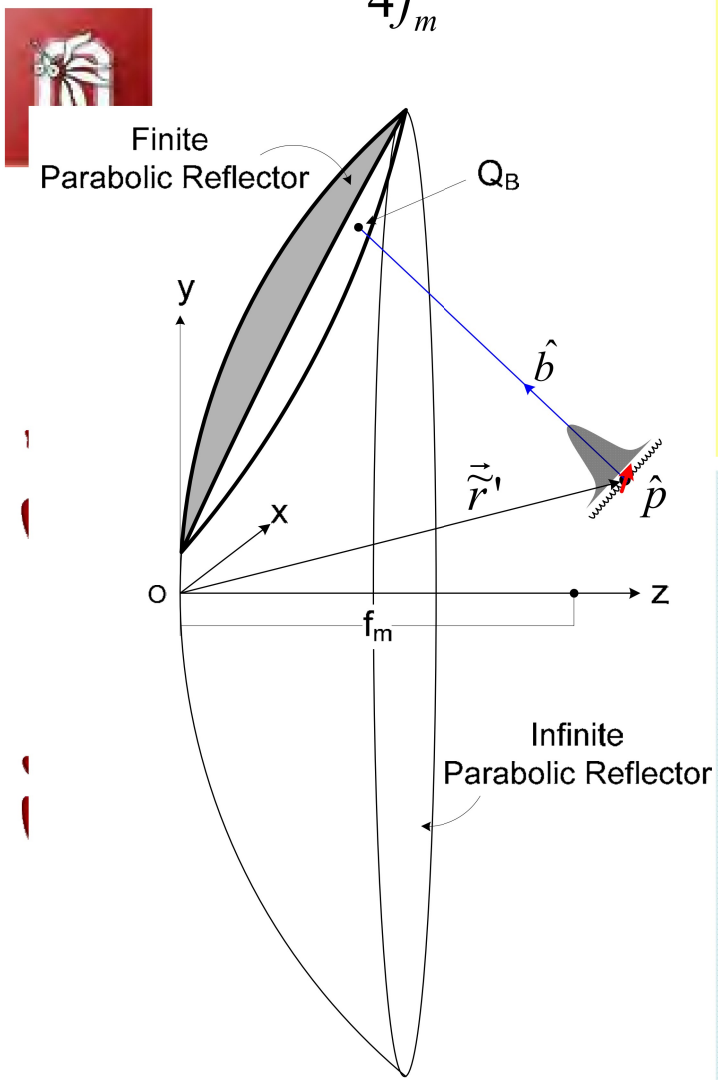

- **The present CSB-UTD & CSB-EUTD solution** for a CSB excited PEC curved wedge is obtained by analytically continuing the UTD solution for a PEC curved wedge excited by a real point source (or even real astigmatic ray) to deal with a CSB (or even more generally a complex astigmatic beam, i.e. CAB) illumination of a curved edge in a curved surface.
- The CSB reflected from doubly curved surface become an astigmatic Gaussian beam in paraxial region.

- The **CSB-UTD solution** is valid for analyzing CSB excited focus-fed parabolic reflector antennas since the caustics are now in complex space for the CSB excitation case.
- The **PO analysis for a CSB excited** parabolic reflector
  (a) **loses its accuracy** in the region of the main beam when a CSB axis hits near the edge. → can be improved by adding the additional edge diffraction term based on Physical Theory of Diffraction (PTD).
  (b) **becomes more accurate** when a CSB axis hits the actual reflector surface away from the edge.

CSB-UTD Diffraction by a Curved Wedge (cont.)

Numerical Result ***: Finite parabolic reflector illuminated by a CSB***

$d_M = 60\lambda,\ h = 5\lambda,\ f_M = 35\lambda,\ b = 10\lambda,\ \hat{p} \perp \hat{b},\ Q_B = (10\lambda, 50\lambda),\ S = (40\lambda, 100°, 270°)$

Transverse Plane

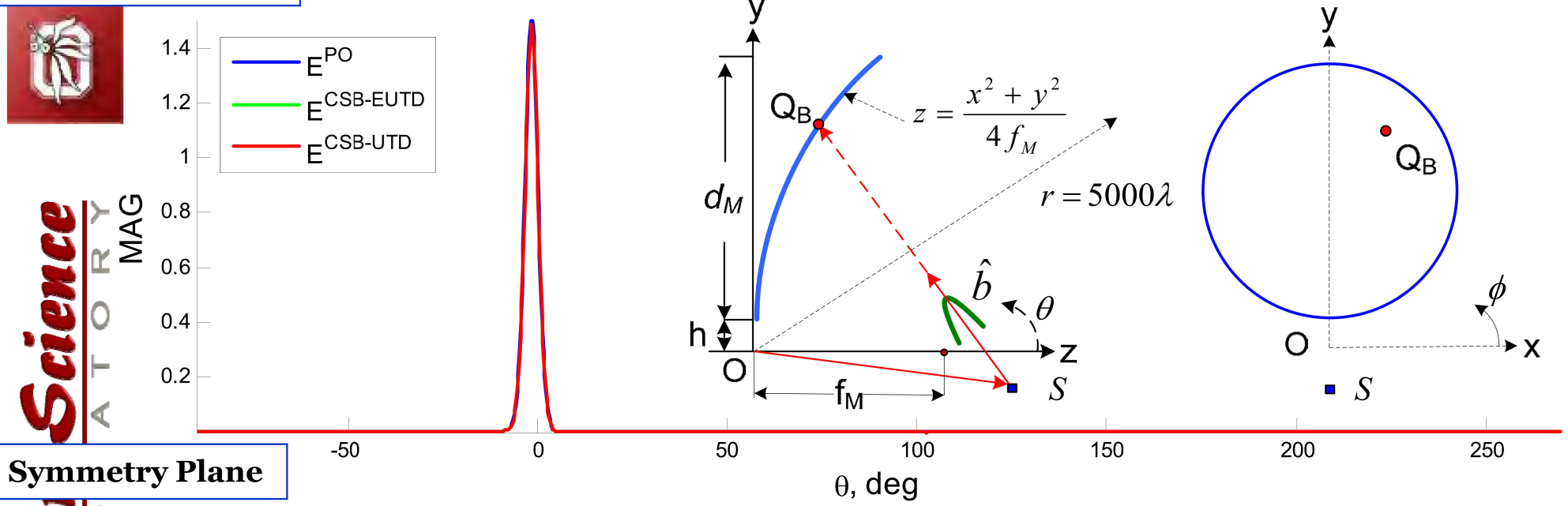

Symmetry Plane

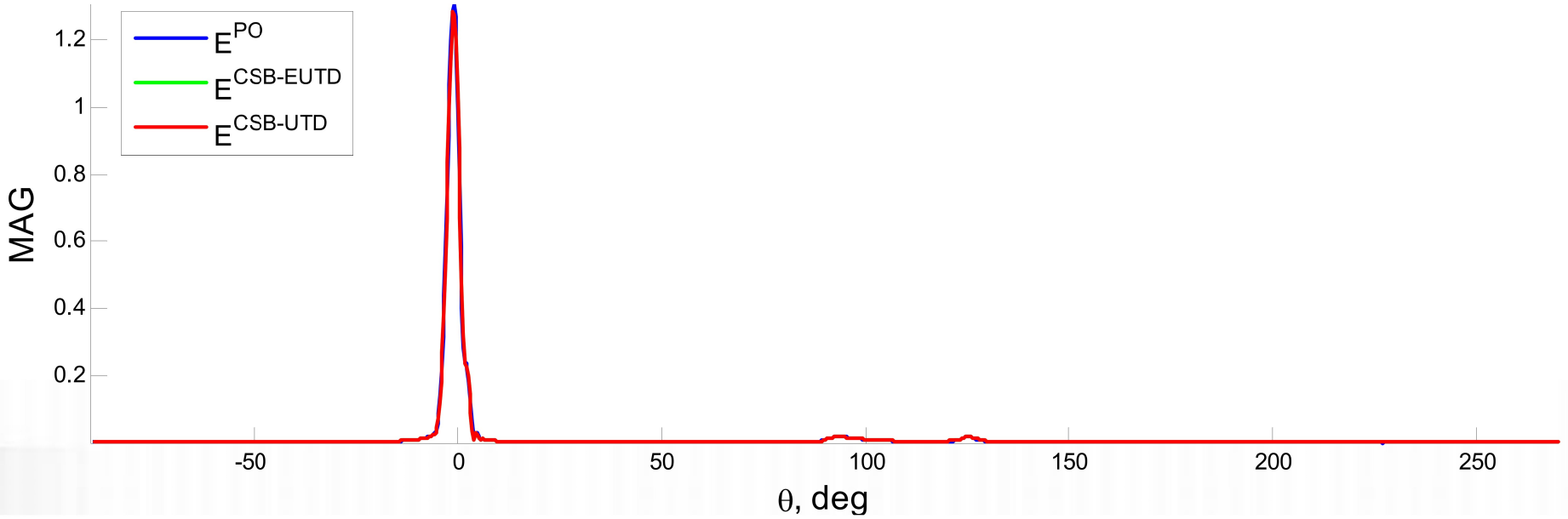

CSB-UTD Diffraction by a Curved Wedge (cont.)

Numerical Result* : *Finite parabolic reflector illuminated by a CSB

Transverse Plane

$d_M = 60\lambda,\ h = 5\lambda,\ f_M = 35\lambda,\ b = 10\lambda,\ \hat{p} \perp \hat{b},\ Q_B = (20\lambda, 60\lambda),\ S = (40\lambda, 100°, 270°)$

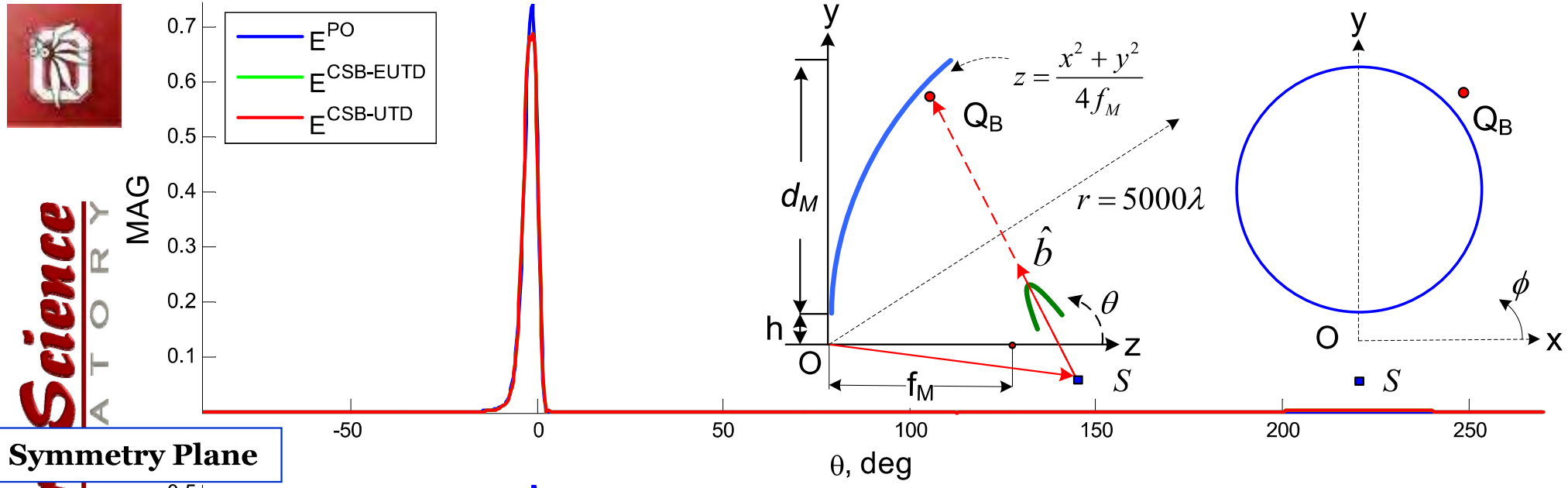

Symmetry Plane

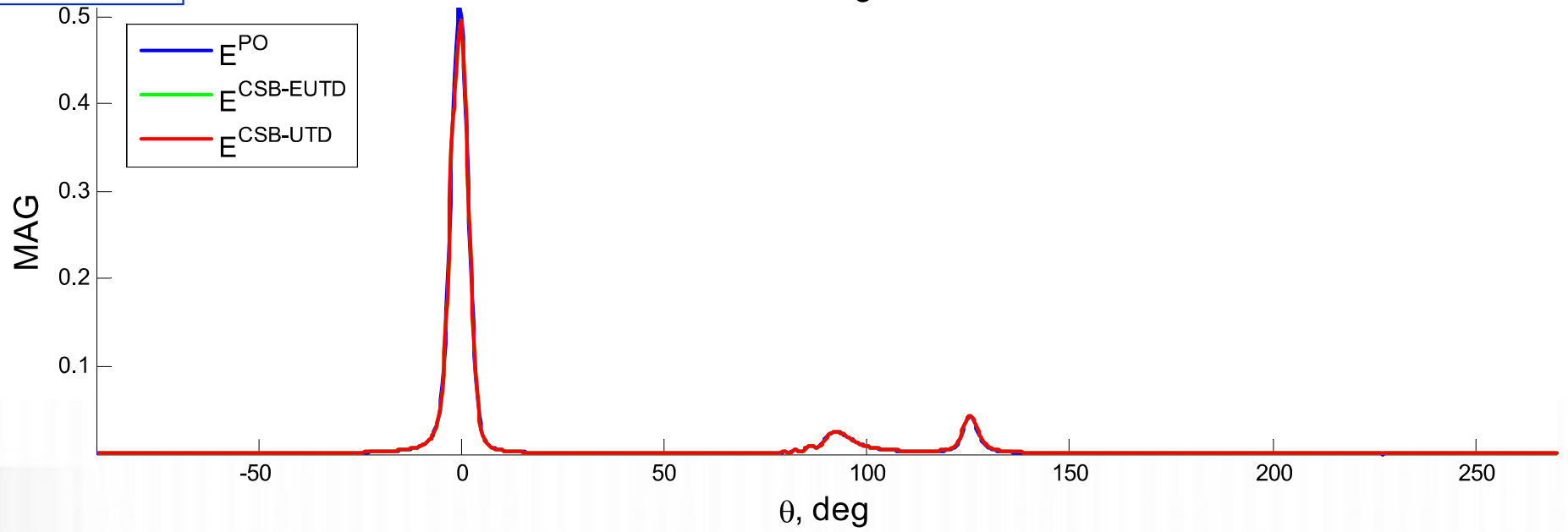

CSB-UTD Diffraction by a Curved Wedge (cont.)

Numerical Result ***: Finite parabolic reflector illuminated by a CSB***

Transverse Plane

$d_M = 50\lambda,\ f_M = 30\lambda,\ b = 10\lambda,\ \hat{p} = \hat{x}\ \ Q_B = (-17\lambda, 10\lambda),\ \ S = (40\lambda, 0°, 90°)$

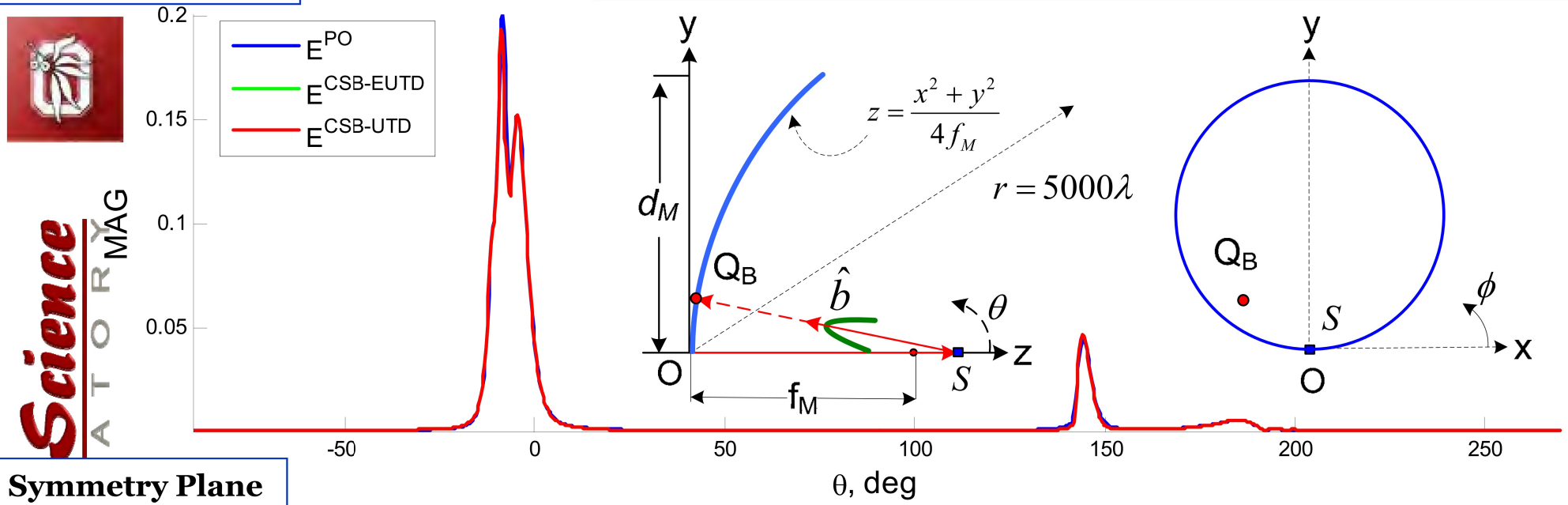

Symmetry Plane

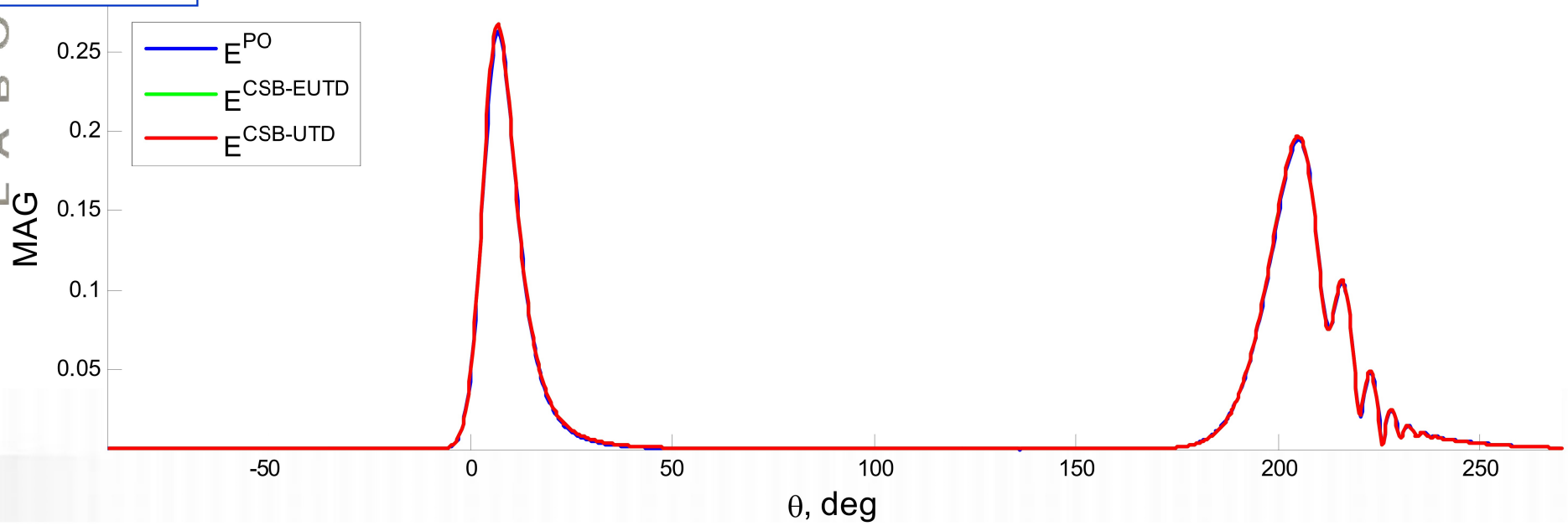

CSB-UTD Diffraction by a Curved Wedge (cont.)

Numerical Result* : *Finite parabolic reflector illuminated by a CSB

Transverse Plane

$d_M = 50\lambda,\ f_M = 30\lambda,\ b = 15\lambda,\ \hat{p} \perp \hat{b}\ \ Q_B = (-20\lambda, 35\lambda),\ \ S = (40\lambda, 10°, 0°)$

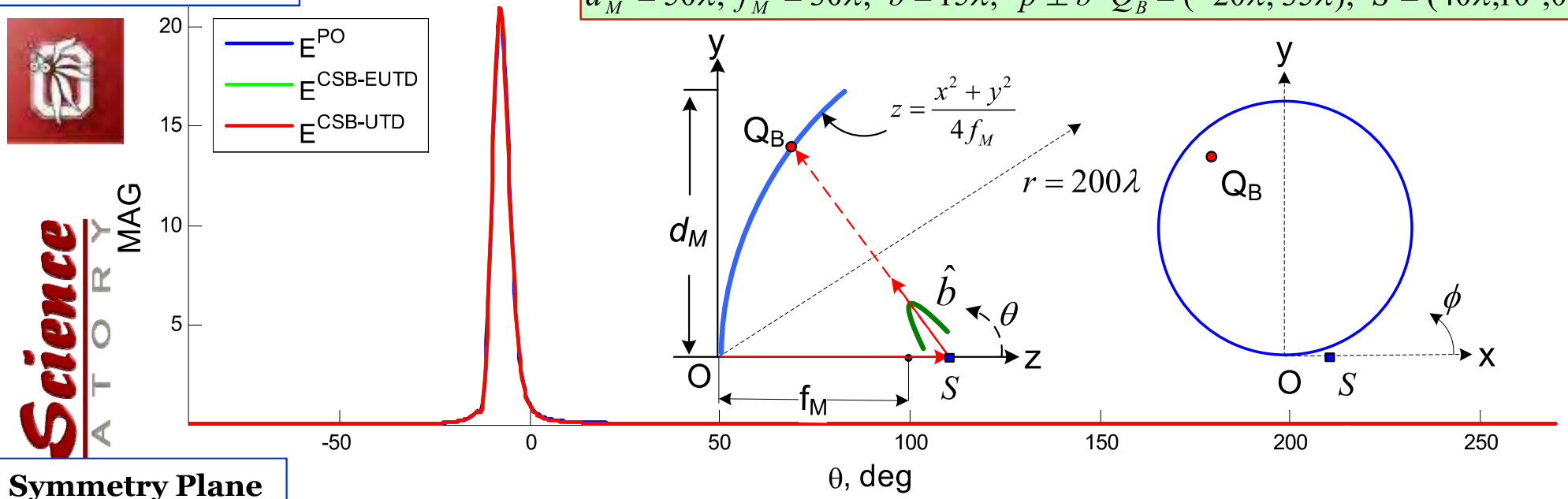

Symmetry Plane

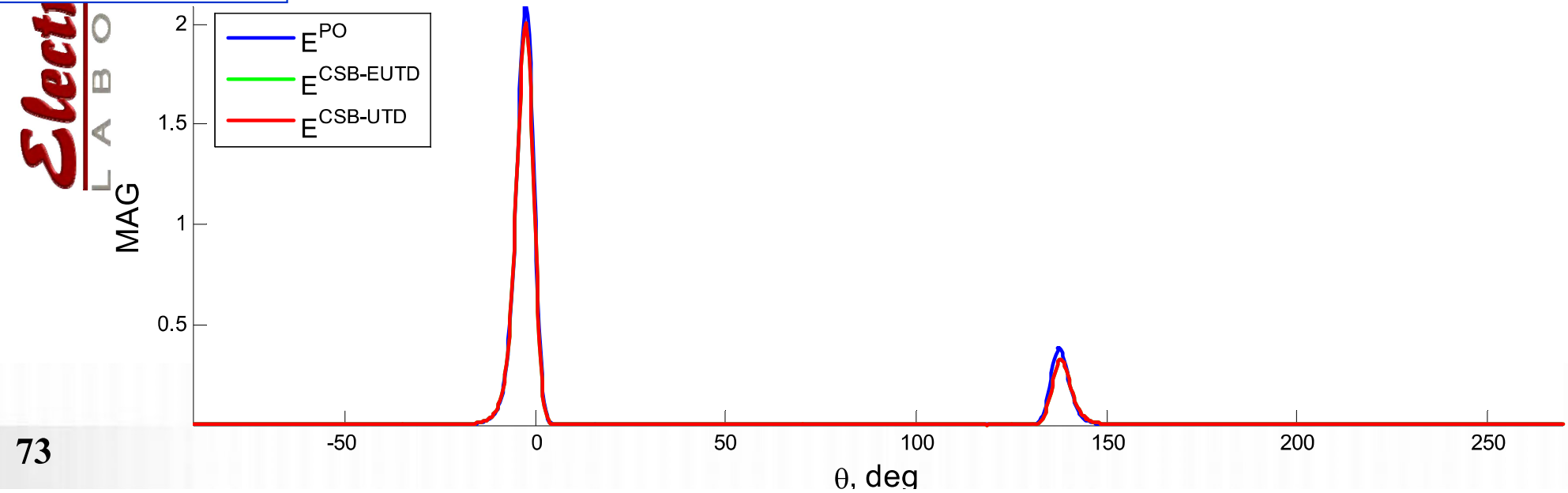

CSBs/GBs Illuminating a reflector

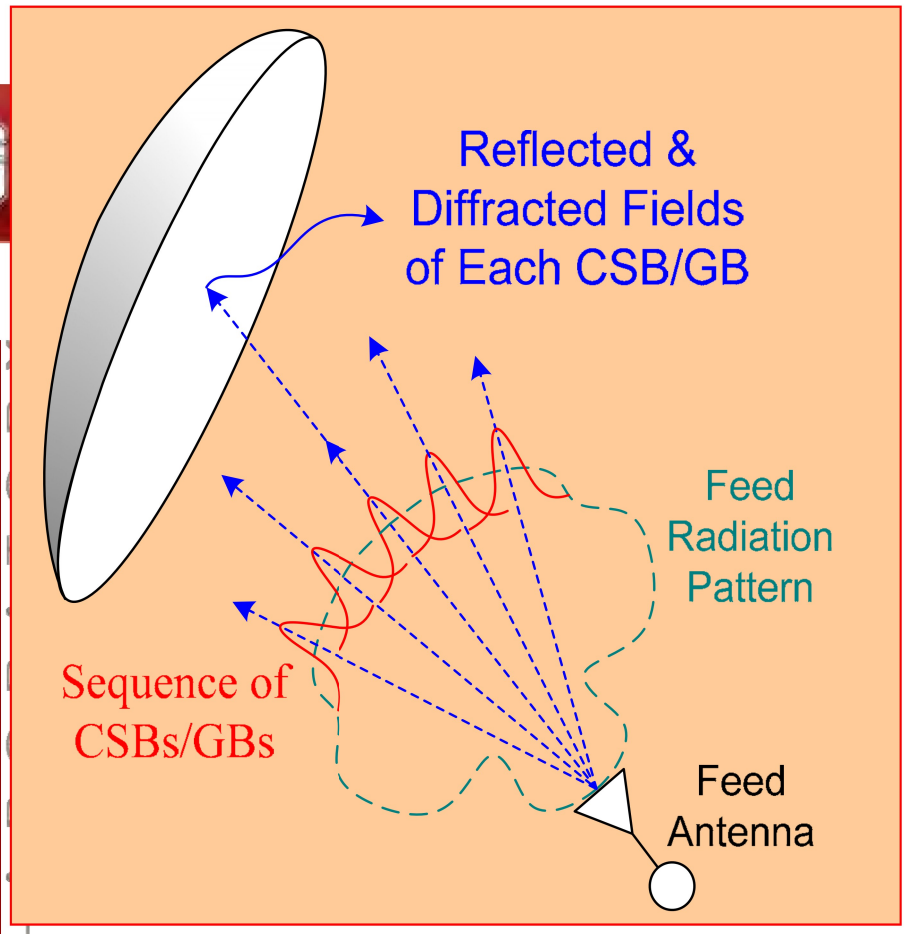

$$\overline{H}_f^i(\overline{r}_f) \sim \frac{e^{-jkr_f}}{r_f}\left[\hat{\theta}_f F_\theta(\hat{r}_f) + \hat{\phi}_f F_\phi(\hat{r}_f)\right]$$

$$\overline{E}_f^i(\overline{r}_f) \sim -Y_0 \hat{r}_f \times \overline{H}_f^i(\overline{r}_f)$$

Feed Radiation

$$\overline{H}_f^i(\overline{r}_f) \cong \sum_{n=1}^{N}\sum_{m=1}^{M} C_{nm}\overline{H}_{nm}(\overline{r}_{fnm})e^{j\psi_{nm}}$$

GB Expansion

n = launching points in feed plane

m = number of GBs from each n

Offset Shaped Reflector for CONUS Contour Beam Using GBs

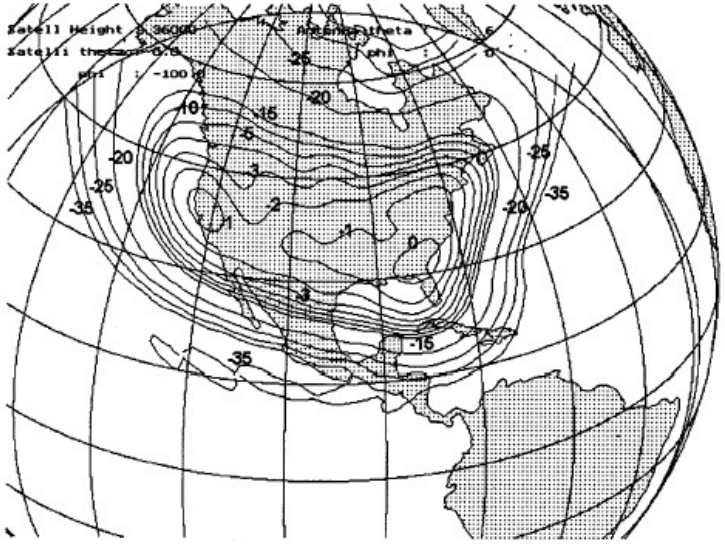

Normalized co-polarized contours based on the GB approach CONUS coverage by a shaped concave reflector with a feed pattern at 12 GHz with I =18.51. Approximately 200GBs were used.

$$D = 85\lambda$$

< 200 GBs

Time < 5 min/iter

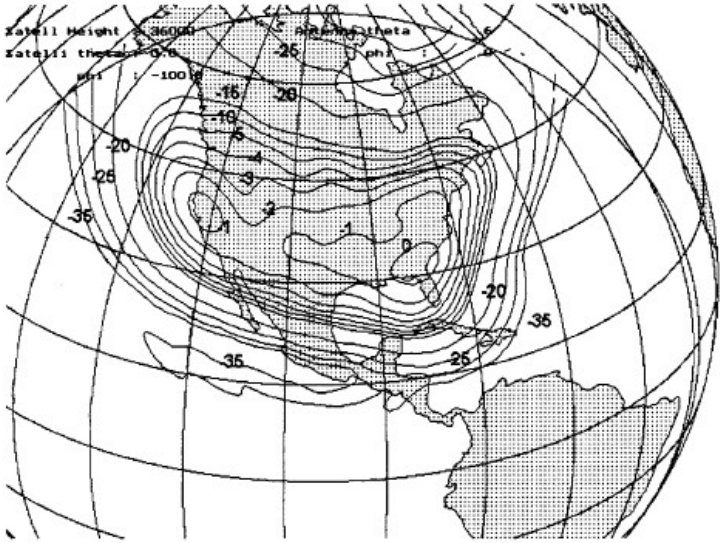

NUM-PO

Time = 5 or 6 hrs/iter

Approx. 30 iter's*

* Rahmat-Samii's paper

?

Normalized co-polarized gain contours based on the numerical PO integration approach for the same shaped reflector case as above.

Conclusions

• CSB expansion methods for EM radiation are presented employing three different variants of the surface equivalence theorem.

• The analytical properties (validity region, truncation, etc.) of the approach are investigated.

• It is shown that accurate and efficient field representations can be obtained by conveniently truncating the beam expansion.

• It is demonstrated that the expansion idea is applicable to a class of EM radiation/scattering problems.

Computational Methods

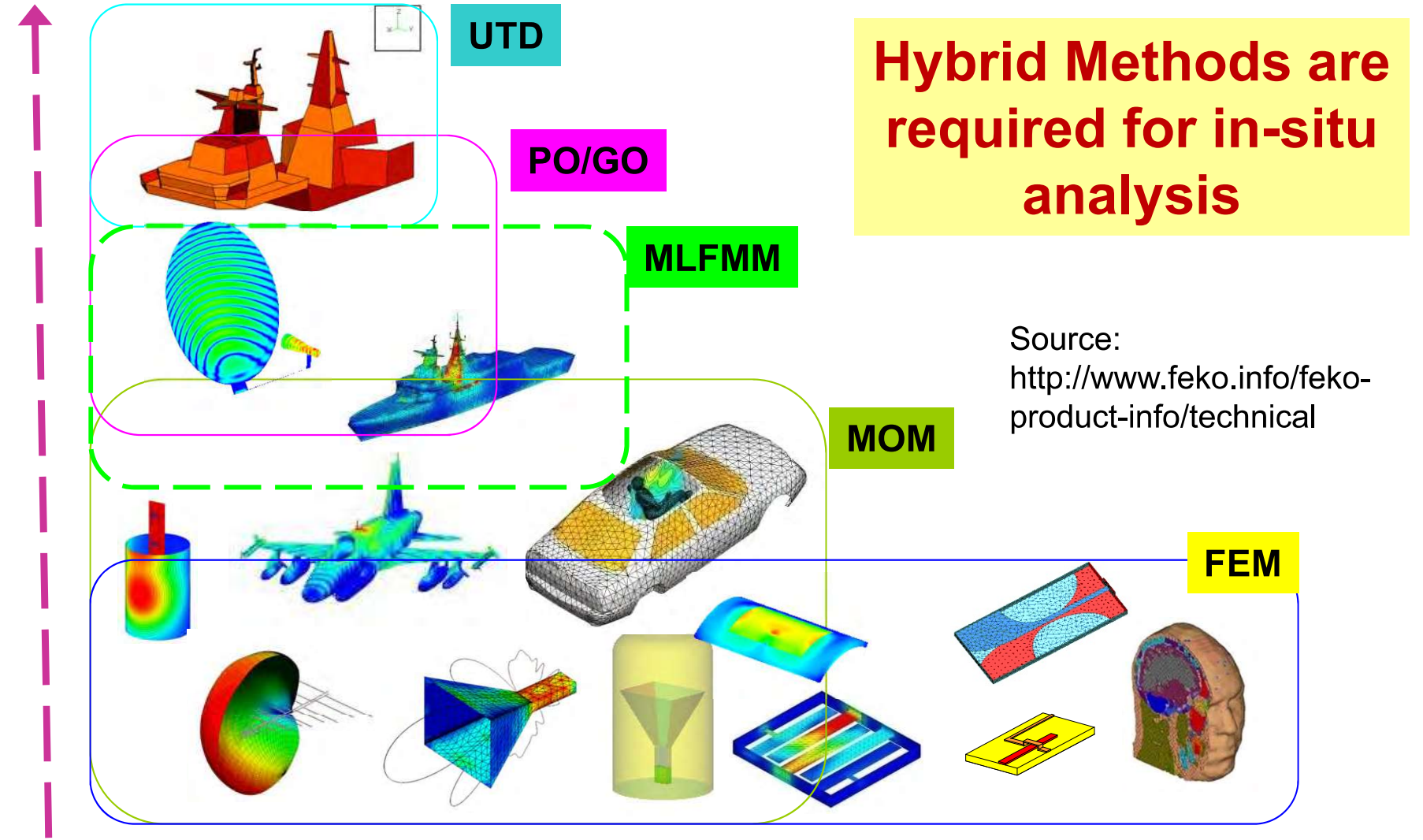

Hybrid Methods are required for in-situ analysis

Source: http://www.feko.info/feko-product-info/technical

ElectroScience LABORATORY

Hybrid Method & Some Applications

ElectroScience LABORATORY

• In many applications, large antennas (arrays) and large antenna platforms contain both large and small features in terms of wavelength.

•For electrically large parts on radiating object, UTD ray method is useful but not valid for electrically small portions.

•For highly inhomogeneous and electrically small region (e.g. complex antenna elements/arrays) the FE-BI or numerical methods are useful, and UTD is not applicable here.

•A hybrid combination of FE-BI (or other suitable numerical methods) and UTD could handle the entire problem not otherwise tractable by each single approach by itself.

Conformal Array Configurations

Simple slot phased array in a convex PEC surface

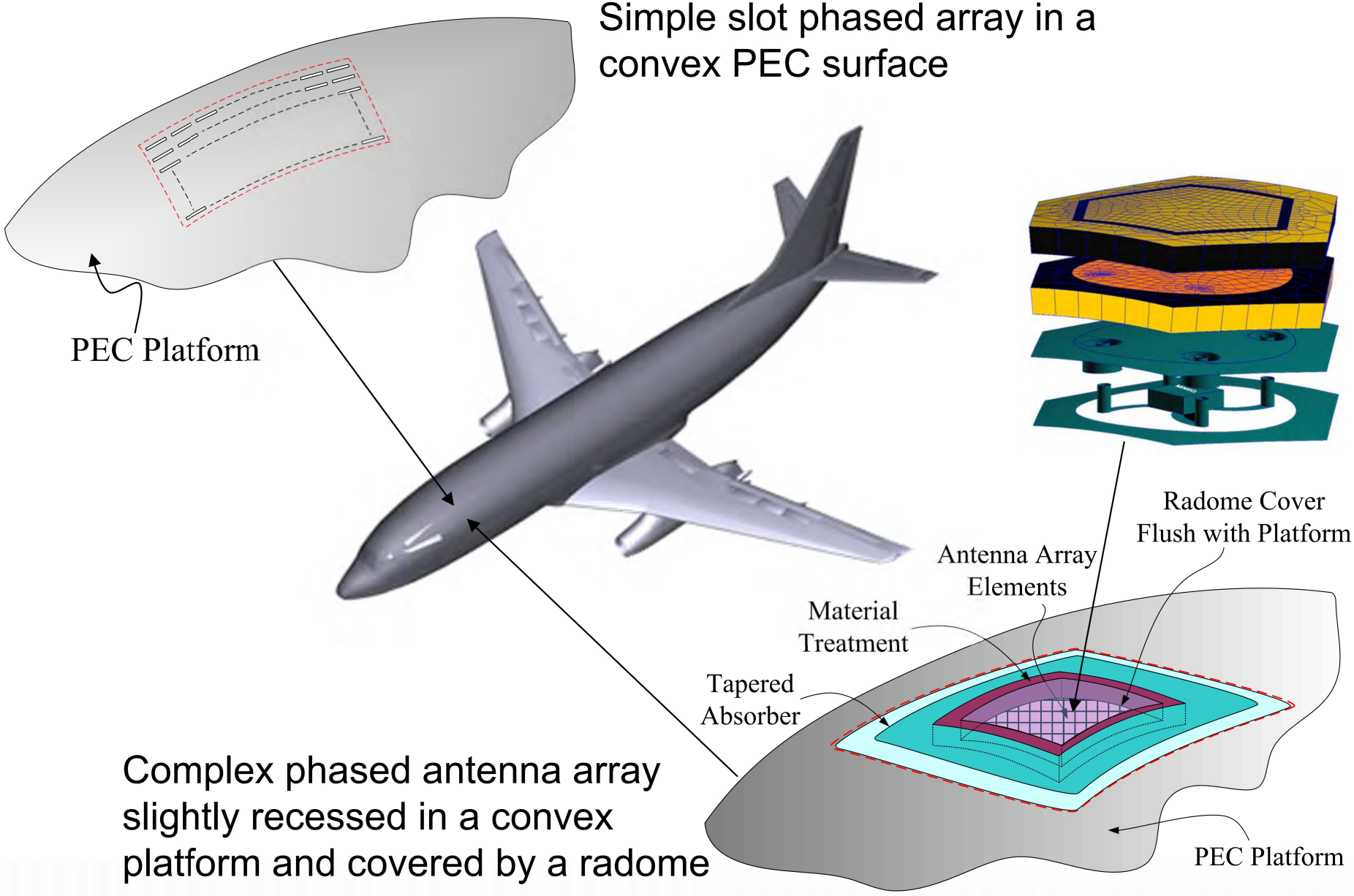

Complex phased antenna array slightly recessed in a convex platform and covered by a radome

Proposed Hybrid Numerical-UTD Approach

ElectroScience LABORATORY

Local Array Part
treated by full wave numerical methods.

Present Collective UTD Solution
converts numerical array solution into rays launched from array aperture.

External Platform Part
Collective UTD rays launched from aperture efficiently excite external platform which is analyzed by UTD.

Local Array Part Treated by FEM, FE-BI

ElectroScience LABORATORY

Actual problem

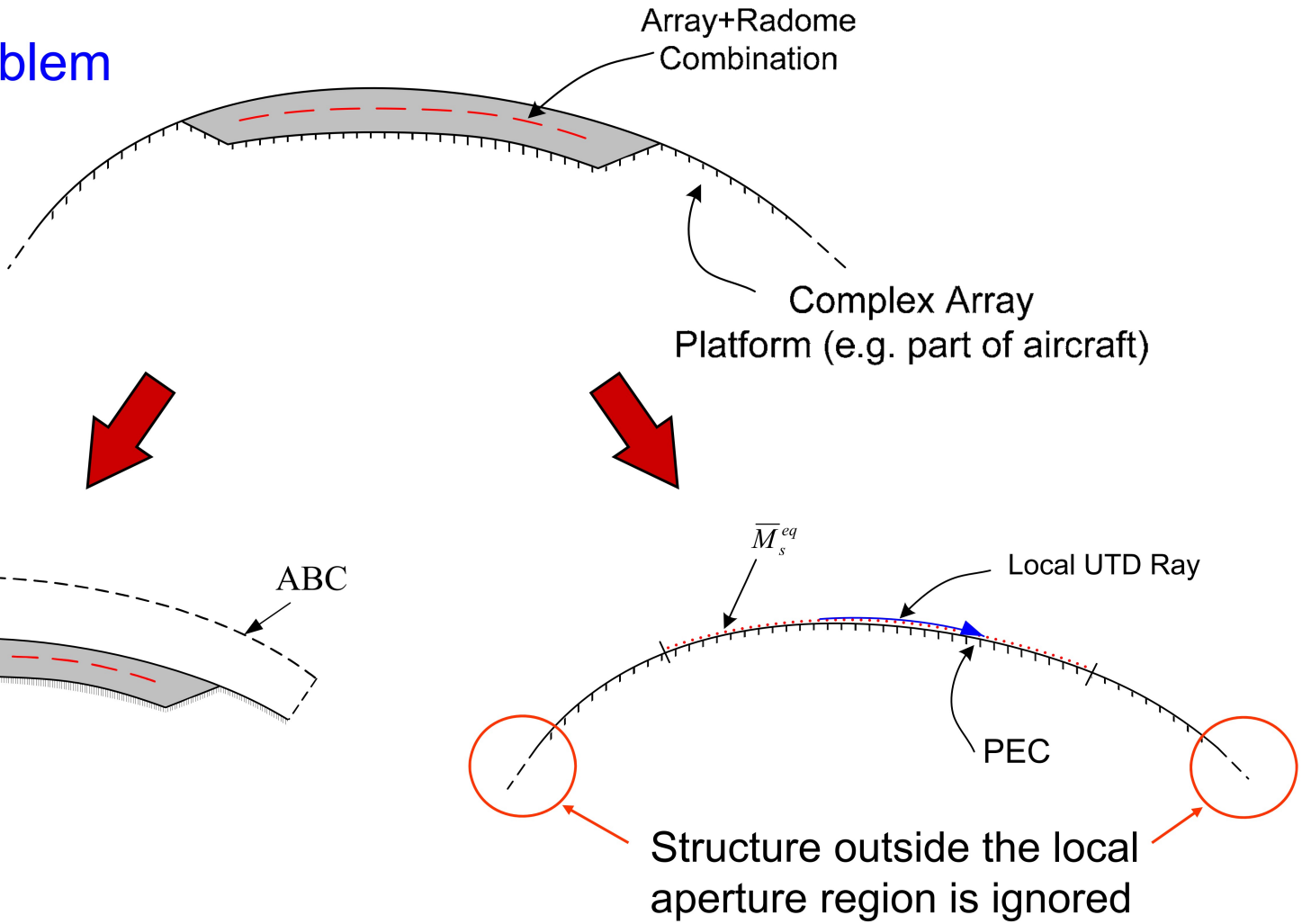

A local array modeling for **FEM**

A local array modeling for **FE-BI**

Collective UTD Rays

Panuwat Janpugdee and Prabhakar H. Pathak

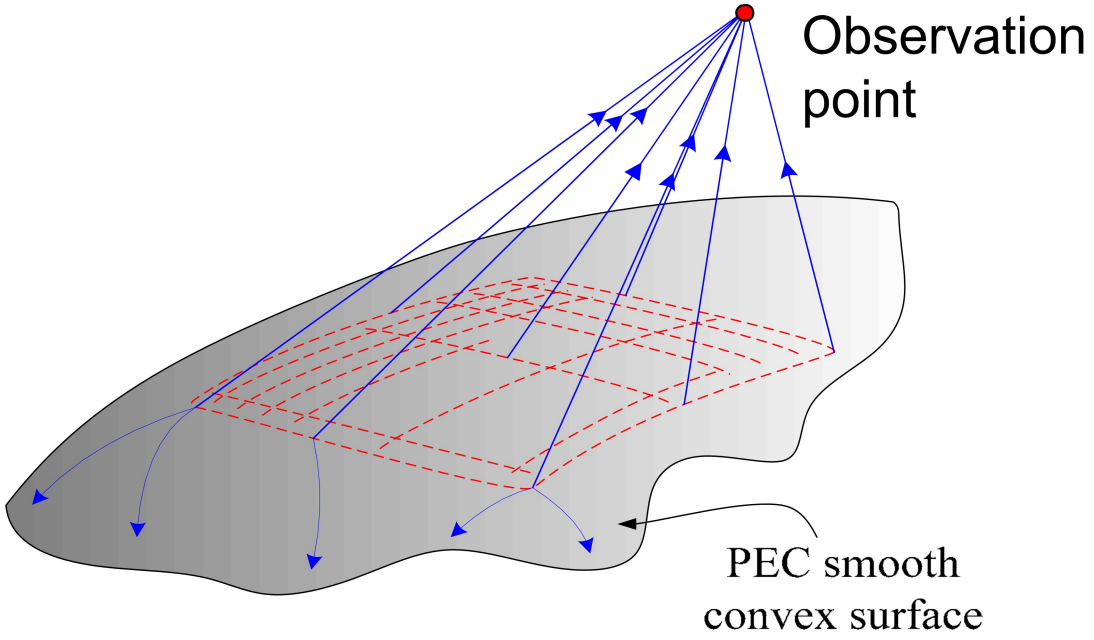

- Collective UTD rays launched by array aperture distribution obtained via numerical solution to local array part.
- Collective UTD rays launched from a few flash points in the array aperture.

External Platform Interaction Part

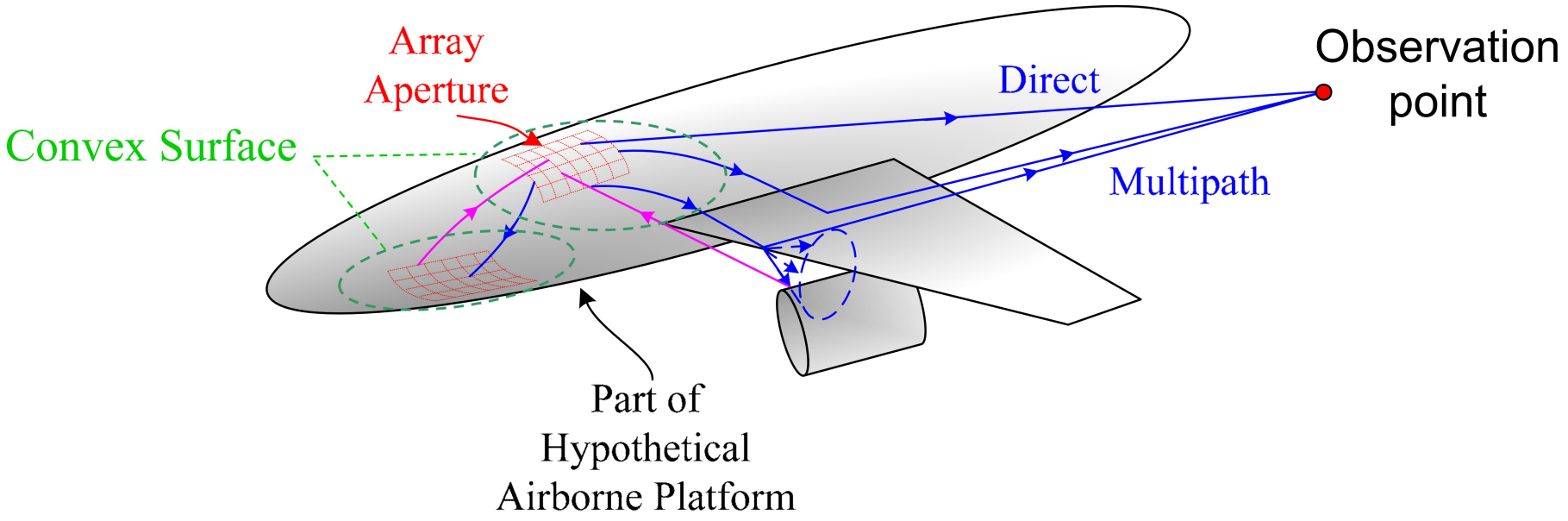

- Collective UTD rays efficiently launched from array aperture interact with external platform.
- Rays from platform could interact back with the array and so on. These effects can be included if desired.
- Collective UTD surface rays provide direct coupling between two arrays located on the same platform.

Comparison with Conventional Element-by-element UTD Field Summation Approach

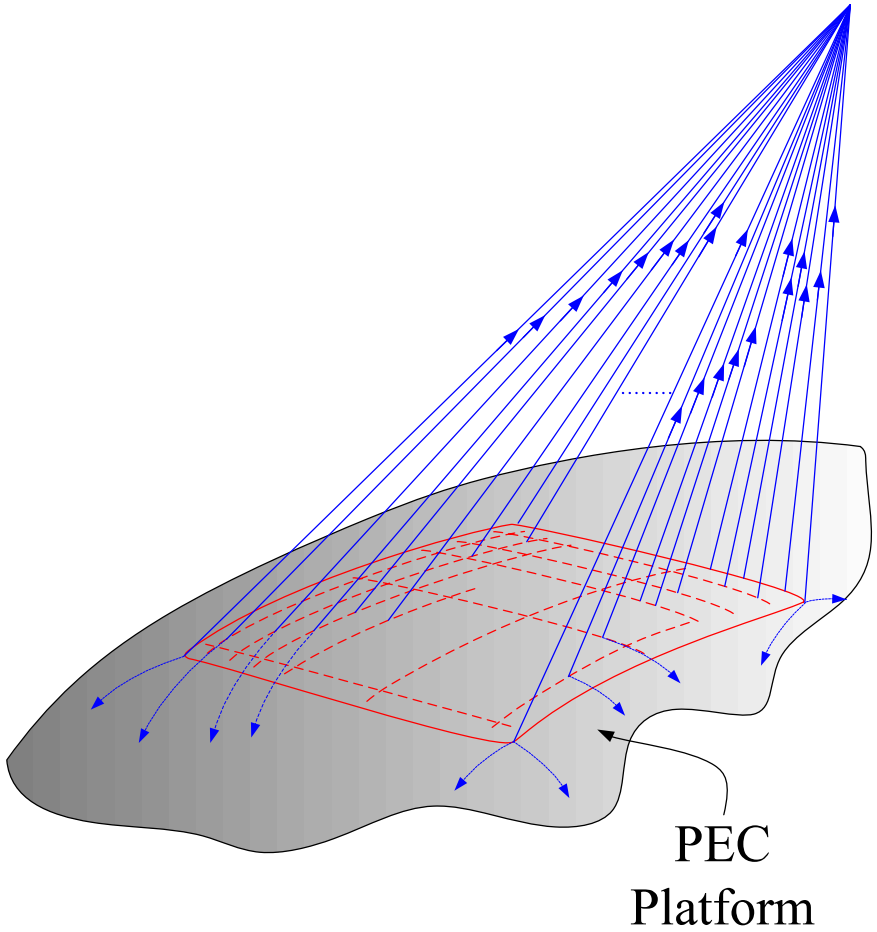

Less efficient for large arrays – need to trace a large number of rays (with all the **constructive & destructive interference** effects).

Lacks physical picture for describing collective array radiation and surface field excitation mechanisms.

Integration to existing UTD codes for predicting the platform interaction effects via UTD is straightforward – but less efficient.

Conventional EBE Sum Utilizes UTD Solution for a Single Current Source

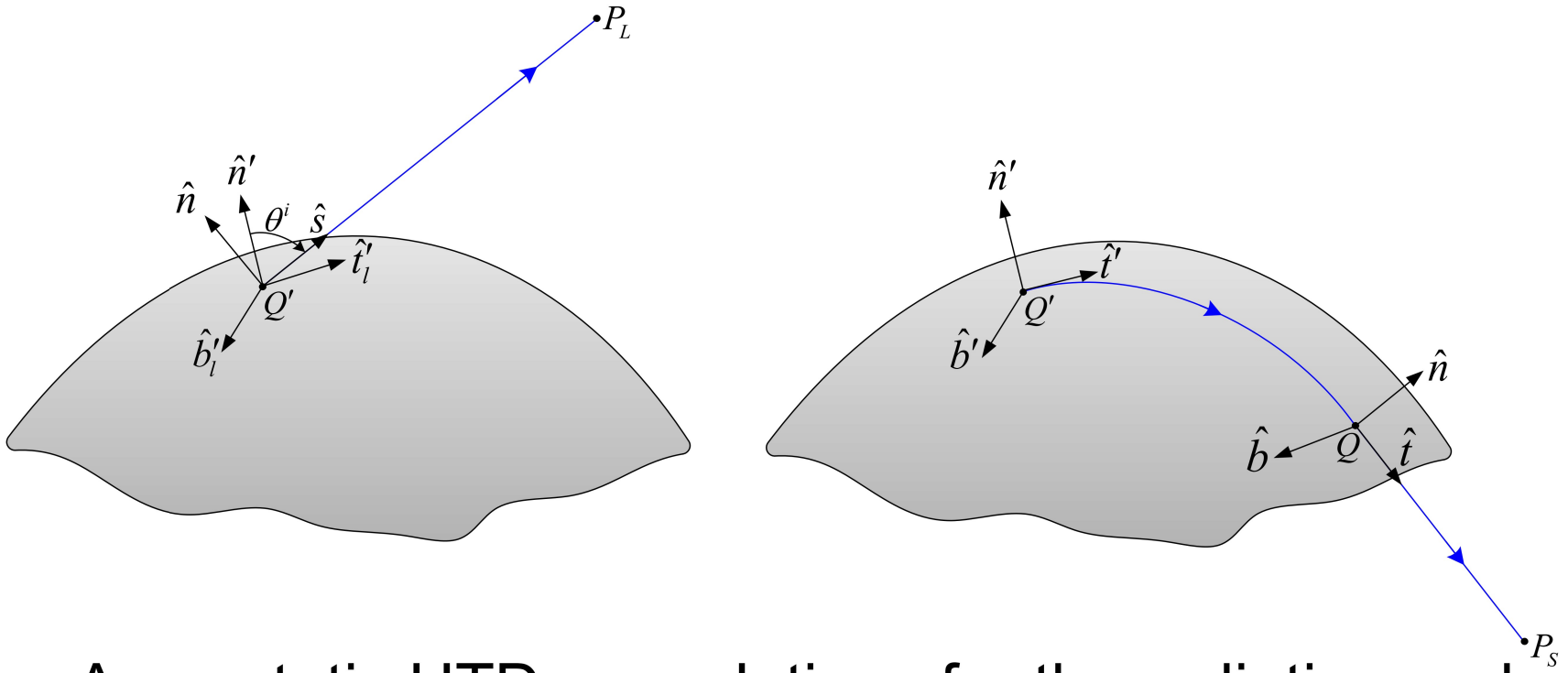

- Asymptotic UTD ray solutions for the radiation and surface fields produced by a **single point current source** on a smooth convex surface have been developed previously by Pathak *et al*.

Pathak *et al*., *IEEE Trans. AP*, vol. AP-29, pp. 609-622, Jul. 1981.
Pathak *et al*., *IEEE Trans. AP*, vol. AP-29, pp. 911-922, Nov. 1981.

Example of a LARGE Array

Hypothetical Example

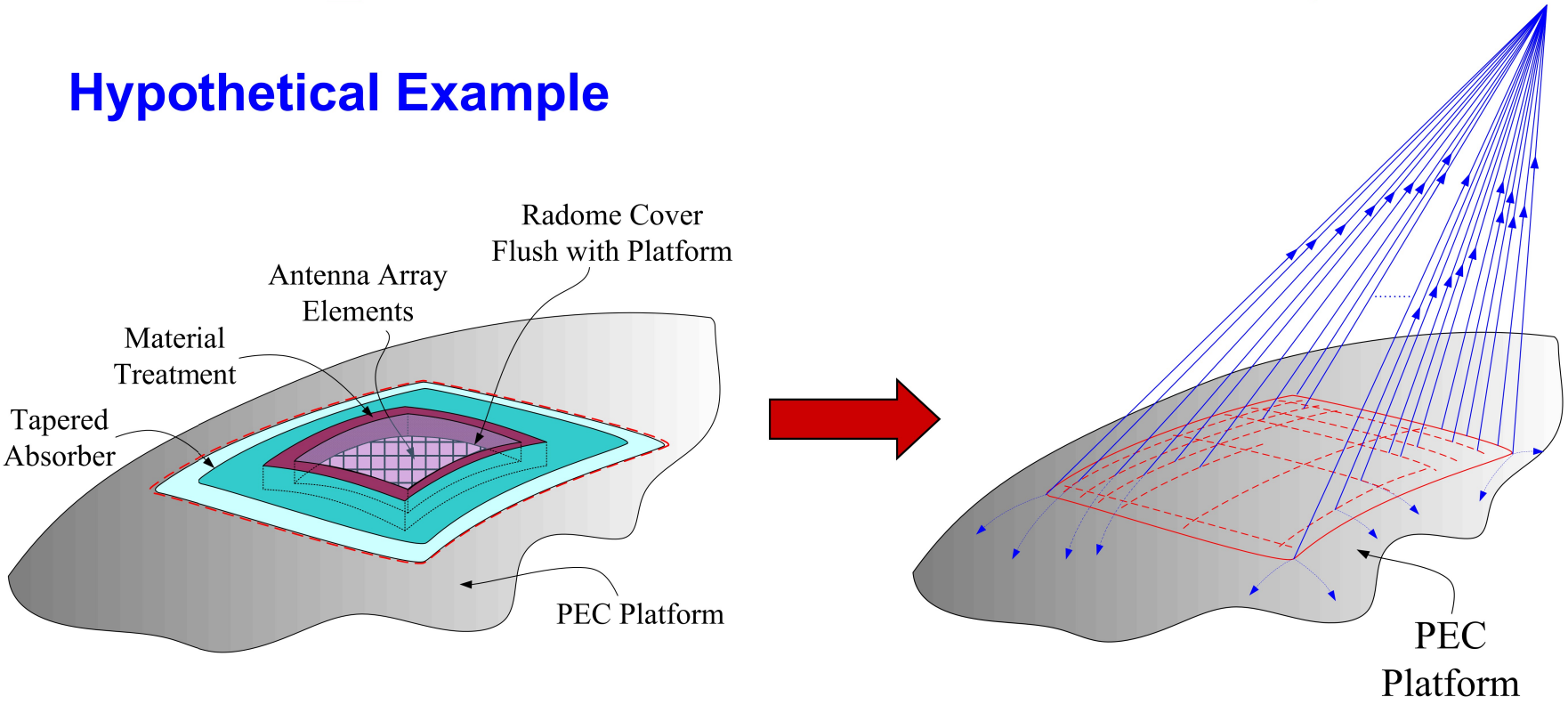

- Antenna array operated at 25 GHz (K-band); λ = 1.2 cm
- Aperture size = 1 ft. $\times$ 1 ft. = 25.4 $\lambda \times$ 25.4 λ
- If sampling at every $\lambda/4$, one needs $\approx 102 \times 102$ (**10,404**) sample points and needs to trace such large number of rays.
- Conventional UTD approach becomes less efficient than collective UTD approach.

Present Collective UTD Ray Approach

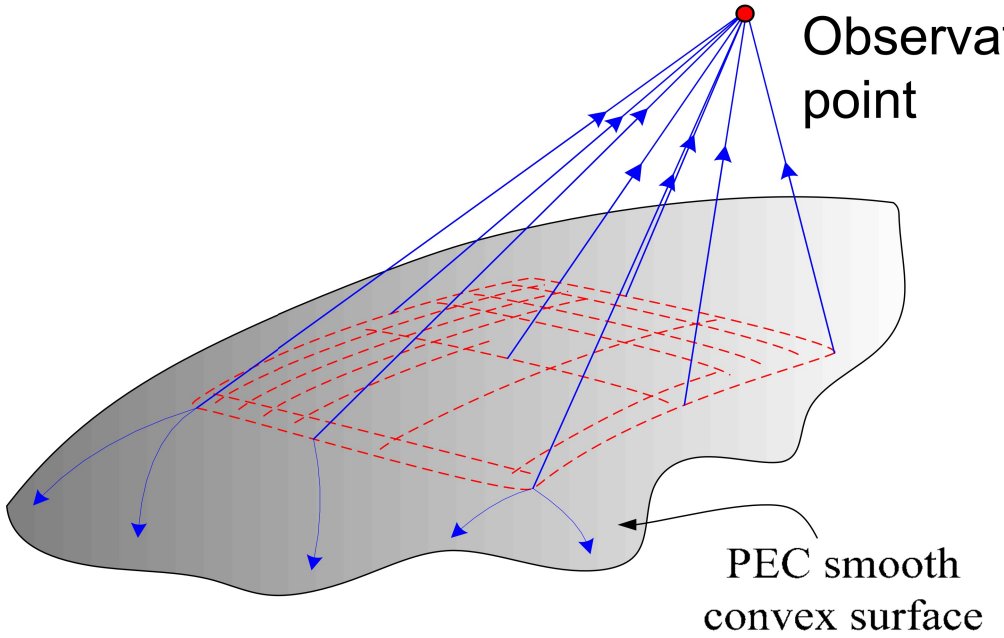

☺ Describes fields produced by the whole array aperture at once in terms of only a few UTD rays arising from specific points in the interior, and on the boundary of the array aperture – **highly efficient**.

☺ **Provides physical picture** for describing collective array radiation and surface field excitation mechanisms.

😐 Integration to most existing UTD codes for predicting the platform interaction effects via UTD is not direct because it requires some code modifications to allow for a new input description.

Curved Surface Modeling

- A scanning phased array on a slowly varying convex platform can be modeled by a parametric surface patch, such as a **bi-quadratic** surface, etc.

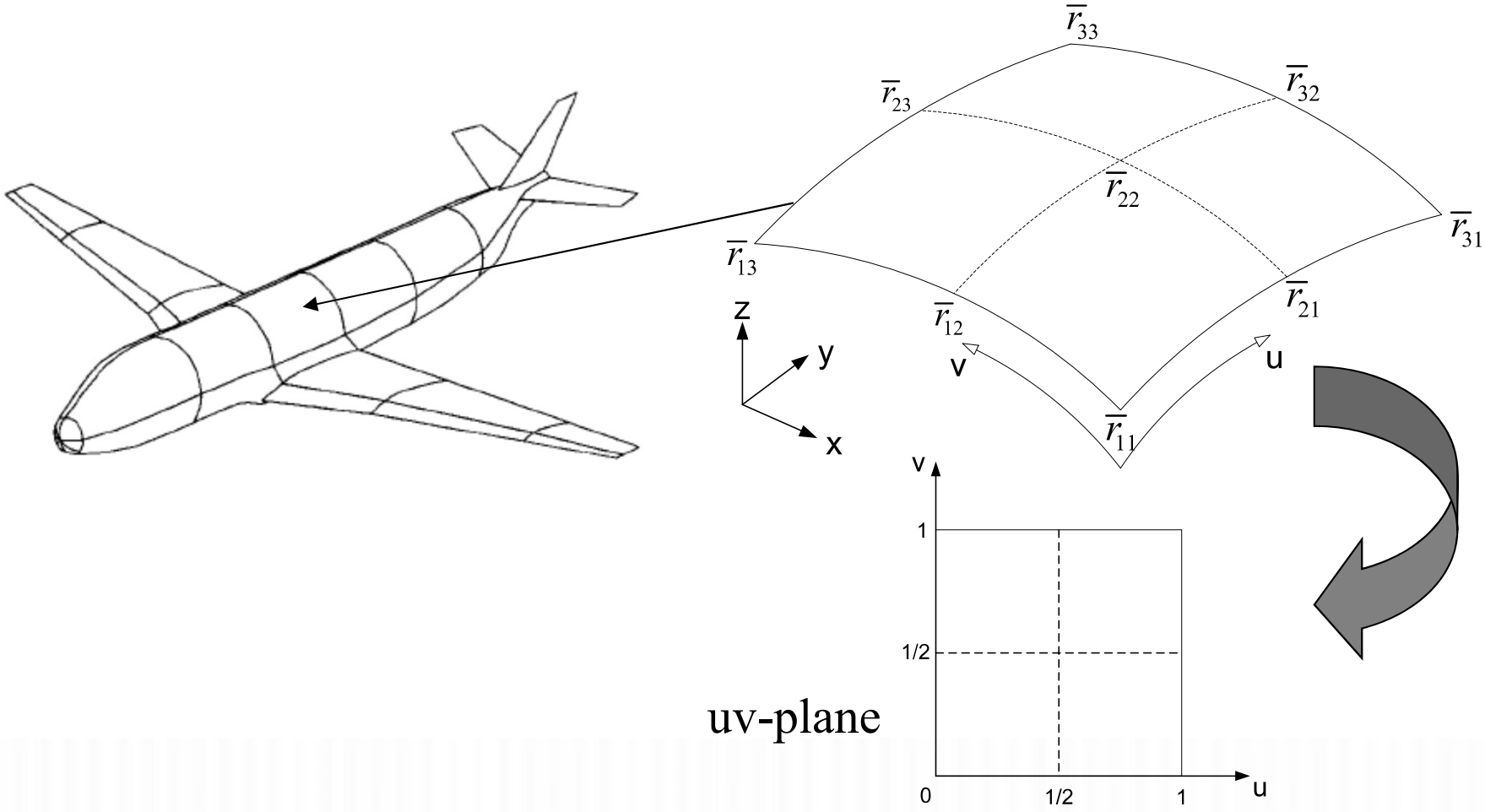

Traveling Wave Expansion

- A traveling wave (**TW**) expansion for realistic aperture distributions obtained from **FEM**, **FE-BI**, etc.

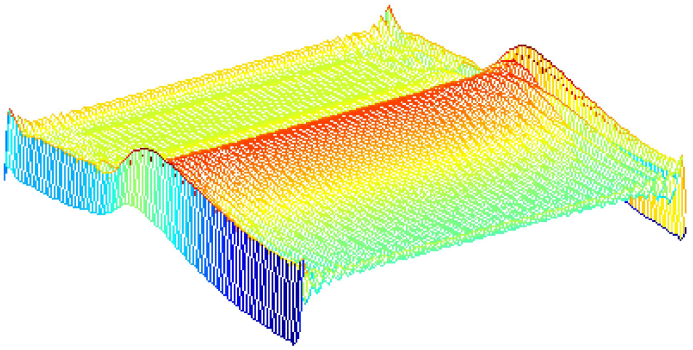

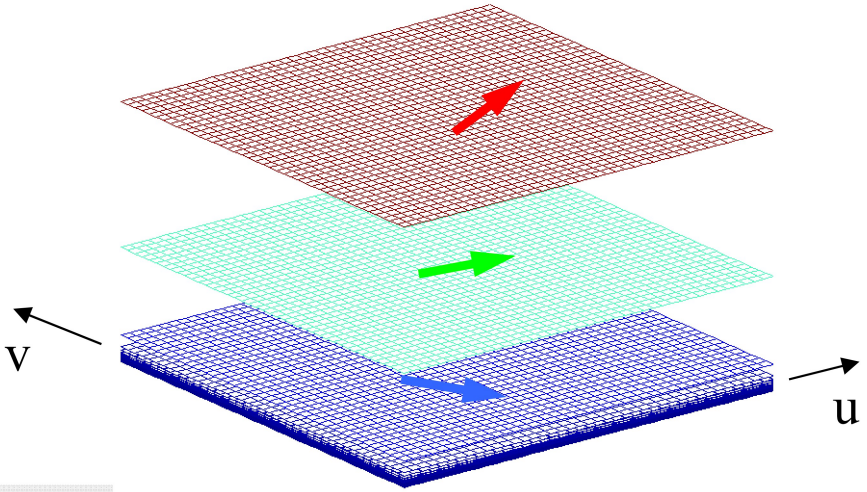

$$A(\vec{r}'(u,v)) \approx \sum_{i=1}^{K} C_i e^{-j(\beta_u^i u + \beta_v^i v)}$$

uv-space

Found numerically by matching to the actual distribution

* Fields produced by each **TW** can be represented in terms of a set of **UTD** rays.

TW Extraction Methods

ElectroScience LABORATORY

- DFT (**D**iscrete **F**ourier **T**ransform)
- CLEAN (or “Extract and Subtract”)
- Prony’s Method
- Other Available Methods

Collective UTD Ray Fields

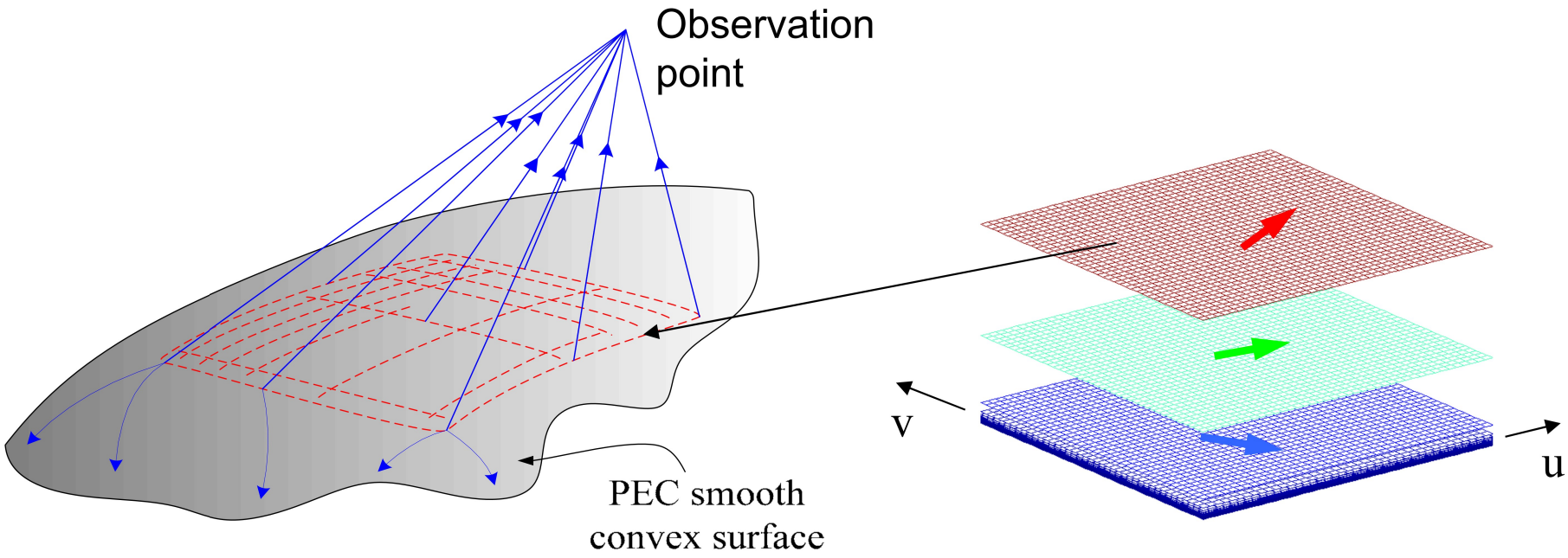

Each TW current radiates a small set of **collective** UTD rays.

$$\overline{E}(P) \approx \sum_{l=1}^{K} \overline{E}^{l}_{UTD}$$

Transition fields

$$\overline{E}_{UTD} = \overline{E}^{GO} U_{GO} + \sum_{i=1}^{4} \overline{E}^{ed}_{i} U_{ei} + \sum_{j=1}^{4} \overline{E}^{cd}_{j} + \left\{ \Delta\overline{E}^{GO} + \sum_{i=1}^{4} \Delta\overline{E}^{ed}_{i} \right\}$$

Geometrical Optics or Local Floquet Wave

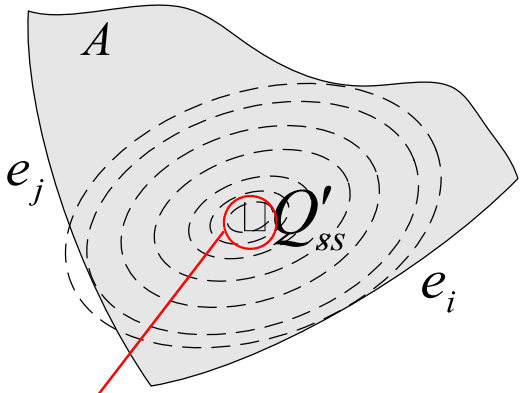

Astigmatic Ray Field

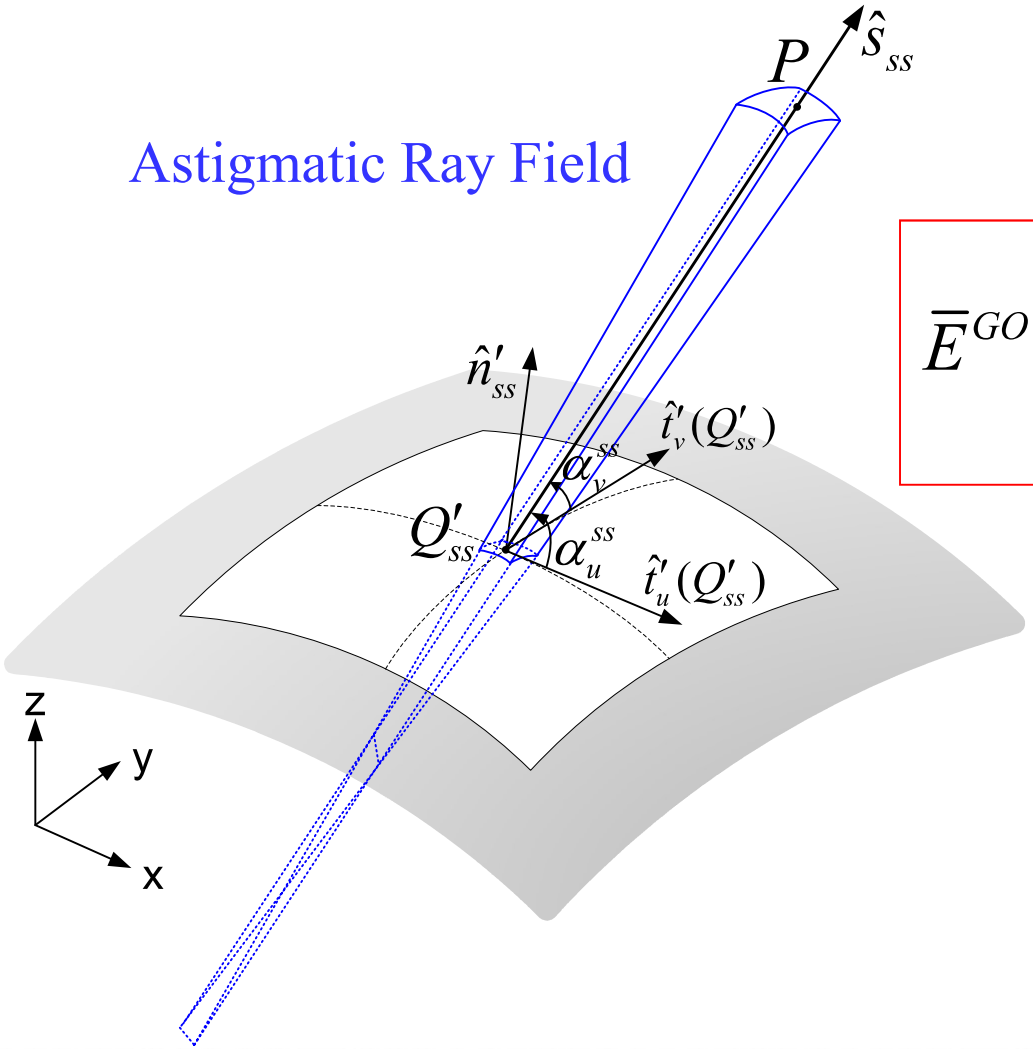

$$\bar{E}^{GO} = \bar{A}_{ss}\sqrt{\frac{\rho_1^{ss}\rho_2^{ss}}{(\rho_1^{ss}+s_{ss})(\rho_2^{ss}+s_{ss})}}e^{-jks_{ss}}$$

$$\bar{A}_{ss} = \overline{\overline{T}}_L(P\,|\,Q'_{ss})\bullet\hat{\tau}'L_{ss}$$

$$L_{ss} = \frac{(-2\pi j)J(Q'_{ss})}{k\sqrt{\Lambda_{ss}}}e^{-jk\chi(Q'_{ss})}$$

Edge Diffracted Fields

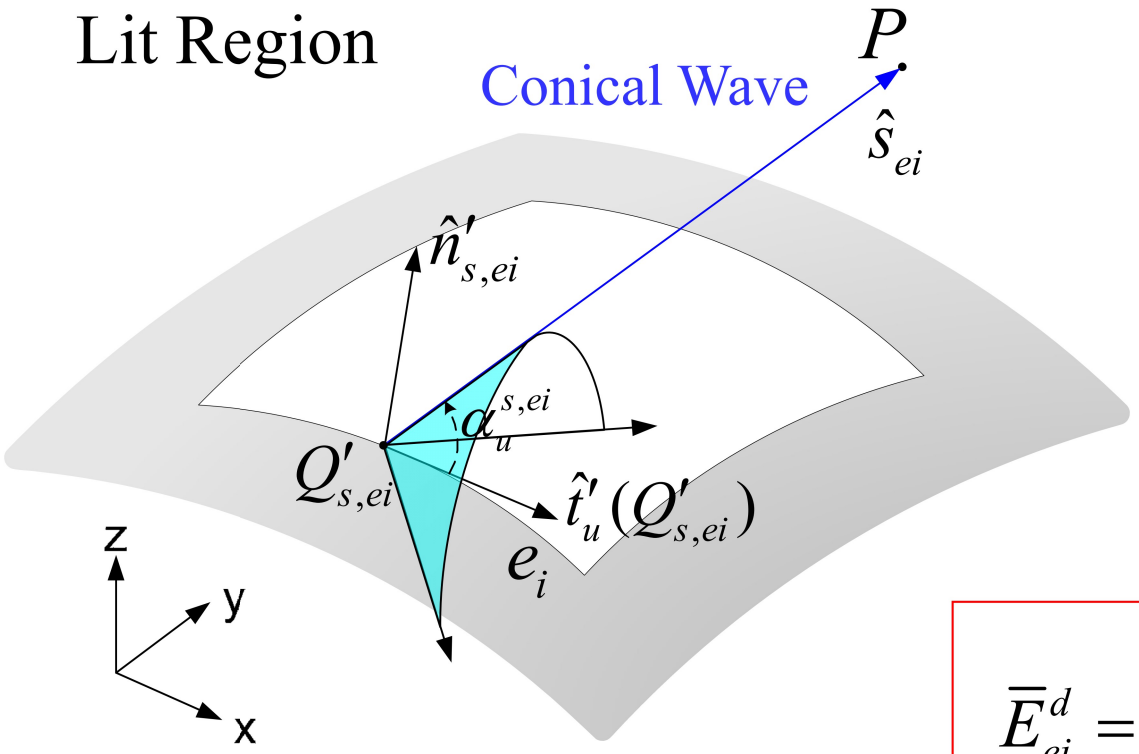

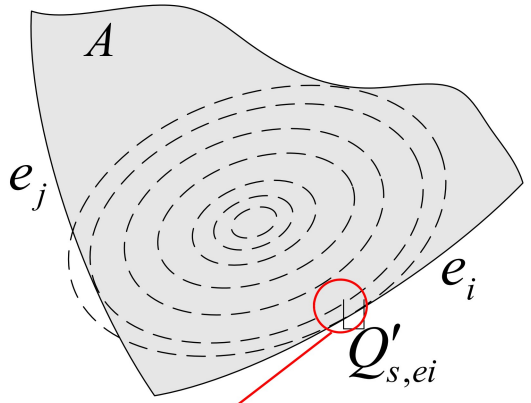

$$\bar{E}^d_{ei} = \bar{A}_{ei}\sqrt{\frac{\rho_{ei}}{s_{ei}(\rho_{ei}+s_{ei})}}e^{-jks_{ei}}$$

$$\bar{A}_{ei} = \overline{\overline{T}}_L(P \mid Q'_{s,ei}) \bullet \hat{\tau}' D^d_{ei}$$

$$D^d_{ei} = \frac{\varepsilon_{ei} j\sqrt{2\pi}e^{-j\pi/4}J(Q'_{s,ei})}{k[\hat{s}_{ei} \bullet \bar{r}'_v - \Omega_v]} \frac{e^{-jk\chi(Q'_{s,ei})}}{\sqrt{k \mid E_{ei} - \Omega_u^2 \mid}}$$

Edge-Excited Surface Diffracted Fields

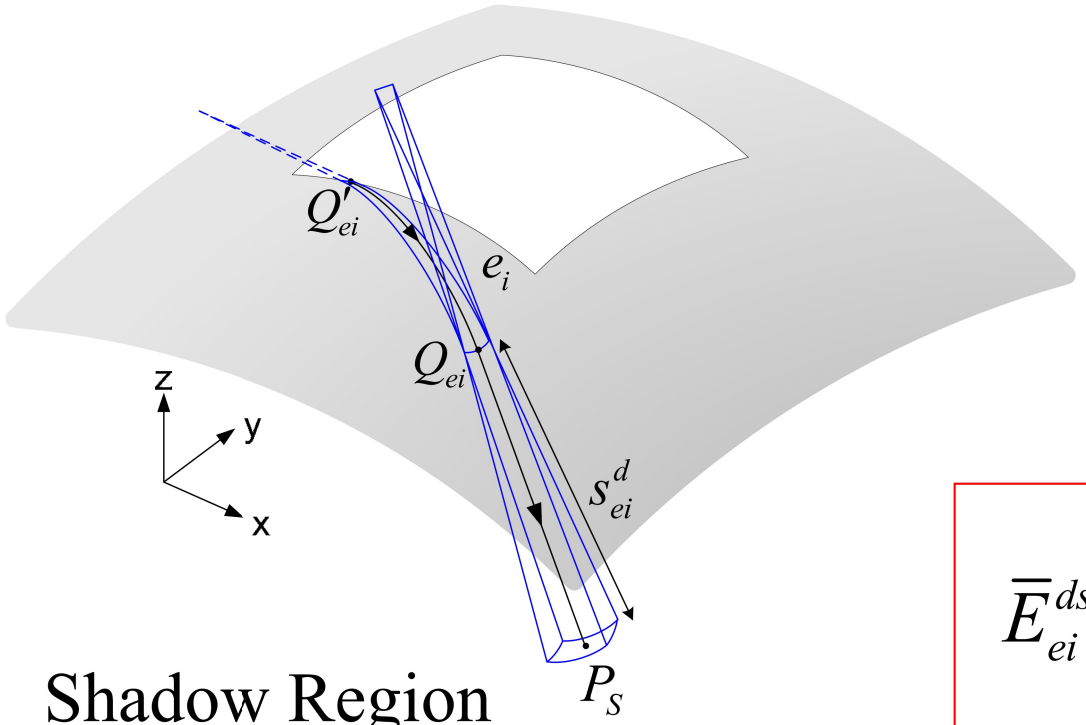

Shadow Region

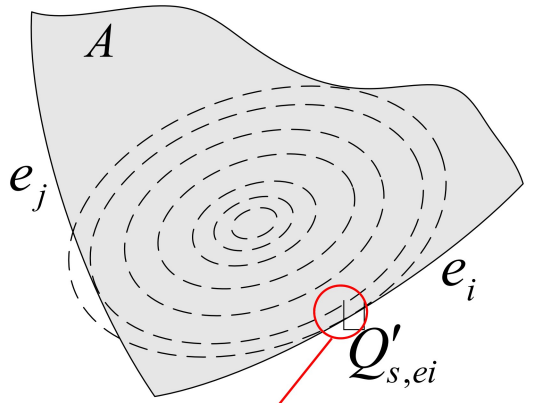

$$\bar{E}^{ds}_{ei} = \bar{A}^{s}_{ei}\sqrt{\frac{\rho^{d}_{ei}}{s^{d}_{ei}(\rho^{d}_{ei}+s^{d}_{ei})}}e^{-jks^{d}_{ei}}$$

$$\bar{A}^{s}_{ei} = \overline{\overline{T}}_S(P\,|\,Q'_{s,ei})\bullet\hat{\tau}' D^{ds}_{ei} e^{-jkt_{ei}}\sqrt{\frac{d\eta(Q'_{s,ei})}{d\eta(Q_{s,ei})}}\left[\frac{\rho_g(Q_{s,ei})}{\rho_g(Q'_{s,ei})}\right]^{1/6}$$

$$D^{ds}_{ei} = \frac{\varepsilon_{ei} j\sqrt{2\pi}e^{-j\pi/4}J(Q'_{s,ei})}{k[\hat{t}'_{ei}\bullet\bar{r}'_v-\Omega_v]}\frac{e^{-jk\chi(Q'_{s,ei})}}{\sqrt{k\,|\,E_{ei}-\Omega^2_u\,|}}$$

Corner Diffracted Fields

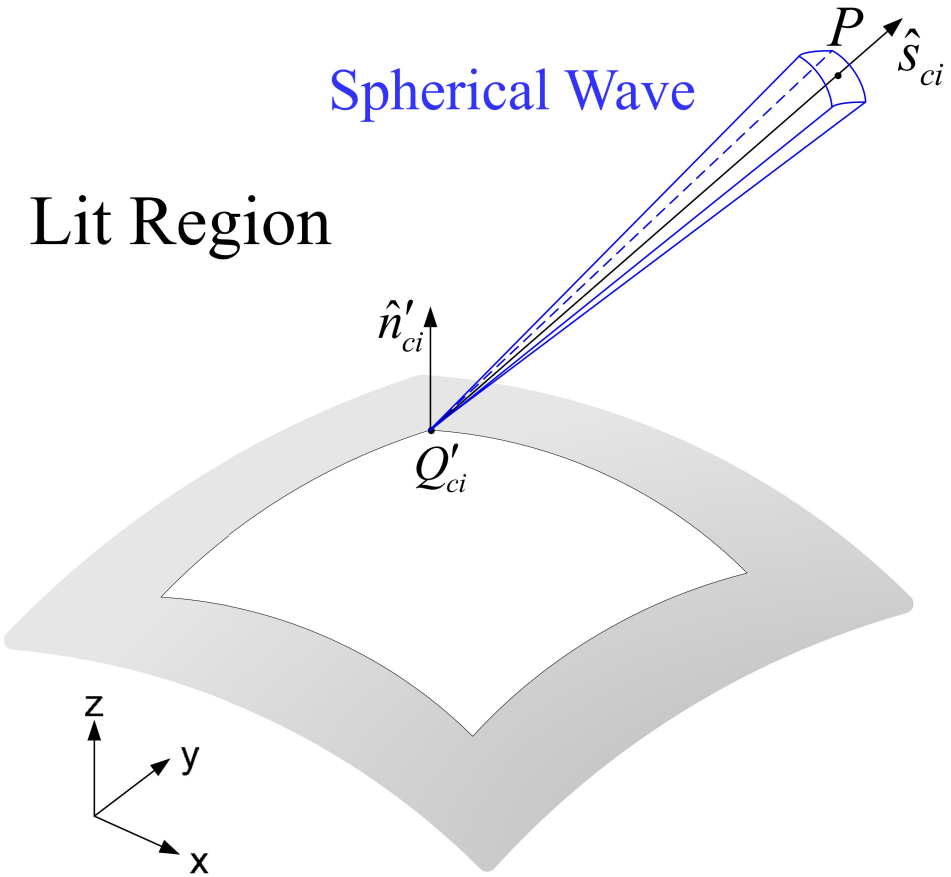

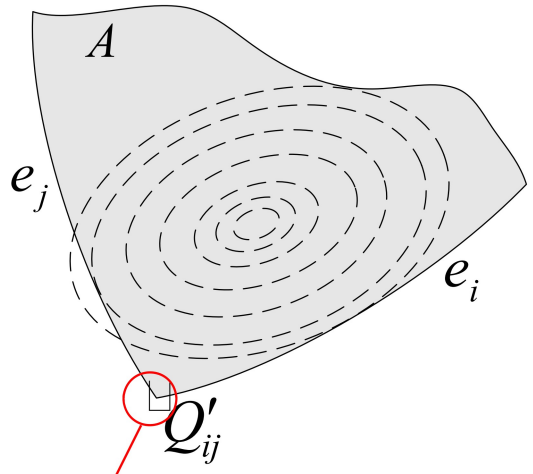

$$\bar{E}^c_{ij} = \bar{A}_{ij} \frac{e^{-jks_{ij}}}{s_{ij}}$$

$$\bar{A}_{ij} = \overline{\overline{T}}_L(P \mid Q'_{ij}) \bullet \hat{\tau}' D^c_{ij}$$

$$D^c_{ij} = -\frac{\varepsilon_{ei}\varepsilon_{ej} J(Q'_{ij}) e^{-jk\chi(Q'_{ij})}}{k^2[\hat{s}_{ij} \bullet \vec{r}'_u - \Omega_u][\hat{s}_{ij} \bullet \vec{r}'_v - \Omega_v]}$$

Corner-Excited Surface Diffracted Fields

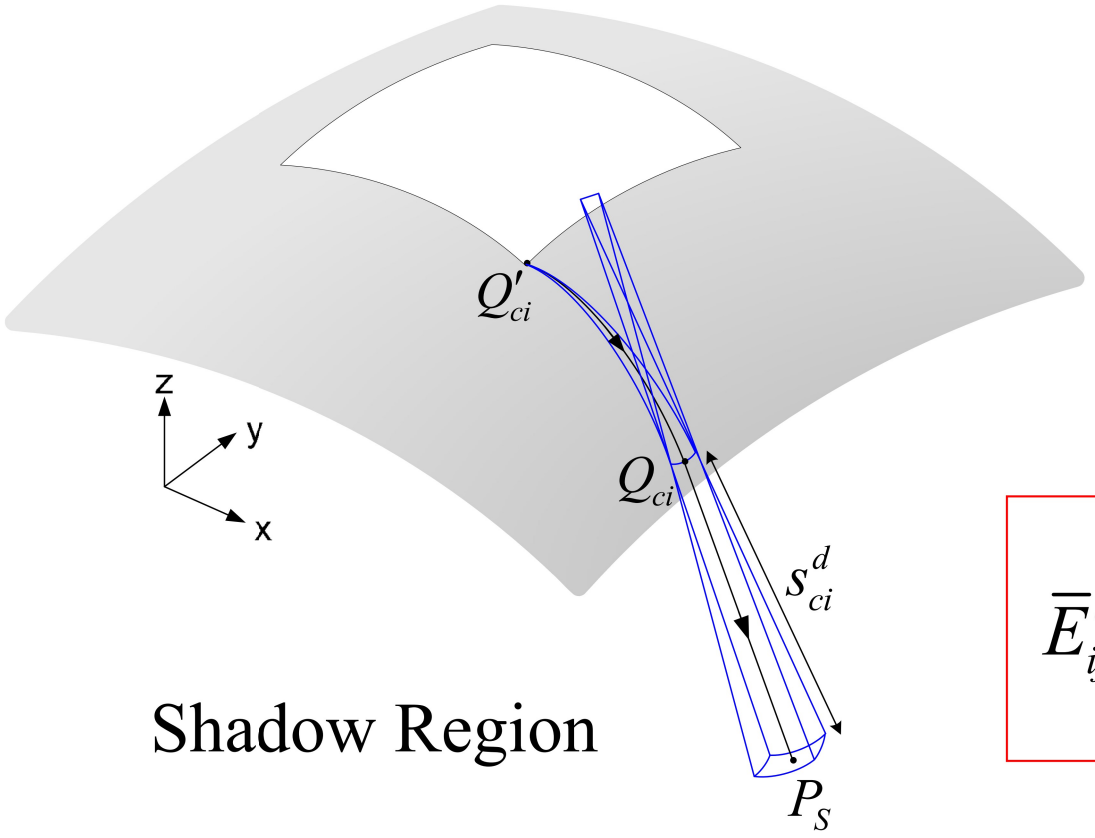

Shadow Region

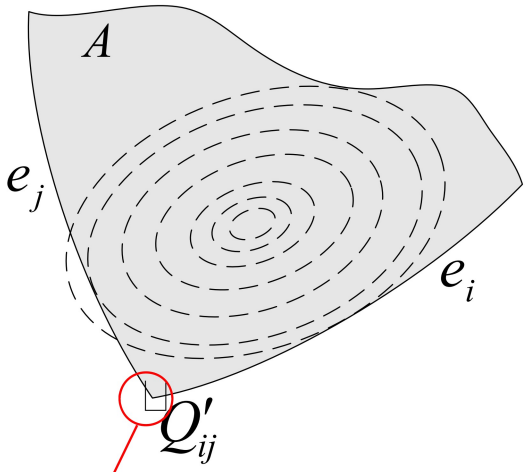

$$\bar{E}^{cs}_{ij} = \bar{A}^{s}_{ij}\sqrt{\frac{\rho^d_{ij}}{s^d_{ij}(\rho^d_{ij}+s^d_{ij})}}e^{-jks^d_{ij}}$$

$$\bar{A}^{s}_{ij} = \overline{\overline{T}}_S(P_s \mid Q'_{ij}) \bullet \hat{\tau}' D^{cs}_{ij} e^{-jkt_{ij}} \sqrt{\frac{d\psi_0}{d\eta(Q_{ij})}}\left[\frac{\rho_g(Q_{ij})}{\rho_g(Q'_{ij})}\right]^{1/6}$$

$$D^{cs}_{ij} = -\frac{\varepsilon_{ei}\varepsilon_{ej}J(Q'_{ij})e^{-jk\chi(Q'_{ij})}}{k^2[\hat{t}'_{ij}\bullet\vec{r}'_u-\Omega_u][\hat{t}'_{ij}\bullet\vec{r}'_v-\Omega_v]}$$

Fields in Transition Regions

$$\Delta\bar{E}^{GO} = \bar{E}^{GO}\left\{\sum_{i=1}^{2}\sum_{j=3}^{4}\frac{e^{-j(k\delta_{ij}^2+\frac{\pi}{4})}}{4\pi k\delta_{ij}^2}W(\sqrt{k}\delta_{ci,j},\sqrt{k}\delta_{ei},\sqrt{k}\delta_{cj,i},\sqrt{k}\delta_{ej})\varepsilon_{ei}\varepsilon_{ej}\right.$$
$$+\sum_{i=1}^{2}\frac{e^{-j(k\delta_{ei}^2+\frac{\pi}{4})}}{2\sqrt{\pi}\sqrt{k}\delta_{ei}}\left[1-F(k\delta_{ei}^2)\right]\varepsilon_{ei}U_{ei}$$
$$\left.+\sum_{j=3}^{4}\frac{e^{-j(k\delta_{ej}^2+\frac{\pi}{4})}}{2\sqrt{\pi}\sqrt{k}\delta_{ej}}\left[1-F(k\delta_{ej}^2)\right]\varepsilon_{ej}U_{ej}\right\}$$

$$W(x_1,y_1,x_2,y_2)=\left(\frac{x_1}{y_1}+\frac{x_2}{y_2}\right)-\frac{\left(x_1^2+y_1^2\right)}{x_1y_1}F(x_1^2)-\frac{\left(x_2^2+y_2^2\right)}{x_2y_2}F(x_2^2)$$
$$+\left(\frac{y_1}{x_1}+\frac{y_2}{x_2}\right)T(x_1,y_1,x_2,y_2)$$

$$\Delta\bar{E}_{ei}^{d}=\bar{E}_{ei}^{d}\left\{\sum_{j=3}^{4}\frac{e^{-j(k\delta_{ci,j}^2+\frac{\pi}{4})}}{2\sqrt{\pi}\sqrt{k}\delta_{ci,j}}\left[1-F(k\delta_{ci,j}^2)\right]\varepsilon_{ej}\right\}$$

Aperture on a PEC Circular Cylinder

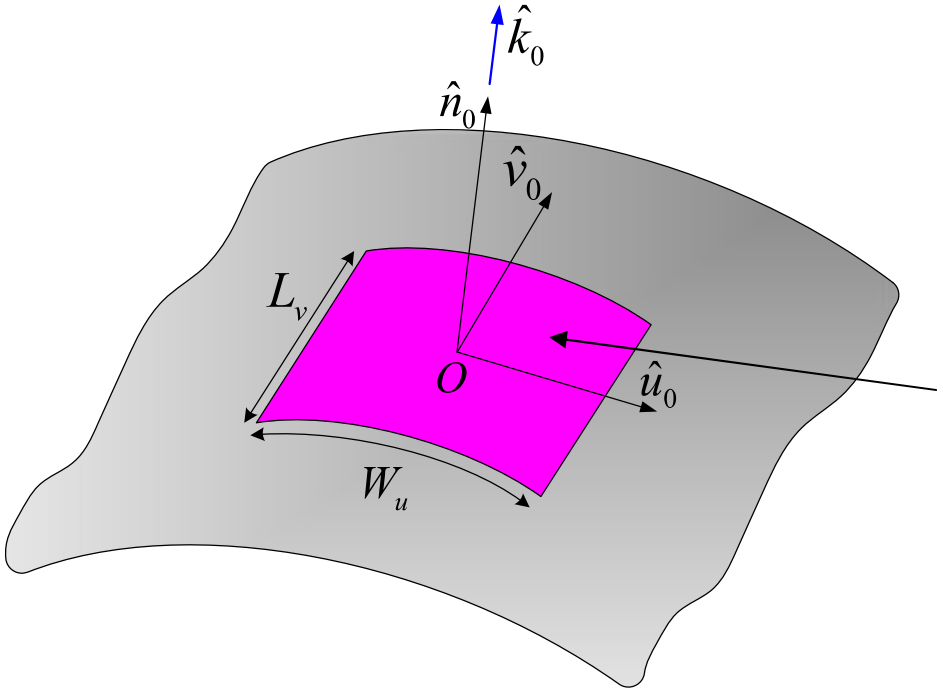

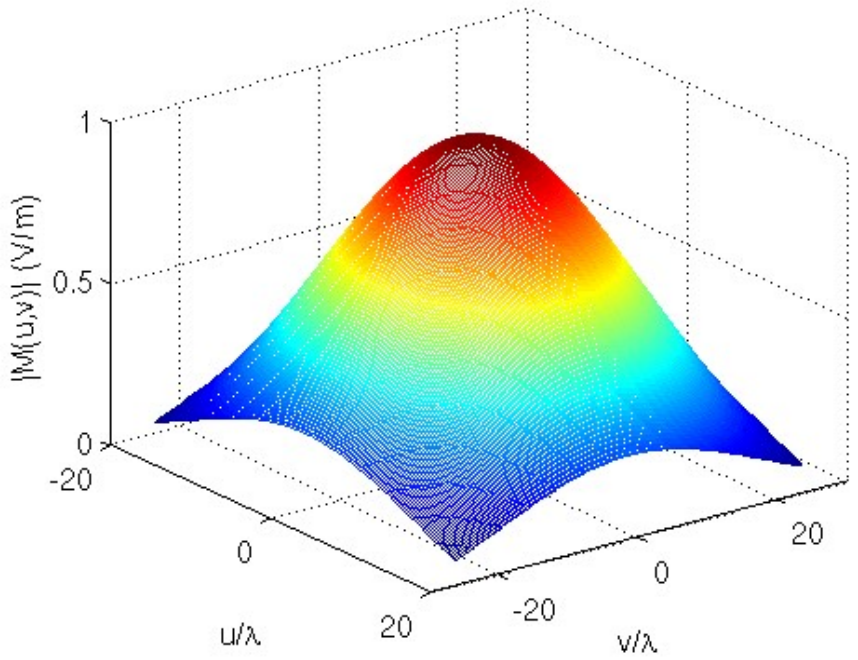

Taylor distribution

f = 24 GHz
a = 150.0 cm (120.0 λ)
W_u = 37.5 cm (30.0 λ)
L_v = 50.0 cm (40.0 λ)
Broadside scan
Current polarization: 45° w.r.t. axial direction

105 TWs were used !!

Aperture on a PEC Circular Cylinder (cont.)

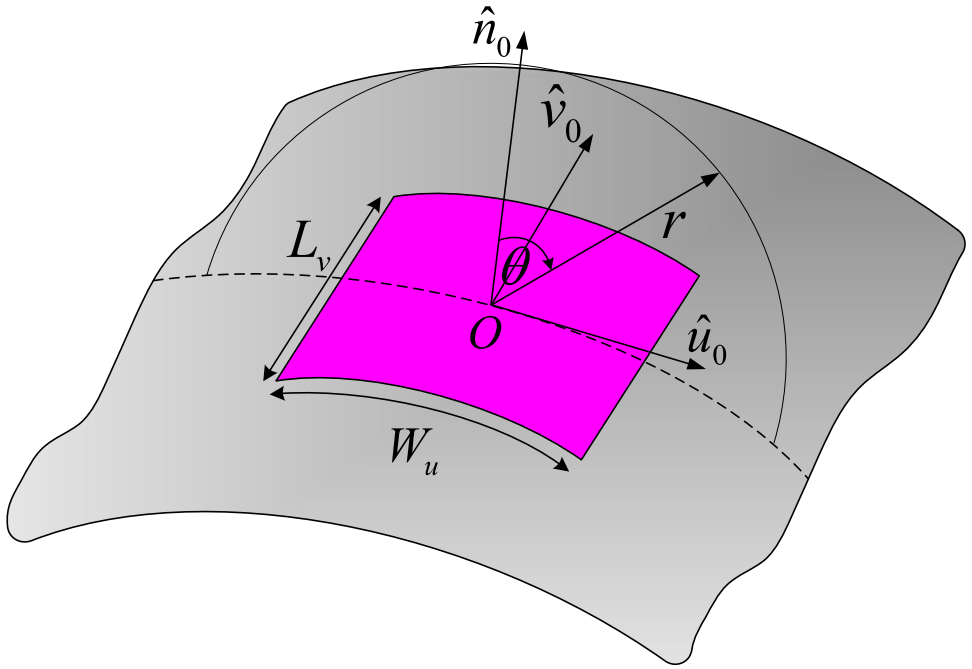

Circumferential plane cut
r = 40 λ (**near zone**)
REF: 25.36 sec.
TW-UTD: 3.78 sec.

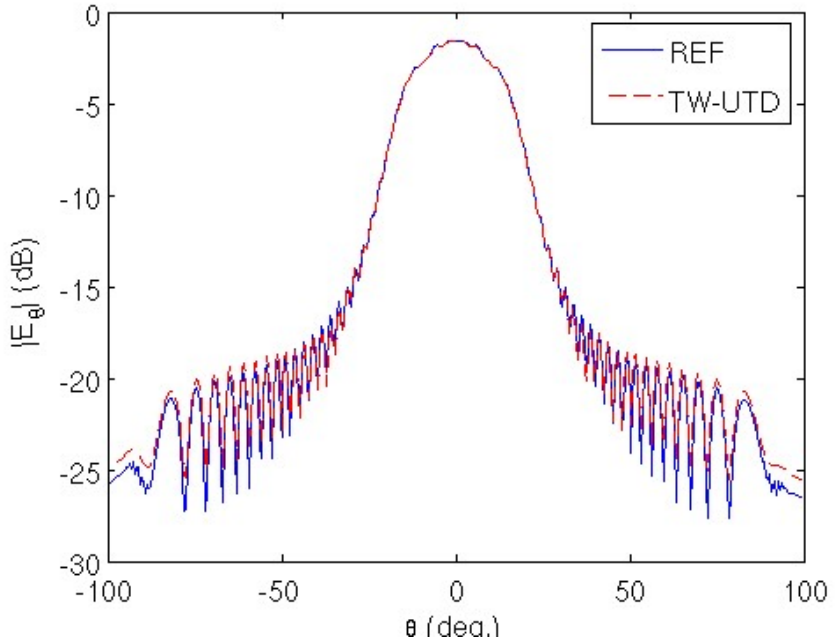

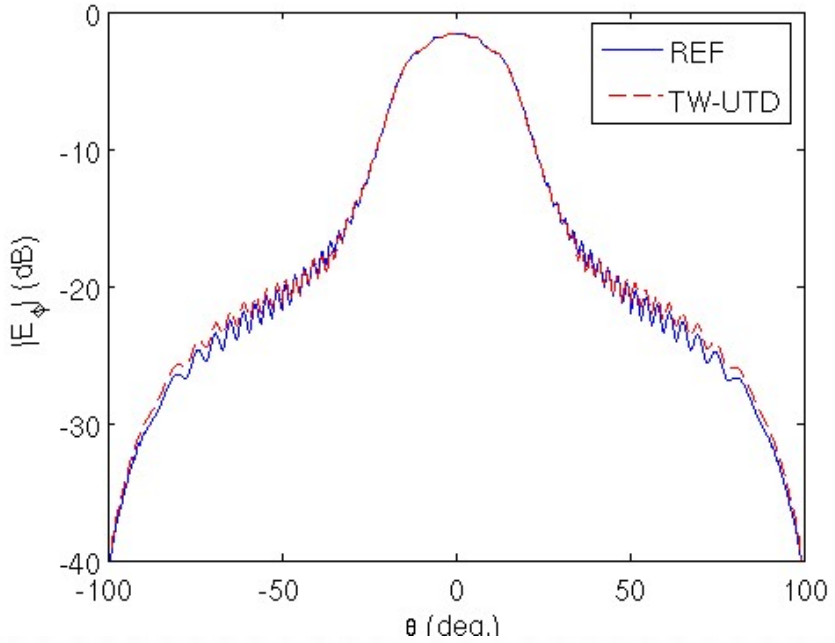

Aperture on a PEC Circular Cylinder (cont.)

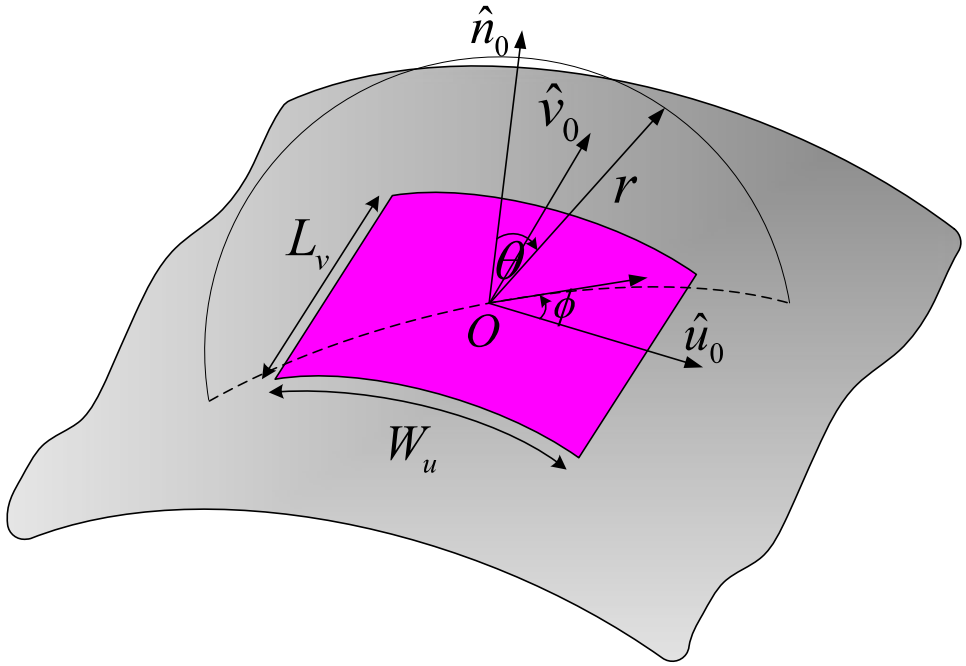

Oblique plane cut: ϕ = 40°
r = 40 λ (**near zone**)
REF: 24.24 sec.
TW-UTD: 3.76 sec.

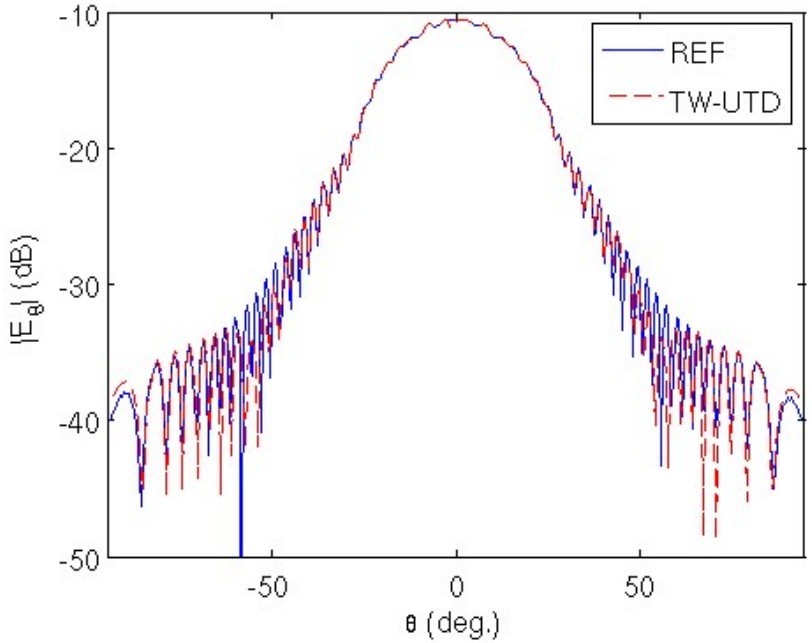

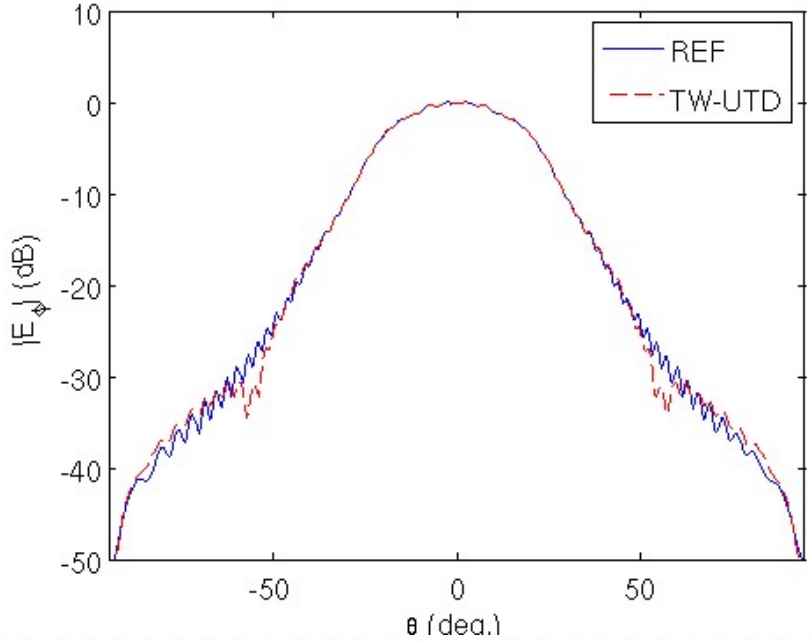

Aperture on a PEC Circular Cylinder (cont.)

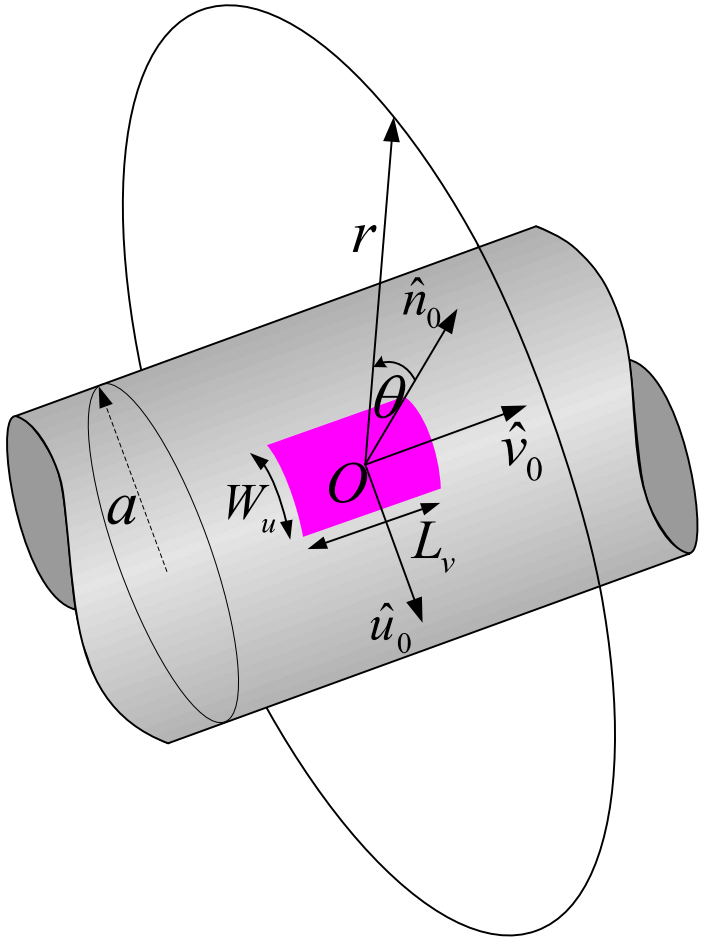

Circumferential plane cut
r = 9600 λ (**far zone**)
REF: 31.25 sec.
TW-UTD: 4.18 sec.

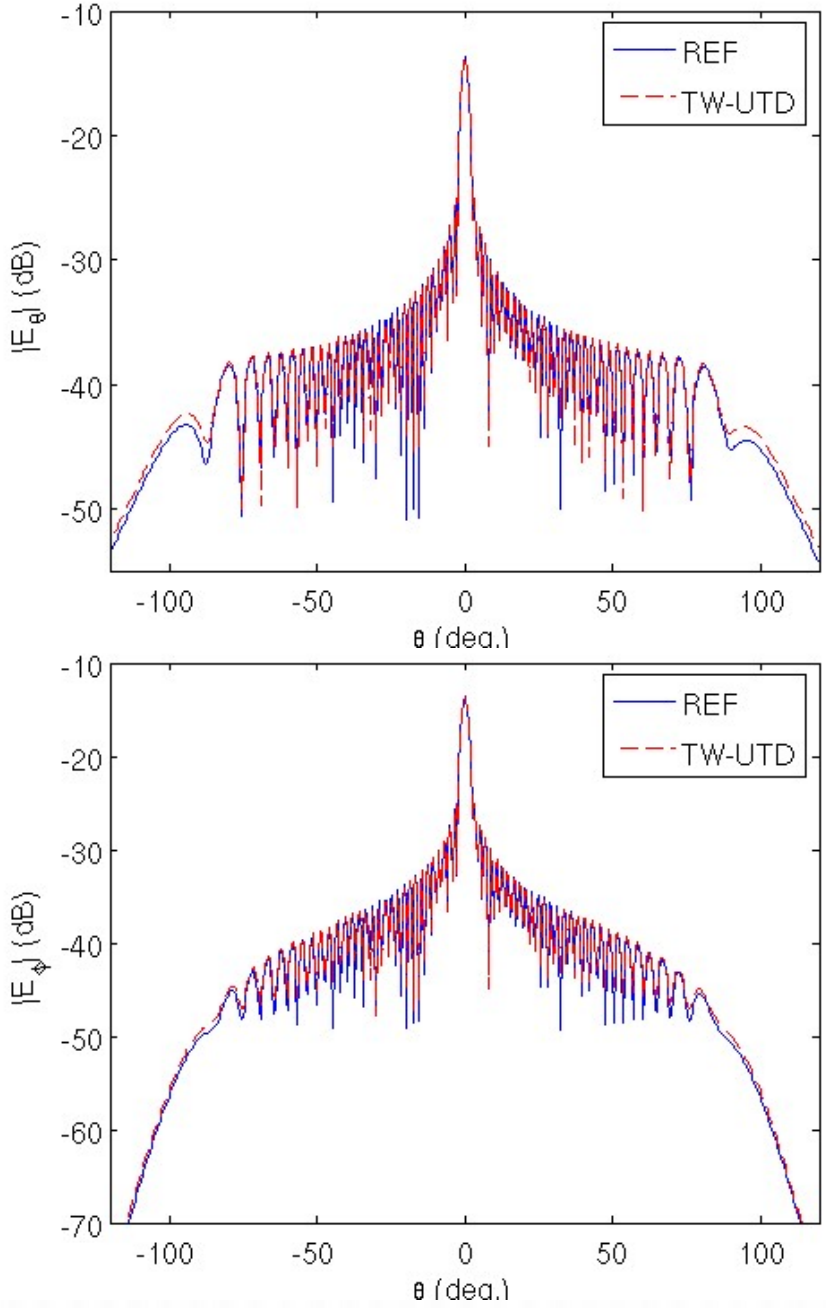

Slot array on a PEC Circular Cylinder

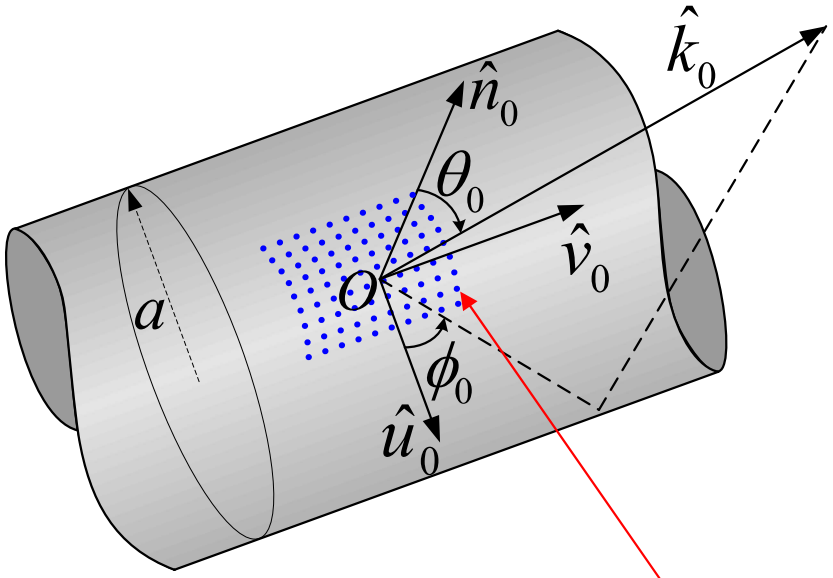

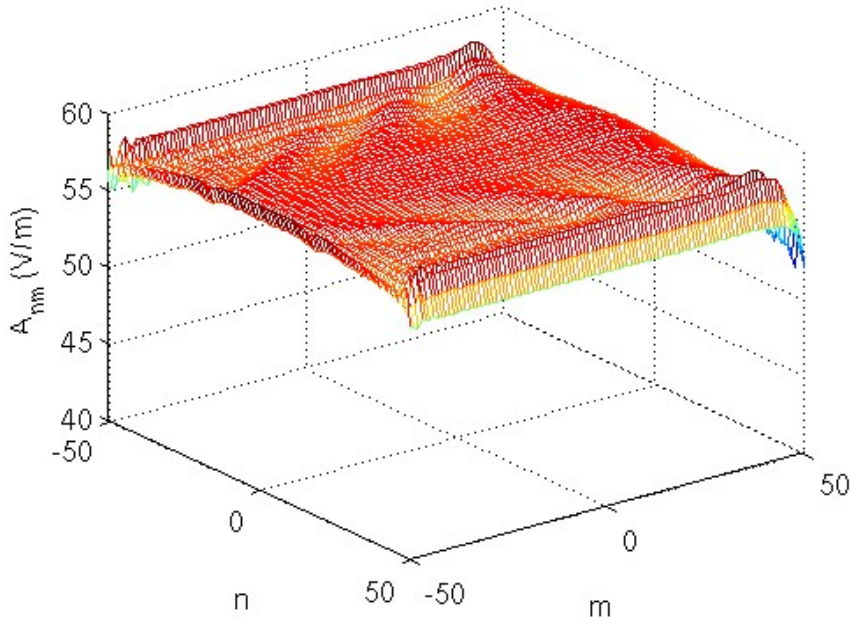

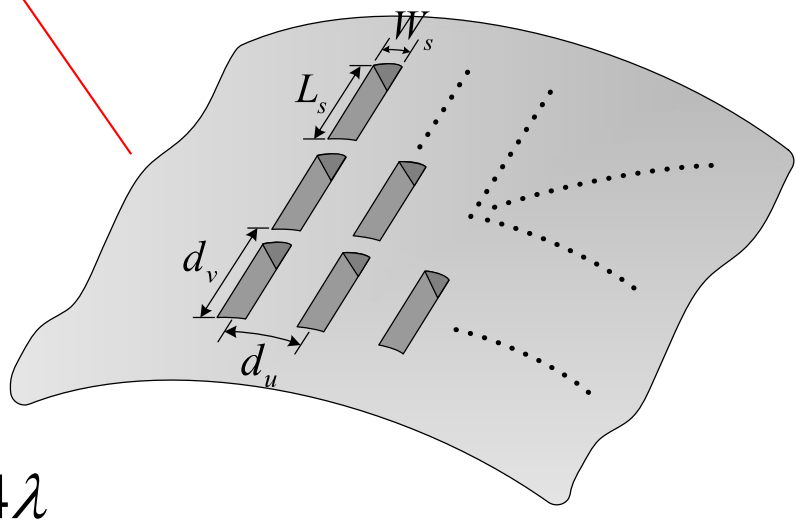

$f = 9.0$ GHz

$a = 100.0\lambda$

101×101 elements

$d_u = d_v = 0.65\lambda$

$L_s = 0.55\lambda, \quad W_s = 0.244\lambda$

Scan direction: $\theta_0 = 30^\circ, \phi_0 = 90^\circ$

93 TWs (≈0.9%) were used !!

Slot array on a PEC Circular Cylinder (cont.)

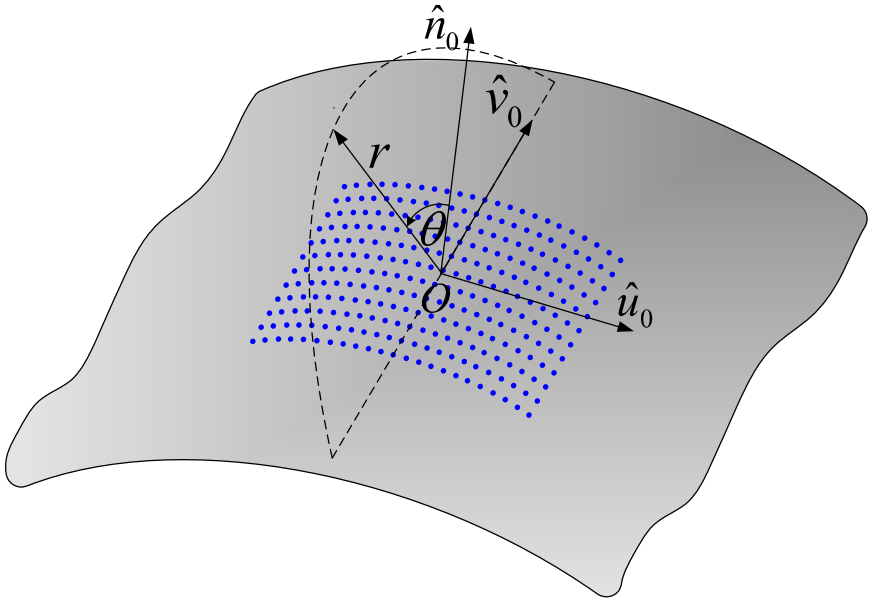

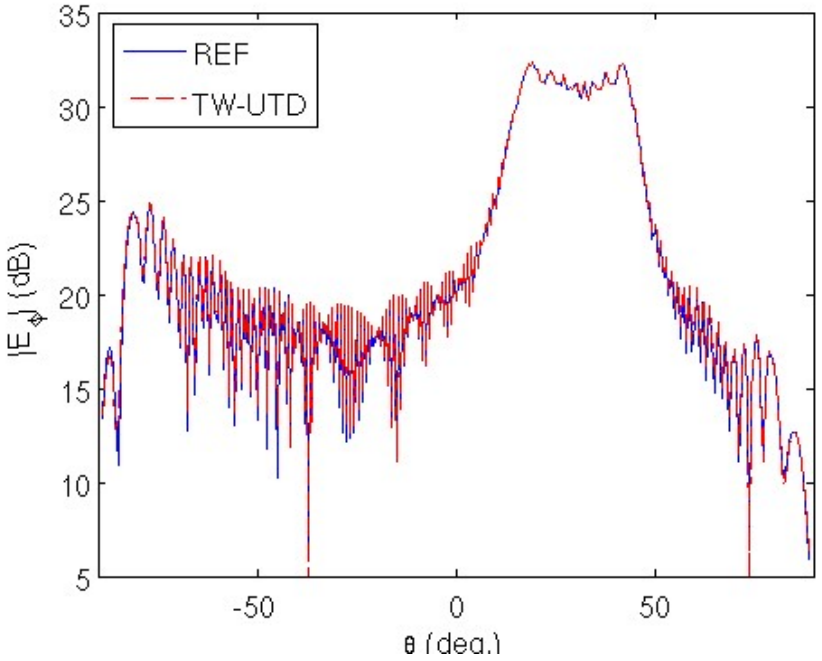

Axial plane cut (**scan plane**)

r = 100 λ (**near zone**)

REF: 34.57 sec.

TW-UTD: 5.47 sec.

Slot array on a PEC Circular Cylinder (cont.)

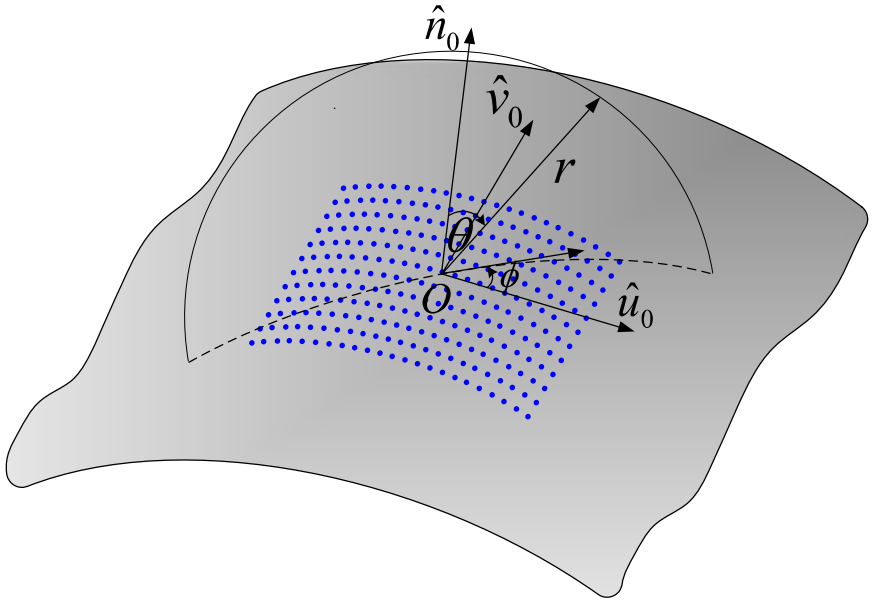

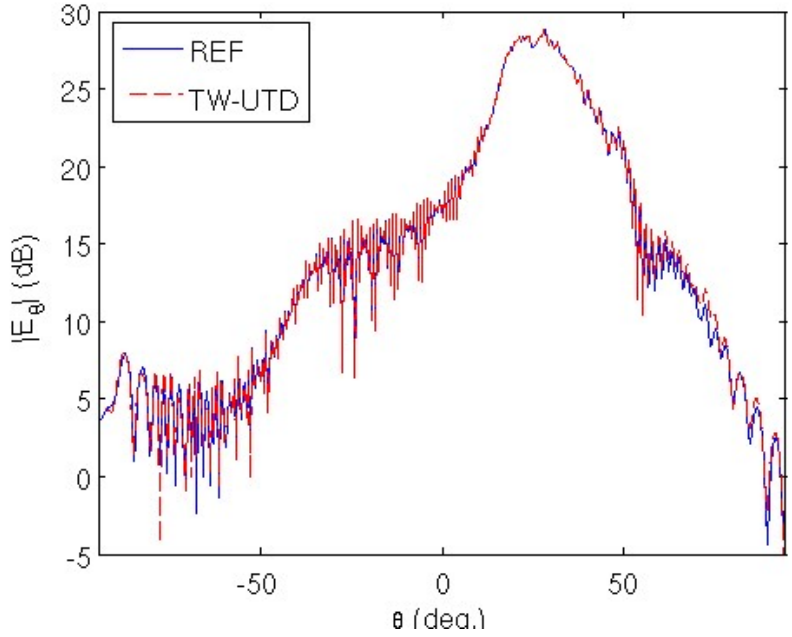

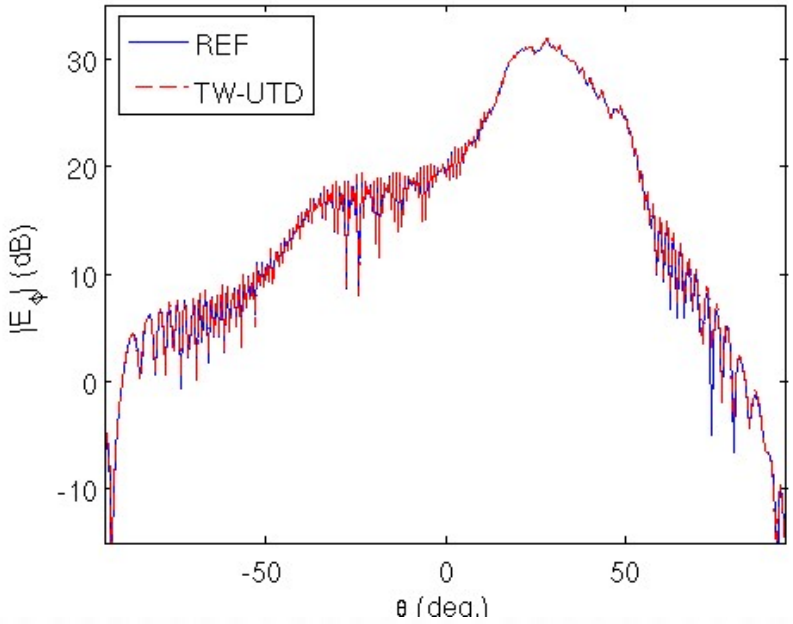

Oblique plane cut: $\phi = 60°$
r = 100 λ (**near zone**)
REF: 38.40 sec.
TW-UTD: 6.12 sec.

Slot array on a PEC Circular Cylinder (cont.)

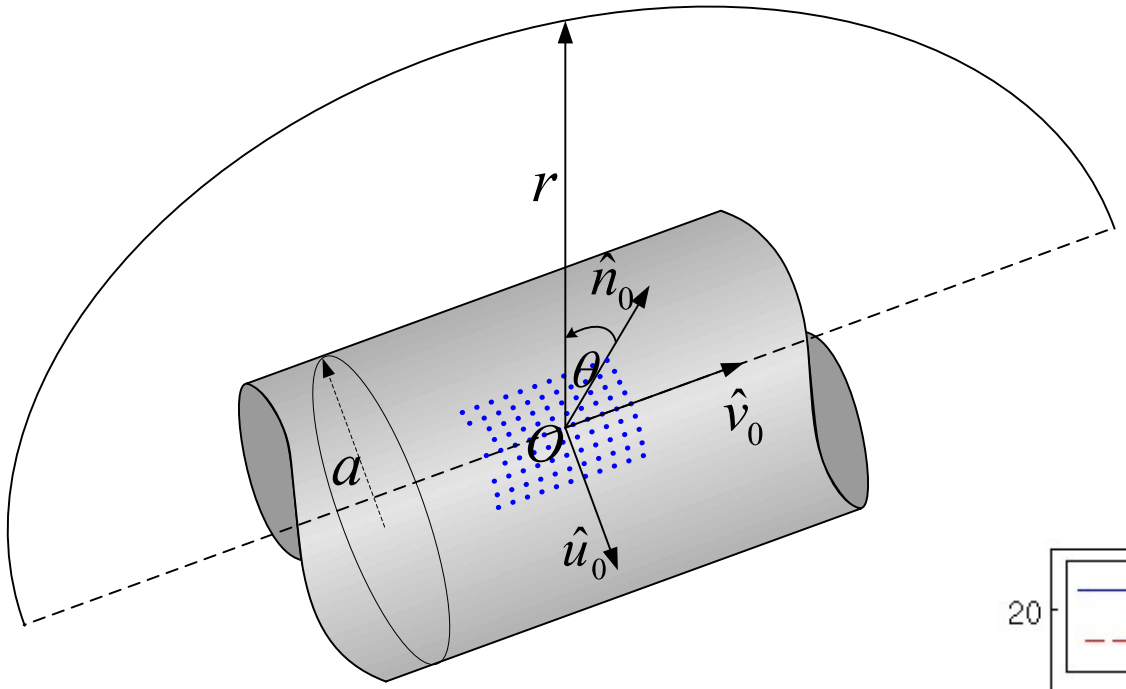

Axial plane cut (**scan plane**)
far zone
REF: 33.48 sec.
TW-UTD: 4.39 sec.

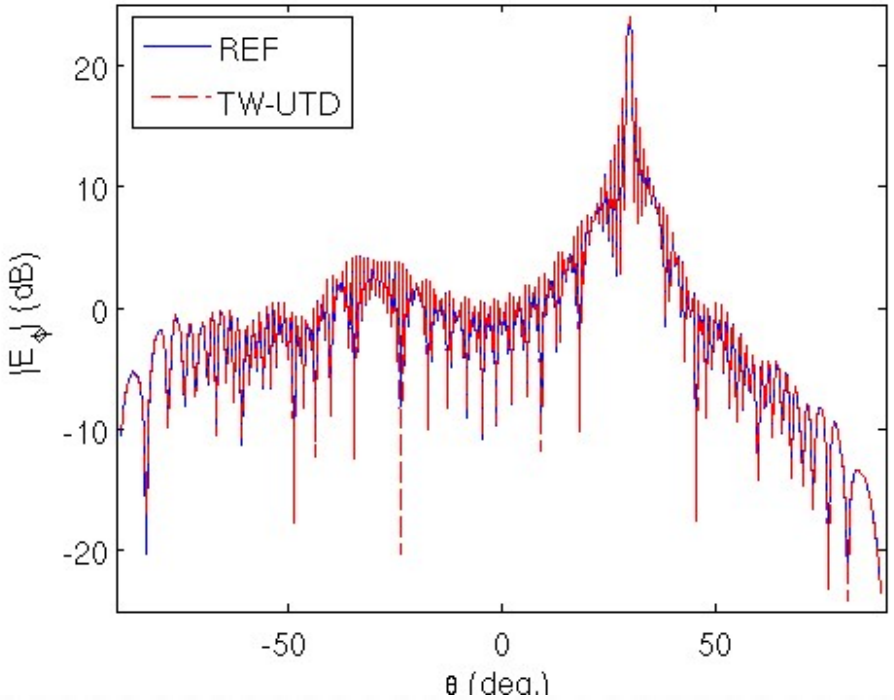

Slot array on a PEC Circular Cylinder (cont.)

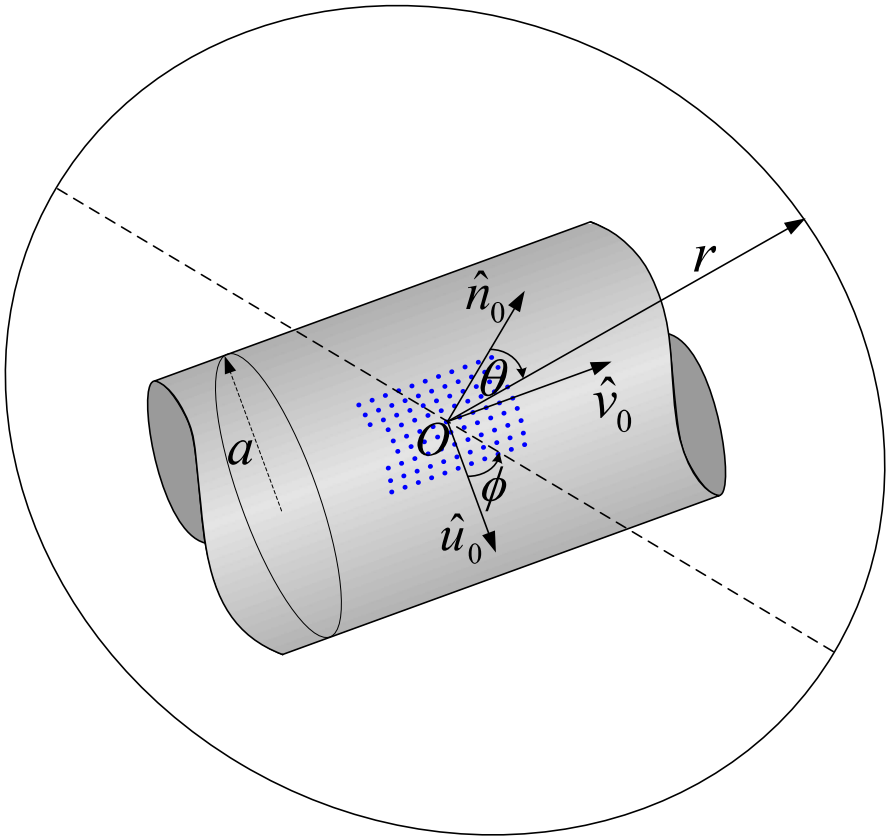

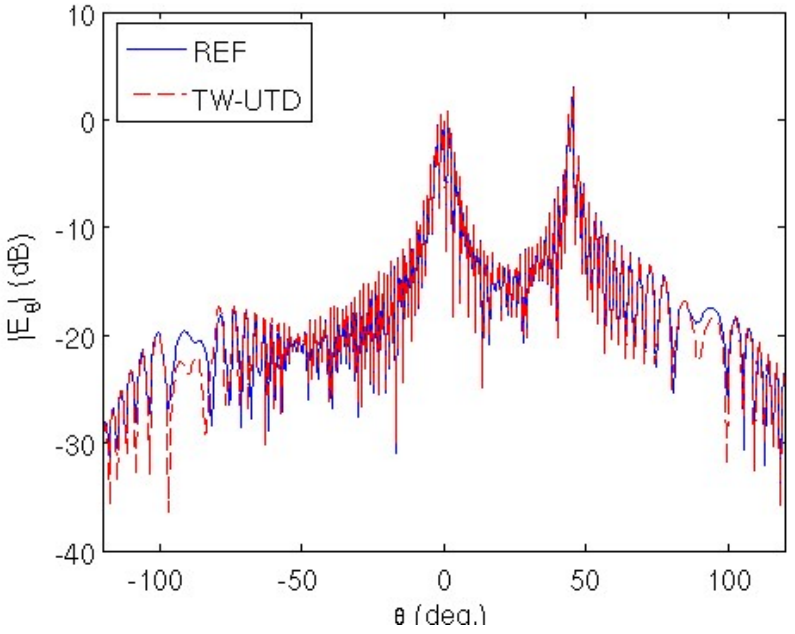

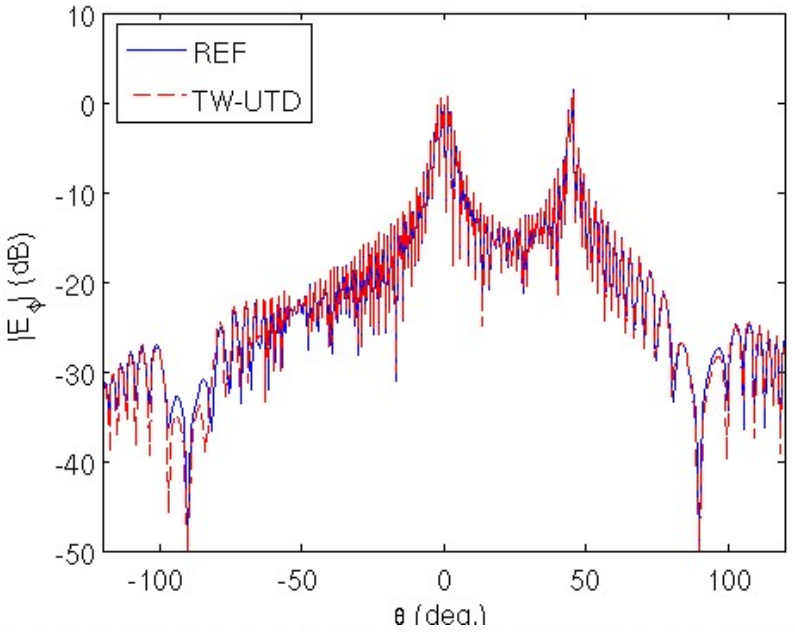

Oblique plane cut: ϕ = 45°

far zone

REF: 51.39 sec.

TW-UTD: 6.08 sec.

Interface between Full-Wave solver and High Frequency method

- Simulate the antenna region with surrounding part of cavity.*
- Take the tangential field on the aperture opening.
- Let $\vec{M} = -\hat{n} \times \vec{E}$ to be the excitation source put on the surface of platform without aperture.
- UTD code NewAir is used to do the high frequency calculation for the *sources on the smooth surface*.**

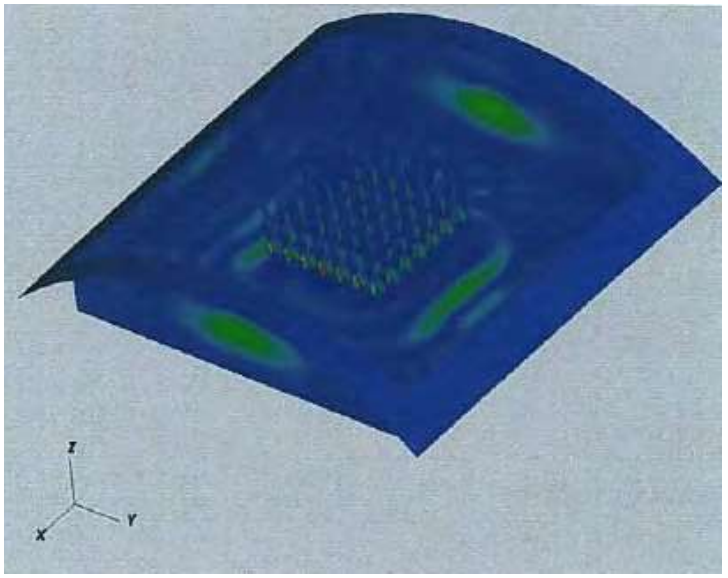

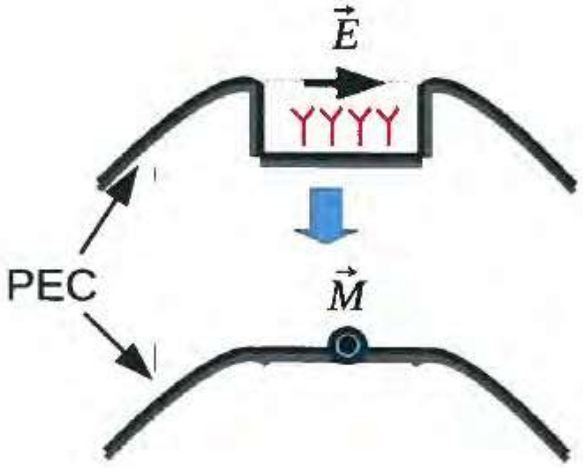

* J-F. Lee's DD FEBI code.

** P.H. Pathak, et al. A Uniform GTD Solution for the Radiation from Sources on a Convex Surface. TAP-29, No. 4, pp. 609-22.

Solution of 7 by 7 Vivaldi array mounted on F16 Platform

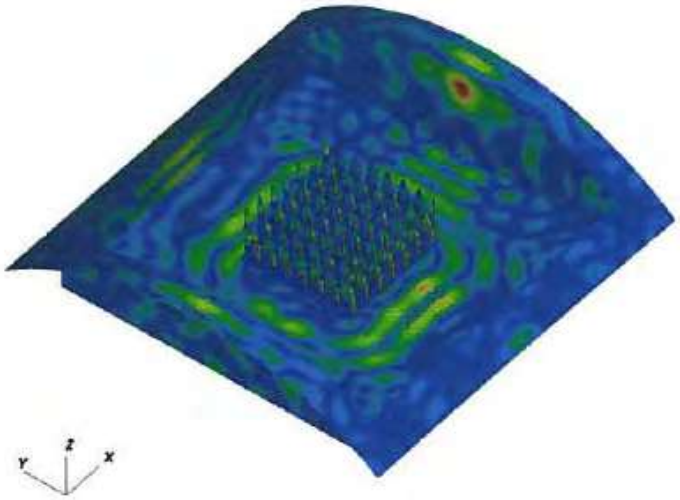

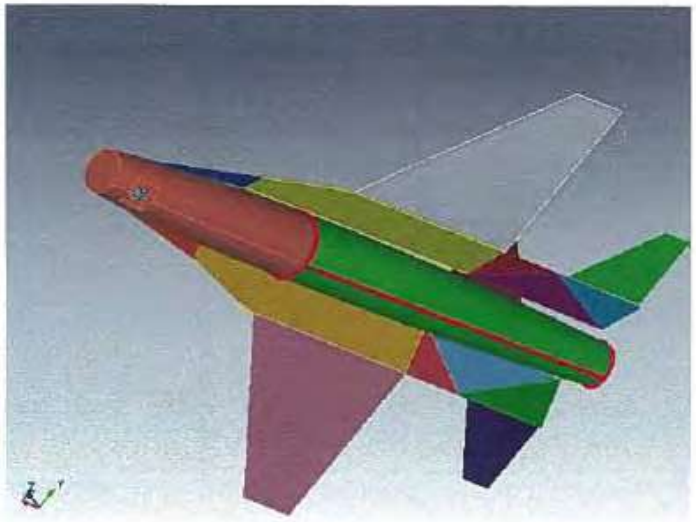

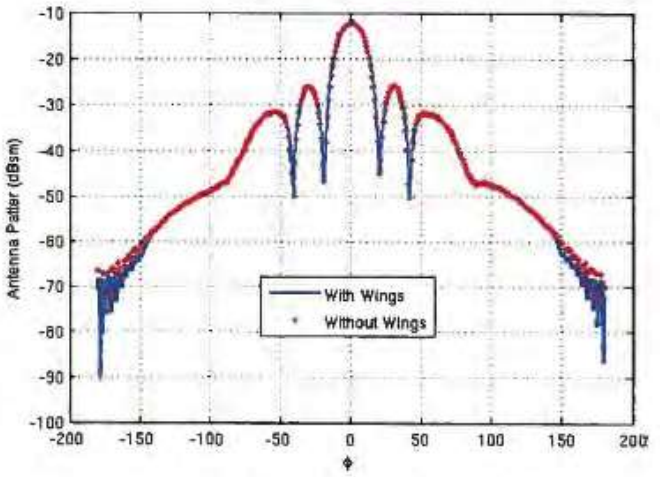

Antenna Pattern (co-polar)

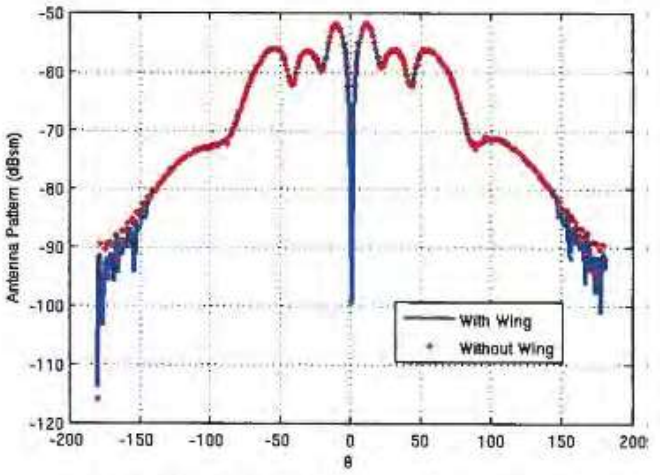

Antenna Pattern (cross-polar)

Solution of 7 by 7 Vivaldi array mounted on F16 Platform

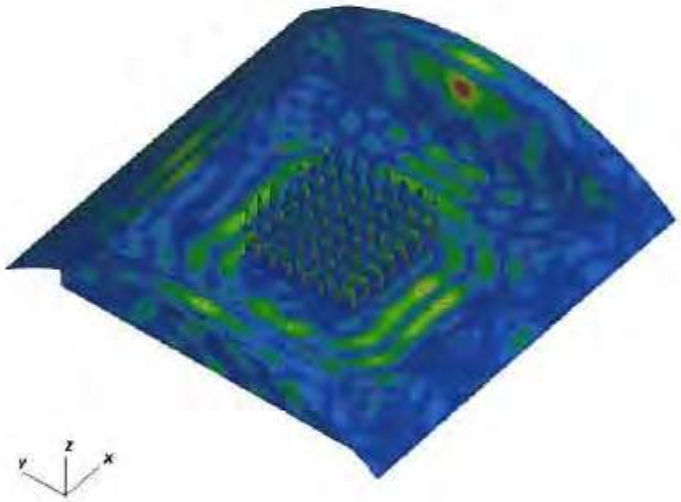

Computational Statistic
Iteration Number: 14

	CPU time	Memory Cost	Unknowns
Antenna	1:27:10	95M	1,878,372
Cavity	1:56:24	49M	29,895
Coupling	0:25:02		
OuterLoop	0:0:50	54M	
High Freq	0:18:33		

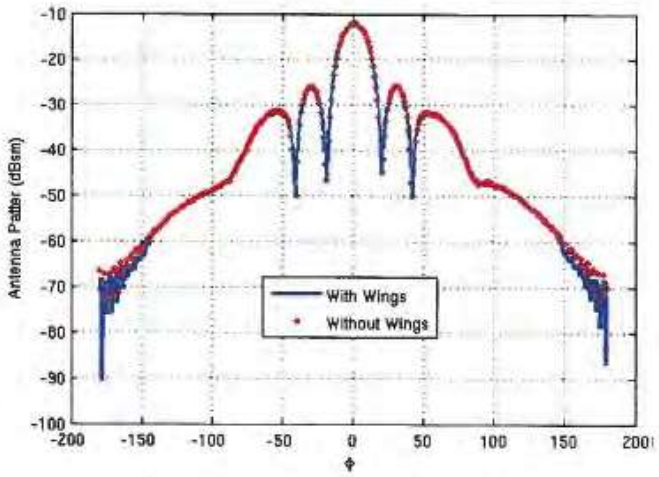

Antenna Pattern (co-polar)

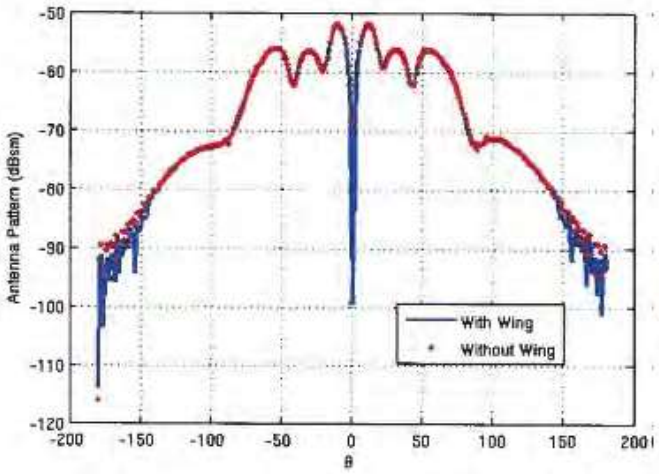

Antenna Pattern (cross-polar)

20 by 20 Vibaldi array mounted on larger platform

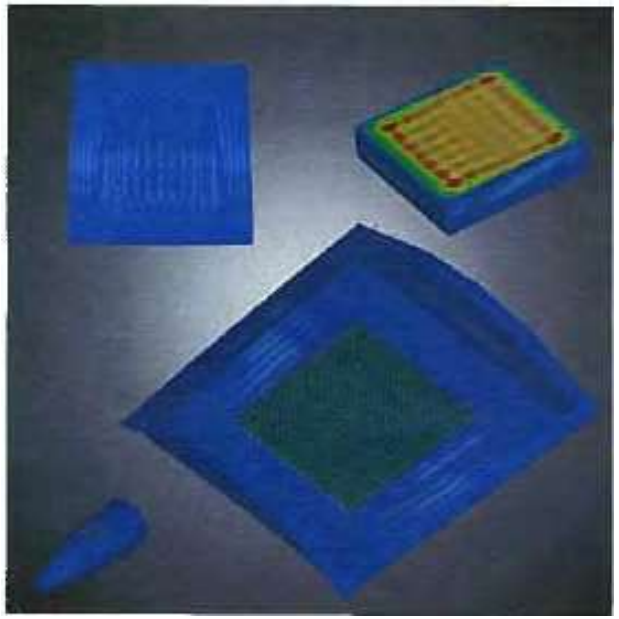

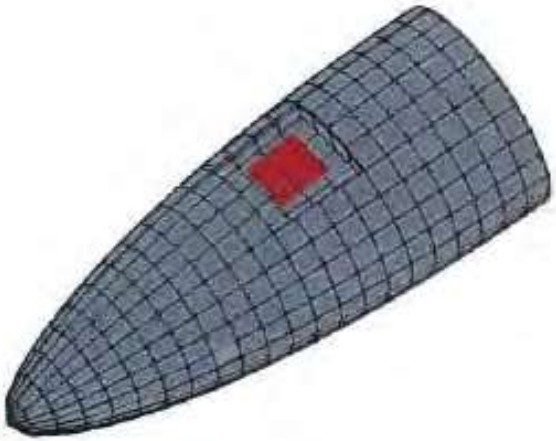

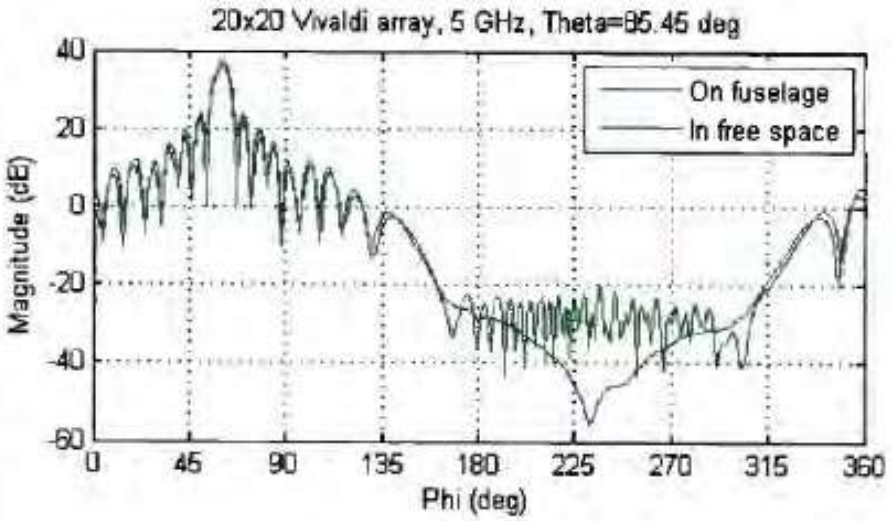

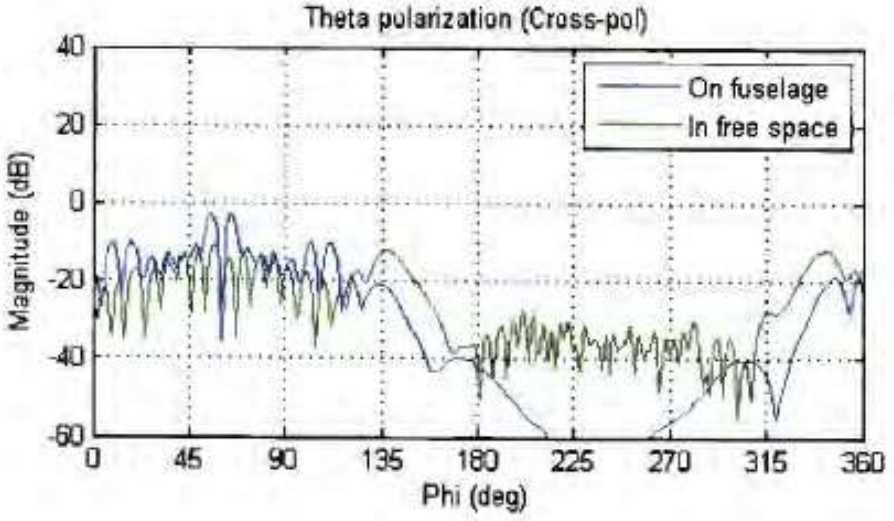

ElectroScience LABORATORY

20 by 20 Vibaldi array mounted on larger platform

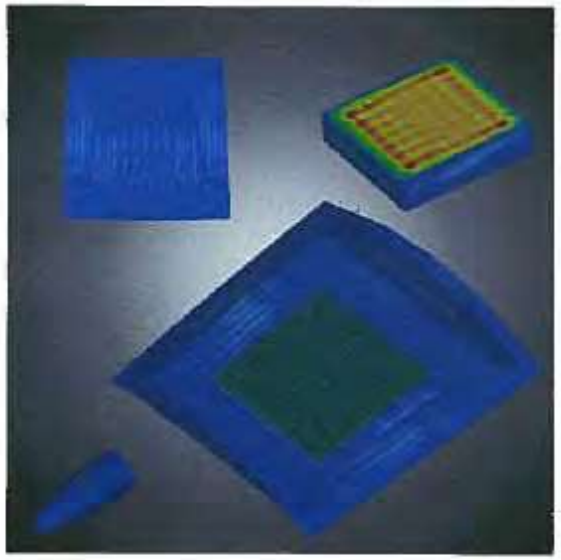

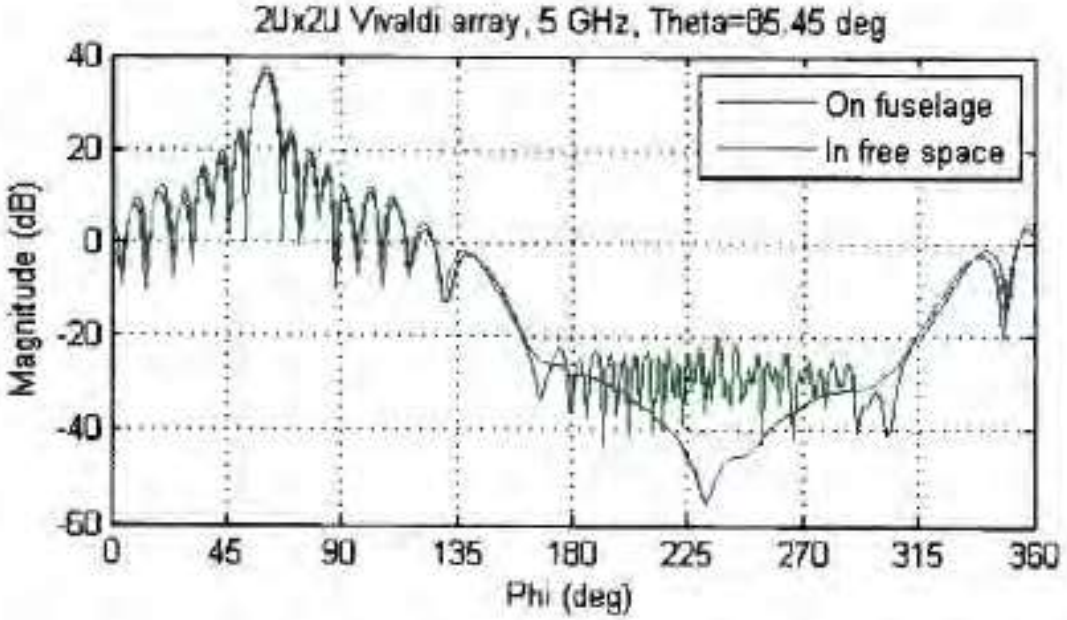

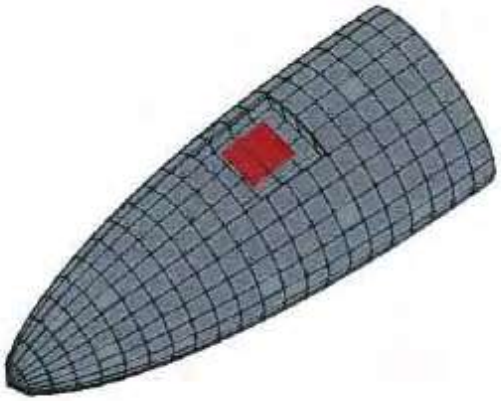

Computational Statistic
Iteration Number: 18

	CPU time	Memory Cost	Unknowns
Antenna	11:10:48	400M	8,288,904
Cavity	2:29:06	330M	167,580
Coupling	2:41:42		
OuterLoop	0:3:0	223M	
High Freq	0:5:30		

Conclusions

• An asymptotic **UTD** ray solution has been developed for describing, in a **collective** fashion, the fields radiated by large conformal antenna arrays on a doubly curved, smooth convex surface.

ElectroScience LABORATORY

• The present solution will provide an **efficient link** between the local array part to be analyzed numerically and the full external platform part to be analyzed by UTD, in a **hybrid method** for analyzing large complex antenna phased arrays integrated into a realistic complex platform.

• The present collective UTD ray solution shows a good agreement with the conventional element-by-element UTD field summation solution.

The work presented is done in conjunction with the following researchers

The Ohio State Univ. (OSU), ElectroScience Lab.(ESL), Columbus, Ohio, USA

(1) Prof. Robert J.Burkholder
(2) Dr. Youngchel Kim
(3) Dr. His-Tseng Chou (now Prof. at Yuan-Ze Univ. Taiwan ROC)
(4) Dr. Titipong Lertwriyaprapa (now at King Mongkut university)
(5) Dr. Pawuwat Janpugdee (Was member of research staff at TEMASEK Labs. NUS, Singapore; Now at Chulalongkorn univ.)
(6) Dr. Koray Tap (Now at ASELSAN, Ankara, Turkey)
(7) Prof. W.D. Burnside
(8) Dr. R.J. Marhefka
(9) Dr. Nan Wang
(10) Prof. Jin-Fa Lee

Univ. of Siena, Italy

(1) Giorgio Carluccio
(2) Prof. Matteo Albani
(3) Prof. Stefano Maci

Applied EM

(1) Dr. Cagatay Tokgoz
(2) Dr. C. J. Reddy